UCSF
UC San Francisco Electronic Theses and Dissertations

Title
Cell-intrinsic Mechanisms of Odor Preference and Discrimination in C. elegans Olfactory Neurons

Permalink
https://escholarship.org/uc/item/78q1c6q4

Author
Tsunozaki, Makoto

Publication Date
2008-08-27

Peer reviewed|Thesis/dissertation

eScholarship.org Powered by the California Digital Library
University of California

Cell-intrinsic Mechanisms for Odor Preference and Discrimination in C. elegans Olfactory Neurons

by

Makoto Tsunozaki

DISSERTATION

Submitted in partial satisfaction of the requirements for the degree of

DOCTOR OF PHILOSOPHY

in

Cell Biology

in the

GRADUATE DIVISION

of the

UNIVERSITY OF CALIFORNIA, SAN FRANCISCO

Copyright (2008)
By
Makoto Tsunozaki

This dissertation is dedicated to my parents

Acknowledgements

This work would not have been possible without the guidance, encouragement and good company of friends and family. I am grateful for:

Cori, for her constant encouragement, insights and mentorship;

Sreekanth, for his energy, for his magic, for always being there when you need him;

My classmates/lab mates, Andy, Jason and Sarah, for sharing a unique graduate school experience spanning two coasts;

Holly, for her amazing capacity to care for everybody in lab, and every bird;

Rockefeller people: Tapan, for our late-night/early morning conversations on sports, movies and science; Adrés, for our musical and culinary excursions; Navin, for knowing everything about everything American; Chrisitian, for being normal; My bay mates Nichos "Ernesto" Chronis and Bibi, for putting up with Shrek; Manoush and Hernan, for keeping the worms happy; Present Bargmann lab members for creating a fun lab environment;

UCSF people: Paul, for teaching me the first chemotaxis assay; Jesse, for teaching me worm behavior, starting with burning plastic; My baymates, Jami and Miri, for tolerating some not-so-pleasant odors; all the former Bargmann lab members, for making the lab a cool place to work in; Emmitt and Annie, for convincing me to come to UCSF; My classmates, for making the best skit for the Tetrad retreat;

My Thesis committee members, Henry Bourne and Herwig Baier, for their guidance and support; My Orals committee members, Sandy Johnson, Ulrike Heberlein, and Henry Bourne, for their support;

My former roommates: Jason and Mike, for introducing me to Tenacious D, Leprechauns, and forties; Charles, David, Jason and Mike, for making Placey a special place; The Towerball team, for good times in winning and in losing; 19th Ave Japanese Baptist Church youth group members, for spiritual support in uncertain times;

Steven Lee, for his seemingly unbounded generosity, for always being on my side; The Lee family, for accepting me as family;

My Grandparents, Jun and Nobuko Shiozaki, for always welcoming me home; Aunty Eiko-san, for her dedication and kindness to all of our family;
My siblings, Kentaro and Takeshi, for keeping our family stable in Japan so that I can explore life in the US;
My parents, Etsuko and Toshio Tsunozaki, for all of their support, and their trust;

The Chi family, for their generosity and support;
Candace, for her smiles, humor, creativity, patience, and kindness.

Cell-intrinsic Mechanisms for Odor Preference and Discrimination in *C. elegans* Olfactory Neurons

Makoto Tsunozaki

Abstract

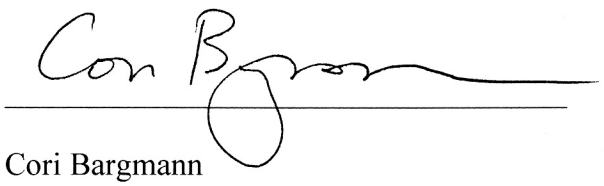
Two fundamental questions regarding the neural basis of sensation are how stimuli are encoded in the nervous system and how animals discriminate between stimuli. In chemosensory systems there is a diversity of chemoreceptors that matches the diversity in chemical space. Volatile chemicals, or odors, are often represented in the periphery by a combinatorial code of neuronal activity. By contrast, the more simple qualities of soluble tasted chemicals, such as bitter and sweet, are sensed by anatomically distinct populations of cells that drive stereotyped behaviors. The nematode *Caenorhabditis elegans* senses and discriminates between many soluble and volatile chemicals, and exhibits plasticity in chemosensory behavior. This thesis addresses the cellular and molecular mechanisms underlying *C. elegans* chemosensory behaviors through genetic analysis, quantitative analysis of behavior and measurement of neuronal activity.

C. elegans discriminates among certain food-related odors by mechanisms that require multiple olfactory cell types. In this study, animals with only one type of functional neuron are shown to discriminate between some odors. Therefore, cell-intrinsic mechanisms may participate in certain kinds of odor discrimination, in addition to combinatorial mechanisms.

Some chemosensory cues drive innate behaviors by activating a hardwired, "labeled-line" circuit connecting sensory input to motor output. However, this thesis shows that *C. elegans* AWC olfactory neurons that drive attraction can also drive

avoidance in some contexts. cGMP and PKC signaling in olfactory neurons reverses odor preference by altering neurotransmission at the first sensory synapse. Therefore, a hardwired circuit can generate opposite behavioral outcomes through alternative modes of synaptic transmission.

Further analysis of cGMP signaling mutants revealed that neuronal cGMP signaling is involved not only in chemosensory behaviors in *C. elegans* but also in regulating adaptive behavioral responses to osmotic stress. These results provide a striking parallel to the role of cGMP signaling in vertebrate water homeostasis. The adaptive response to osmotic stress has been mapped to a set of candidate mechanosensitive neurons. These neurons are distinct from those that sense mechanical touch stimuli along the body or the nose. Thus mechanosensation and osmosensation may arise from segregated neuronal pathways, which could facilitate discrimination between the different types of mechanical stimuli.



Cori Bargmann

Graduate Advisor

Table of Contents

Title Page i

Copyright ii

Dedication and Acknowledgements iii

Abstract vi

Table of Contents viii

List of Tables ix

List of Figures x

Chapter 1: Introduction 1

Chapter 2 : The role of olfactory neuron diversity in *C. elegans* odor discrimination 43

Chapter 3: A behavioral switch: cGMP and PKC signaling in olfactory neurons reverses odor preference in *C. elegans* 67

Chapter 4: Genetic analysis of *gcy-28* function in AWC chemotaxis 135

Chapter 5: cGMP signaling regulates hypo-osmotic stress responses in *C. elegans* 168

Chapter 6: Perspectives and future directions 199

Library Release Form 218

List of Tables

Chapter 2

Table 2-1. Odor specificity of olfactory neurons 60

Table 2-2. Cell-fate mutants that reduce olfactory neuron diversity 61

Chapter 4

Table 4-1. Fractional rescue of butanone chemotaxis in *gcy-28* mutants.....158

Table 4-2. Expression pattern of promoters 159

Table 4-3. Chemotaxis index of *gcy-28* mutants rescued with different promoters.....161

Chapter 5

Table 5-1. Tissue-specific rescue of *gcy-28* mutants.....191

Table 5-2. Candidate mutants tested for hypo-osmotic stress response 192

List of Figures

Chapter 2

Figure 2-1. Discrimination defect of *nsy-1* mutants 62

Figure 2-2. AWC^{ON} can discriminate between some odors, but cannot discriminate between butanone and 2,4,5-trimethylthiazole..... 63

Figure 2-3. Discrimination between 2,3-pentanedione and 2,4,5-trimethylthiazole..... 64

Figure 2-4. AWC^{OFF} can discriminate between odors..... 65

Figure 2-5. Odor discrimination in candidate mutants 66

Chapter 3

Figure 3-1. AWC^{ON} mediates odor avoidance instead of attraction in *gcy-28* mutants ..101

Figure 3-2. Regulated turning during chemotaxis to odors.....103

Figure 3-3. Ablation of AWC^{ON} abolishes turning bias in wild type and *gcy-28* animals 106

Figure 3-4. Sequence analysis of *gcy-28*.....108

Figure 3-5. Spatial and temporal sites of GCY-28 action.....110

Figure 3-6. *gcy-28* and DAG/PKC signaling interact to transform behavior 112

Figure 3-7. Olfactory plasticity is altered in *gcy-28*.....114

Supplementary Figure 1. Characterization of *gcy-28* mutants 116

Supplementary Figure 2. Turning biases during chemotaxis 118

Supplementary Figure 3. Ca^{2+} response of AWC^{ON} neurons in *gcy-28* animals.....120

Supplementary Figure 4. Genetic interactions between *gcy-28* and *egl-4* PKG loss-of-function and gain-of-function mutants 122

Supplementary Figure 5. Ca^{2+} response of AWC^{ON} neurons in *pkc-1* animals 124

Supplementary Figure 6. Salt and temperature plasticity in *gcy-28* mutants 125

Supplementary Figure 7. Butanone conditioning without food can rescue *gcy-28* 127

Chapter 4

Figure 4-1. Effect of a *gcy-28.d*-specific deletion on chemotaxis.....162

Figure 4-2. Effect of extracellular domain deletion on *gcy-28* activity.....163

Figure 4-3. Genetic interaction between *gcy-28* and *daf-3*, a suppressor of PKG mutants 164

Figure 4-4. Genetic interaction between *gcy-28* and cAMP signaling.....165

Figure 4-5. Genetic interaction between *gcy-28* and the BK channel mutant, *slo-1*.....166

Figure 4-6. Genetic interaction between *gcy-28* and circuit mutants.....167

Chapter 5

Figure 5-1. Measuring the effect of hypo-osmotic stress on *C. elegans*.....193

Figure 5-2. Effect of hypo-osmotic stress on locomotion in wild-type and *gcy-28* mutant animals 194

Figure 5-3. Hypo-osmotic stress-induced paralysis in *gcy-28* mutants.....195

Figure 5-4. Hypo-osmotic stress response of PKG *egl-4* mutants 196

Figure 5-5. Aldicarb resistance in *gcy-28* mutants.....197

Figure 5-6. Hypo-osmotic stress-induced paralysis in mechanosensory mutants.....198

CHAPTER 1

Introduction

Summary

Many animals respond to chemical cues directly related to food, mating or harm with innate behaviors. Chemosensory neurons that drive these innate behaviors are often coupled to a hardwired circuit. However, a complex, shifting environment poses two challenges. The first challenge, which is general to all sensory behaviors, is discriminating between different sensory cues and identifying the important ones. In other words, what aspects of the sensory environment does the nervous system encode? Secondly, how does a hardwired circuit adapt to changes in the environment? How is plasticity generated in a fixed neural circuit? Recent work in mice, *Drosopila* amd *Caenorhabditis elegans* has uncovered the basic mechanisms the encode innate behaviors in peripheral of olfactory and gustatory systems. A common principle emerging from these studies is the transformation of sensory information using anatomically segregated, "labeled-line" neuronal pathways. How the neuronal pathways specify behavior, or how plasticity is built into innate behaviors, is less well understood.

The olfactory behavior of *C. elegans* is an ideal system to study questions of sensory coding, discrimination and plasticity. *C. elegans*, with its small nervous system, demonstrates surprising sophistication in its behavioral repertoire, including odor discrimination, odor adaptation and olfactory learning. Studying sensory behaviors in *C. elegans* can shed light on the molecular and neural mechanisms underlying the transformation of sensory input into behavioral output. In this overview of chemosensory coding and behavior, the basic principles will be first described in mammalian and *Drosophila* olfaction and taste systems. This will serve as a framework to compare *C. elegans* chemosensation and behavior.

A. Coding sensory information

A common principle underlying sensory coding is an organized anatomical representation in neural circuits of information contained within a stimulus. For example, one part of the information space of a visual cue is the spatial distribution of light intensity. In the vertebrate visual system, the spatial properties of the stimulus are maintained from retinal ganglion cells to higher brain areas such that neighboring regions in the retina are represented as neighboring regions in the primary visual cortex (Hubel and Wiesel, 1962). In the vertebrate auditory system, hair cells in the cochlea are activated by different frequency of sound, depending on where they lie along the organ of Corti (Hudspeth, 1989). This frequency space is transformed into a linear spatial map of hair cell activity that is repeated in the thalamus and cortex.

Chemosensory systems are also organized, but there are important differences that arise from the different nature of the stimuli; unique properties of the chemosensory system start with the diversity of receptors.

1) Chemosensory receptors

Odor and taste information space consists of the structures and concentrations of chemicals. Animals detect countless numbers of volatile and soluble chemicals, using receptors that belong to large gene families. Olfactory receptors (ORs) are encoded by hundreds of genes in the genomes of mammals and *C. elegans*, and by ~50 genes in *Drosophila* (Buck and Axel, 1991; Godfrey et al., 2004; Malnic et al., 2004; Robertson and Thomas, 2006; Vosshall et al., 2000). In vertebrates and *C. elegans*, ORs are G protein-coupled receptors (GPCRs), which couple to intracellular cAMP or cGMP second

messenger signaling pathways regulating cyclic nucleotide-gated channels (reviewed in Bargmann, 2006; Schild and Restrepo, 1998). *Drosophila* ORs are proposed to be ligand-gated cation channels that can depolarize the cell in the absence of known second messenger signaling pathways (Sato et al., 2008; Wicher et al., 2008).

Mammalian taste receptors for sugars, amino acids and bitter substances are GPCRs that come in two flavors – T1R and T2R (reviewed in Chandrashekar et al., 2006). The T1R family, which are distantly related to metabotropic glutamate receptors, has only three members (T1R1, T1R2, and T1R3) and different combinations of the three members specify different tastes: T1R3 expressed with T1R2 forms the receptor for sugars, and T1R3 expressed with T1R1 forms the receptor for amino acids (Li et al., 2002; Nelson et al., 2002; Nelson et al., 2001). On the other hand, there are ~30 T2R receptors that sense bitter compounds (Adler et al., 2000; Chandrashekar et al., 2000). These taste receptors use the lipid signaling pathway including phospholipase C and the transient receptor potential (TRP) cation channel TRPM5 (Zhang et al., 2003). *Drosophila* gustatory receptors (GRs) are related to *Drosophila* ORs and are encoded by 68 genes (Scott et al., 2001).

2) Chemosensory coding in mammals

Each olfactory sensory neuron (OSN) in mice expresses only one OR (Chess et al., 1994), which detect multiple odors, and a single odor may stimulate multiple OSNs expressing different receptors (Duchamp-Viret et al., 1999; Malnic et al., 1999; Touhara et al., 1999). The odor specificity of OSN responses is determined by that of the receptor expressed in the OSN (Araneda et al., 2000), and the tuning bandwidth of a given OSN is

concentration dependent (Malnic et al., 1999; Touhara et al., 1999). Lower concentrations of odor activate fewer and more selective sets of OSNs, and higher concentrations of odor activate more OSNs. Thus, odors are represented by a combinatorial code of OSN activity.

Anatomical segregation of chemosensory inputs is observed at the first relay downstream of the sensory neurons. In the mouse olfactory system each OSN sends an axon to the olfactory bulb (OB) and synapses onto feed-forward output neurons (mitral cells and tuft cells) and local interneurons (reviewed in(Mori et al., 1999). In the OB, projections from OSNs expressing the same receptor converge onto distinct structures called glomeruli (Ressler et al., 1994; Vassar et al., 1994). Each odor activates a set of glomeruli and a single glomerulus is activated by multiple odors (Rubin and Katz, 1999; Uchida et al., 2000; Wachowiak and Cohen, 2001). Thus, chemical space is remapped onto a spatial distribution of glomerular activity in the OB. Mitral cells and tufted cells project to numerous brain regions; the olfactory maps at these higher levels are largely uncharacterized.

In the gustatory system, T1R-expressing sensory cells represent three distinct populations: T1R1 + T1R3 (amino acids), T1R2 + T1R3 (sugars) and T1R3 alone (unknown function) (Nelson et al., 2002; Nelson et al., 2001). The T1R2/3 sugar receptor senses many different sugars, and the T1R1/3 amino acid receptor senses many L-amino acids. The T1R and T2R expressing cells define two distinct populations of cells, and a bitter-sensing gustatory cell may express multiple T2R receptors (Adler et al., 2000). Some T2R receptors are narrowly tuned to detect specific compounds while others are broadly tuned, sensing a variety of compounds (Behrens et al., 2004). Sour

sensing cells in mice represent another population of cells distinct from both sweet and bitter sensing cells (Huang et al., 2006). Therefore, taste quality such as sweet, bitter and sour are represented by segregated populations of sensory cells, but within each taste quality, there is no clear pattern of representation for individual chemicals. The mapping of taste quality beyond sensory cells is poorly understood.

3) Chemosensory coding in insects

Drosophila OSNs express one or two OR that determine odor specificity and an additional obligatory OR common to all OSNs (Larsson et al., 2004; Vosshall et al., 2000). Again, OR expression determines the receptive field of an OSN, an OR can recognize multiple odors, and multiple ORs can recognize a single odor (Hallem and Carlson, 2006). OR tuning to a large panel of odors shows a graded scale of tuning bandwidth – some receptors preferentially recognize one odor, and others recognize many (Hallem and Carlson, 2006; Schlief and Wilson, 2007).

The insect olfactory system is organized with an odotopic architecture similar to mice. OSNs are located in the antennae and send out axons to the antennal lobe (AL), where they segregate into glomeruli based on the OR expressed by each OSN (Couto et al., 2005; Fishilevich and Vosshall, 2005; Gao et al., 2000; Vosshall et al., 2000). The anatomical segregation of OSN inputs gives rise to a combinatorial code of glomerular activity that is unique to the odor (Wang et al., 2003).

Within the AL, glomeruli distribute lateral excitatory information to each other and distribute lateral inhibitory information onto sensory axon terminals (Shang et al., 2007; Wilson et al., 2004). Projection neurons integrate these signals and relay them in

anatomically precise patterns to two higher brain centers, the mushroom bodies and the lateral protocerebrum (Marin et al., 2002; Wong et al., 2002).

Sweet sensing and bitter sensing neurons in the *Drosophila* gustatory system represent distinct populations (Scott et al., 2001; Wang et al., 2004). Gr5a, a trehalose receptor, and Gr66a are two receptors that are expressed in non-overlapping sets of gustatory receptor neurons (GRN). Gr5a-expressing GRNs are required for sensing various sugars and Gr66a-expressing GRNs are required for sensing bitter compounds. Similar to the mouse gustatory system, each sensory neuron expresses multiple receptors (Jiao et al., 2007; Slone et al., 2007). Gr5a is coexpressed with a related family of six receptors, Gr64a-f. Gr5a is required for trehalose sensing, whereas Gr64a-f are required for sensing many sugars, including glucose, sucrose and trehalose.

Gustatory neurons in the proboscis project to the subesophageal ganglion (SOG) (Scott, 2005). SOG projections from sugar-sensing neurons and those from bitter-sensing neurons are distinct (Wang et al., 2004). Therefore, the GRNs represent taste quality, but not the whole chemical space, by anatomically distinct neuronal populations. There is some evidence, however, of cell-intrinsic mechanisms of discrimination between different stimuli sensed by a single sensory neuron (see below).

4) Dynamic ensemble coding

In addition to the spatial representation of chemical space, the temporal dynamics of population responses can also contribute to odor coding. The odor-evoked activity of projection neurons (PN), which are the target of OSNs in the glomerulus of insects, become synchronized in an oscillatory pattern (Laurent and Davidowitz, 1994). Odor-

specific information is entrained to the pattern of PN activity in each oscillation cycle (Wehr and Laurent, 1996), and inhibiting this oscillatory synchronization can reduce performance in behavioral discrimination tasks using structurally related odors (Stopfer et al., 1997). Oscillatory dynamics may divide olfactory information into discrete pulses to facilitate discrimination between odor quality and intensity (Stopfer et al., 2003), and allow more complex features of the stimulus to be encoded (Broome et al., 2006).

Population dynamics of mitral cells in the mouse olfactory bulb also show unique patterns of activity depending on odor identity (Bathellier et al., 2008). Here, the temporal dynamics correlate with the breathing pattern of the animal, but they also contain information about the odor at time scales shorter than the breathing rate. Therefore, a population of mitral cells encodes odor information in their dynamic pattern of activity at different time scales.

5) Anatomically segregated circuits drive distinct behaviors

Many taste stimuli reliably drive specific behaviors. Presentation of sugar promotes appetitive behaviors, such as licking in mice and proboscis extension in flies, whereas presentation of bitter compounds suppresses these behaviors (Dethier, 1976; Glendinning et al., 2002b). The enhanced licking response to sugar in mice requires the T1Rs, because T1R knockout mice are either insensitive or less sensitive to the sugars (Zhao et al., 2003). Expression of an engineered GPCR (RASSL), which is sensitive only to a synthetic ligand agonist, in the T1R expressing cells causes animals to start licking when the otherwise neutral agonist for the RASSL is presented (Zhao et al., 2003). Expression of the RASSL GPCR in the bitter-sensing cells causes agonist-dependent suppression of

licking behavior (Mueller et al., 2005). Furthermore, expression in mouse sweet-sensing cells of a human bitter receptor that recognizes a compound to which mice do not respond normally, causes animals to increase licking when the "bitter" compound is presented (Mueller et al., 2005). Therefore, the receptors themselves do not define the "value" associated with a ligand, and the taste sensory cells are hardwired to drive specific behaviors.

Drosophila also shows similar coupling of gustatory neurons to specific behaviors (Marella et al., 2006). Flies are attracted to sugars, such as trehalose and sucrose, and avoid bitter substances such as caffeine. Trehalose attraction requires gustatory neurons expressing Gr5a, and caffeine avoidance requires neurons expressing Gr66a. TRPV1 is a cation channel gated by capsaicin, which does not elicit a behavior in wild type flies. TRPV1 expression in Gr5a neurons drives attraction to capsaicin in transgenic animals, while expression in Gr66a neurons drives avoidance of capsaicin.

B. Chemosensory coding, behavior and plasticity in *C. elegans*

C. elegans has a nervous system consisting of 302 neurons (White et al., 1986) and uses about 10 % of its neurons to sense environmental stimuli (reviewed in Bargmann 2006). Chemosensory cues such as odors and salts induce attraction or avoidance behaviors (Bargmann et al., 1993; Ward, 1973) and pheromones can, in addition to attraction or avoidance, regulate development and mating (Butcher et al., 2007; Jeong et al., 2005; Srinivasan et al., 2008; White et al., 2007). These functions have, in many cases, been mapped to specific chemosensory cell types. Like the gustatory system in mice and insects, chemosensory neurons that drive attraction and avoidance behaviors in *C.*

elegans are distinct, but each sensory neuron responds to a broad range of chemical stimuli, most likely using multiple receptors. The presence of a large number of putative GPCR chemoreceptors resembles the olfactory system in mammals. Neuronal diversity contributes to sensory discrimination in *C. elegans*, a result that is analogous to the combinatorial code of odor representation.

1) *C. elegans* chemosensory receptors and neurons

i) Chemosensory receptors

The *C. elegans* genome contains about 2000 genes that encode GPCRs (reviewed in (Robertson and Thomas, 2006)). About 150 encode conserved GPCRs involved in neurotransmission, and at least 1700 encode divergent GPCRs that may be involved in chemosensation. One of the divergent GPCR gene, *odr-10*, encodes a receptor for the attractive odor diacetyl (Sengupta et al., 1996). *odr-10* mutant animals are not attracted to diacetyl, but sense other odors. Expression of *odr-10* in heterologous cells confers sensitivity to diacetyl, as well as to the anionic compounds pyruvate and citrate, which are also attractive to *C. elegans* (Zhang et al., 1997). *odr-10* mutants are able to sense pyruvate and citrate, so there are other receptors that sense these attractants and the biological importance of the *in vitro* results is not clear. *odr-10* may not be the only receptor for diacetyl because o*dr-10* mutant animals can still sense diacetyl at high concentrations (Chou et al., 2001).

Expression analysis of a subset of GPCRs showed that about half are expressed in sensory neurons; most commonly, a receptor is present in a single sensory neuron pair (Troemel et al., 1995). A targeted expression analysis from a pair of olfactory neurons

called AWB indicates that multiple receptors are expressed in these sensory neurons (Colosimo et al., 2004). Therefore, each olfactory neuron likely expresses multiple receptors, an organization that resembles the gustatory system in mice and *Drosophila*. However, neuronal diversity based on differential expression of putative chemoreceptors is also important for sensory discrimination tasks (see below)(Pierce-Shimomura et al., 2001; Wes and Bargmann, 2001). This suggests that closer analysis of receptors and their expression patterns may reveal a combinatorial code of odor representation.

ii) Olfactory and gustatory neurons

The function and specificity of sensory neurons were defined by laser ablation of individual neurons and testing for behavioral responses to various stimuli. *C. elegans* uses two pairs of sensory neurons, called AWA and AWC, to sense attractive odors and uses another three pairs, called AWB, ASH, and ADL, to sense repulsive odors (Bargmann et al., 1993; Troemel et al., 1995; Troemel et al., 1997). At least 50 odors evoke attractive or avoidance responses and the animal can discriminate between at least seven classes of attractive odors (Bargmann et al., 1993). AWA and AWC sense distinct but overlapping sets of odors: AWA senses diacetyl and pyrazine; AWC senses benzaldehyde, isoamyl alcohol, 2,3-pentanedione and butanone; both cells sense 2,4,5-trimethylthiazole (Bargmann et al., 1993; Chou et al., 2001). While there are only a few odors sensed by the avoidance neurons, the limited set suggests that these neurons also sense distinct but overlapping sets of odors: AWB senses 2-nonanone; ASH senses benzaldehyde; both ASH and ADL sense octanol (Troemel et al., 1995; Troemel et al., 1997). Tuning bandwidth of each neuron is dependent on odor concentration because

increasing concentrations of some odors increases the number of neurons that senses the odors. Benzaldehyde is sensed by AWC only at lower concentrations, but ASH and AWB sense it at high concentrations (Bargmann et al., 1993; Luo et al., 2008; Troemel et al., 1995). Diacetyl is sensed by AWA only at low concentrations, but AWC also senses it at high concentration (Chou et al., 2001).

Attractive water-soluble chemicals, or tastes, are sensed mostly by the ASE gustatory neurons, with minor contributions from a few other sensory neurons (Bargmann and Horvitz, 1991). The major soluble repellent-sensing neuron is ASH, which, in addition to sensing odors, senses many different repulsive stimuli (Kaplan and Horvitz, 1993). The receptors in ASE or ASH that sense gustatory cues are unknown.

2) Neuronal diversity contributes to chemosensory discrimination in *C. elegans*

Neuronal diversity is important for olfactory and gustatory discrimination in *C. elegans*. The putative chemoreceptor *str-2* is expressed randomly in one of the two bilaterally symmetric AWC neurons (Troemel et al., 1999). Regulation of *str-2* expression is initiated by the gap junction protein NSY-5, which creates a transient signaling network across multiple sensory neurons, including AWC (Chuang et al., 2007). Subsequently, interaction between the two AWC neurons through their axons leads to stochastic activation of calcium and MAP kinase signaling, including the MAPKKK *nsy-1*, in one of the two cells (Sagasti et al., 2001; Troemel et al., 1999). This in turn suppresses expression of *str-2* in one cell. The *str-2*-expressing AWC neuron is called AWC^{ON} and the other neuron is called AWC^{OFF}.

The two AWC neurons are functionally distinct. AWC^{ON} senses the odor butanone and AWC^{OFF} senses 2,3-pentanedione, while both cells sense benzaldehyde and isoamyl alcohol (Wes and Bargmann, 2001). Thus at least some part of odor space is transformed into distinct neuronal representations. Wild-type *C. elegans* can sense a point source of an attractive odor in the presence of uniform, saturating amounts of another odor (Bargmann et al., 1993). Between AWA and AWC neurons, animals can discriminate between seven classes of odors. Among the AWC-sensed odors, animals can discriminate between butanone and benzaldehyde. However, animals that lack the AWC^{OFF} neuron, due to either laser ablation or genetic lesions that specifically alter the AWC^{OFF} cell fate, fail to discriminate between butanone and benzaldehyde (Wes and Bargmann, 2001). They also have milder defects discriminating between butanone and isoamyl alcohol and 2,4,5-trimethylthiazole.

The ASE gustatory neurons are also asymmetric in their gene expression pattern and function. ASE neurons express at least three receptor guanylate cyclases (rGCs), *gcy-5, 6* and *7*, but *gcy-5* is expressed only in the right ASE, ASER, and *gcy-6* and *7* are expressed only in the left ASE, ASEL (Yu et al., 1997). Functionally, ASER mediates responses to Cl^-, and ASEL mediates responses to Cl^-, Na^+, and K^+ (Pierce-Shimomura et al., 2001). Discrimination between Cl^- and Na^+ is impaired in *lim-6* mutants, which have partially lost ASE left-right asymmetry such that Cl^- is sensed by ASER as well as ASEL (Pierce-Shimomura et al., 2001). Therefore, in both AWC and ASE neurons, reducing neuronal diversity reduces the animal's ability to discriminate between stimuli. This suggests that odor and taste stimuli are partially coded by distinct neuronal representations in the sensory system.

Because of the small number of olfactory neurons (two AWC and two AWA neurons for attraction) relative to the large number of attractive odors, representation of odor space through neuronal diversity alone poses a challenge. A careful examination of all pairwise combinations of five odors sensed by the two AWC neurons alone suggests that the two AWC neurons can discriminate between at least four odors and that there are cell-intrinsic mechanisms for discrimination of odors (Chou, 1998).

Evidence for cell intrinsic forms of sensory discrimination is found in other systems, but the underlying mechanisms are not well understood. In taste sensing and behavior of *Manduca sexta* larvae, animals discriminate between the bitter compounds salicin and aristolochic acid, but not between salicin and caffeine (Glendinning et al., 2002a). All three compounds are sensed by the same set of taste neurons, so coding between salicin and aristolochic acid does not require segregation of sensory inputs. Electrophysiological recordings from the sensory neurons reveal different spiking patterns between salicin and aristolochic acid, but similar patterns of activity between salicin and caffeine. Here, differential activation of a single sensory neuron by two ligands may form the basis of a neural code.

3) cGMP signaling in *C. elegans* sensory transduction

AWC olfaction uses a cGMP signaling pathway for sensory transduction, similar to vertebrate phototransduction (Stryer, 1986). *tax-2* and *tax-4*, two mutants with broad defects in sensory behavior, encode subunits of a cyclic nucleotide-gated (CNG) channel (Coburn and Bargmann, 1996; Dusenbery et al., 1975; Hedgecock and Russell, 1975; Komatsu et al., 1996). CNG channels are non-selective cation channels that are gated by

binding of the cyclic nucleotides cAMP and cGMP (reviewed in Kaupp and Seifert, 2002). *tax-2* and *tax-4* are defective for AWC chemotaxis, they are expressed in AWC among other neurons, and are localized to the cilia (Coburn and Bargmann, 1996; Komatsu et al., 1996), which are sensory structures at the tip of the dendrite in the animal's nose where transduction molecules are localized. Interestingly, *tax-2* is also enriched in the axon and it may have functions independent of primary olfactory transduction. *tax-4* homomeric channels and *tax-4/tax-2* heteromeric channels, when expressed heterologously, are gated by cGMP preferentially over cAMP (Komatsu et al., 1999; Komatsu et al., 1996).

The other components of AWC olfactory signaling are the Gα subunit *odr-3*, and the rGCs *odr-1* and *daf-11* (Birnby et al., 2000; L'Etoile and Bargmann, 2000; Roayaie et al., 1998), which are all expressed in AWC and localized to the cilia. *In vivo* Ca^{2+} imaging shows that odor inhibits AWC activity and odor removal activates AWC (Chalasani et al., 2007). In analogy to phototransduction, odor binding to a GPCR may reduce cGMP levels in the cilia (through activation of an unidentified phosphodiesterase) and close the *tax-2/tax-4* CNG channels, leading to hyperpolarization of the neuron. When odor is removed, cGMP levels rise through the action of *odr-1/daf-11*, the CNG channels may open and the neuron depolarizes.

Many but not all sensory neurons in *C. elegans* use cGMP signaling to mediate sensory behaviors. *tax-2* and *tax-4* animals are defective for salt chemotaxis, thermotaxis, aerotaxis (oxygen preference behavior), and possibly light avoidance. The ASE neurons that sense salts express rGCs, but it is not clear if they function as receptors or as part of the signal transduction pathway. At least one mutation in *gcy-5* does not

cause a chemotaxis defect (Ortiz et al., 2006). There may be functional redundancy with other rGCs expressed in ASE.

The temperature-sensing AFD neurons express *tax-2* and *tax-4*, and proper thermotaxis requires the two channel subunits as well as three partially redundant rGCs (Coburn et al., 1998; Inada et al., 2006; Komatsu et al., 1996). Electrophysiological recordings from AFD show that temperature-evoked currents are missing in the CNG channel mutants and the triple mutant for the rGCs (Ramot et al., 2008).

In aerotaxis, *C. elegans* seeks O_2 concentrations of about 10% and avoid higher or lower O_2 concentrations (Gray et al., 2004). Aerotaxis requires *tax-2* and *tax-4* CNG channels in the O_2-sensing neurons URX, AQR and PQR. These sensory neurons express soluble guanylate cyclases, which are also required for proper aerotaxis (Chang et al., 2006; Gray et al., 2004). O_2 is thought to directly regulate the activity of the cyclases.

C. elegans shows aversive response to short wavelength light in a *tax-2*-dependent manner (Ward et al., 2008). The *tax-2*-expressing neuron ASJ is one light-sensing neuron, although there may be additional cell types. Light depolarizes ASJ, indicating that signal transduction in ASJ may be different from vertebrate phototransduction or AWC olfactory transduction. Regardless, the nematode has repeatedly used the same second messenger, cGMP, to carry out vital sensory transduction roles.

4) Non-sensory roles of rGC/cGMP signaling

rGC/cGMP signaling has important roles outside of sensory transduction in vertebrates. The best-characterized vertebrate rGCs apart from retinal rGCs are the natriuretic peptide

receptors, GCA and GCB, and the receptor for heat-stable enterotoxin (STa) (reviewed in Lucas et al., 2000). GCA is a key player in regulating blood pressure and water balance in mammals. A ligand for GCA, the atrial natriuretic peptide (ANP), is released from the heart atrium into the blood when blood pressure increases (de Bold et al., 1981). ANP acts on GCA in the kidneys to induce natriuresis and diuresis, and acts in the vasculature to cause vasodilation (Holtwick et al., 2002; Kishimoto et al., 1996). Some of the effects of ANP on the kidney and most of the effects on the vasculature are mediated by PKGI, one of two cGMP-dependent protein kinases (PKGs) in the mammalian genome. Thus, GCA knockout mice are hypertensive but PKGI knockout mice are only hypertensive at young age, suggesting redundancy, and vasorelaxation induced by ANP is dependent on PKGI (Lopez et al., 1995; Pfeifer et al., 1998). The second natriuretic peptide receptor GCB, its ligand C-type natriuretic peptide (CNP) and their downstream effector PKGII are all required for proper bone development (Chikuda et al., 2004; Chusho et al., 2001; Miyazawa et al., 2002; Pfeifer et al., 1996; Tamura et al., 2004). Mutations in any one of the signaling components lead to dwarfism due to lack of long bone growth. The third rGC, GCC, is expressed in the intestine where it regulates salt absorption and fluid secretion (Lucas et al., 2000). PKGII also acts downstream of GCC in the intestine (Pfeifer et al., 1996).

A recent survey of all rGCs encoded in the *C. elegans* genome shows that many rGCs are expressed in sensory neurons, but some are expressed in non-neuronal tissues, such as the intestine, hypodermis, excretory canal and gland cells (Ortiz et al., 2006). These cells and tissues are thought to be involved in osmoregulatory functions in *C. elegans* and other nematodes. The intestine and hypodermis are in direct contact with the

extra-organismal environment, and are potential sites of fluid exchange (Fuse et al., 1993). The excretory canal and gland cells are part of the "kidney" of *C. elegans*. Laser ablation of the canal cell causes animals to accumulate fluid and leads to death (Nelson and Riddle, 1984). Therefore, rGCs may have functions in regulating water homeostasis in *C. elegans* as well.

5) From stimulus to behavior

i) Quantitative analysis of sensory behavior

Olfactory and gustatory stimuli drive innate attraction or avoidance behaviors in *C. elegans*. Quantitative analyses of dynamic locomotory patterns reveals computations performed by this small nervous system to convert stimulus to behavior. The trajectory of *C. elegans* locomotion on an agar surface consists of alternating periods of low angular velocity, called runs, and periods of high angular velocity, called turns or pirouettes (Croll, 1975; Pierce-Shimomura et al., 1999). In a gradient of attractive salts, animals tend to suppress turns when the concentration gradient is increasing while they increase turns when the concentration gradient is decreasing (Dusenbery, 1980; Pierce-Shimomura et al., 1999). Closer analysis of turning events showed that on average, turns were not directed – animals were equally likely to be heading in the wrong direction (ie. down the gradient) as in the right direction (ie. up the gradient) as a result of the turn. These properties of nematode motion resemble the biased random-walk mechanism of bacterial chemotaxis (Berg and Brown, 1972). Modeling of nematode turning behavior suggests that the biased random walk mechanism is sufficient to direct migration of animals up a concentration gradient of an attractant (Pierce-Shimomura et al., 1999). This conclusion

also suggested that *C. elegans* measures the gradient by temporal integration of attractant cues.

Direct measurement of *C. elegans* turning behavior in response to temporal shifts in stimulus has been carried out for many sensory modalities, including salts, temperature and odor (Chalasani et al., 2007; Clark et al., 2007; Luo et al., 2008; Miller et al., 2005; Suzuki et al., 2008; Zariwala et al., 2003). In all cases, the animal's turning frequency is modulated to reflect the time derivative of the stimulus intensity (concentration of salts and odors for chemotaxis, temperature for thermotaxis). In general, for an attractive stimulus, turning frequency decreases when the stimulus gradient is positive, and turning frequency increases when the gradient is negative. These patterns of turn modulation are dependent on functional sensory neurons: ASE for salts, AFD for temperature, and AWC for odors. Based on the time course of the behaviors, measurement of stimulus intensity seems to extend 15-30 seconds into the past.

Turning behavior in *C. elegans* consists of a stereotyped series of motion patterns classified as reversals or omega bends (Croll, 1975; Gray et al., 2005). The length of a reversal can vary, and longer reversals tend to end with an omega bend (Gray et al., 2005). An omega bend consists of a forward-movement accompanied by a deep bending of the body such that the head touches the tail end of the body, forming the shape of an Ω. As a result, omega bends result in relatively large changes in direction. Animals can also perform omega bends independently of reversals.

ii) Chemosensory neurons regulate turning behavior

The AWC olfactory neurons are major contributors to the basal frequency of turning. Laser ablation of AWC largely abolishes spontaneous turning events that normally occur in the absence of food (Gray et al., 2005; Tsalik and Hobert, 2003; Wakabayashi et al., 2004). AWC activity, measured by *in vivo* Ca^{2+} imaging, is inhibited by food or odor and increases when these stimuli are removed (Chalasani et al., 2007), similar to the off response observed in vertebrate photoreceptors (Stryer, 1986). The response to odor or food removal is transient and the response peaks ~10 seconds after the shift in stimulus. This suggests that the neuron responds primarily to the downshift in the stimulus and not the absolute level. AWC uses a glutamate transmitter, as do vertebrate photoreceptors, to regulate activity of its downstream synaptic partners AIB and AIY (Chalasani et al., 2007). AWC activates AIB, which promotes turning, through the ionotropic glutamate receptor GLR-1, and AWC inhibits AIY, which suppresses turning, through a glutamate-gated chloride channel, GLC-3 (Chalasani et al., 2007; Gray et al., 2005),. Therefore, the physiological response of AWC to changes in odor concentration correlates with the turning response.

Even though the AWC^{ON} and AWC^{OFF} show functional differentiation in terms of odor specificity, their odor-evoked activity is similar (ie. inhibition by odor, stimulation by odor removal)(Chalasani et al., 2007). By contrast, salt evokes opposite patterns of activity in ASEL and ASER neurons. ASER is similar to the AWCs and responds to a downshift in salt concentration with a Ca^{2+} transient, but ASEL responds with a Ca^{2+} transient to an upshift in salt concentration (Suzuki et al., 2008). Consistent with the behavioral analysis suggesting distinct sensory specificities of ASER and ASEL, ASEL responds weakly to an upshift in both Na^{+} and Cl^{-}, while ASER responds strongly to a

downshift in Cl^- but does not respond to changes in Na^+. Activation of ASER causes animals to increase turning, whereas activation of ASEL causes animals suppress turns (Suzuki et al., 2008). Thus, the salt-sensing system is set up to sense both an increase and a decrease in salt concentration with a positive response in either one ASE neuron, which drives the appropriate behavior. The major synaptic targets of the left and right ASE neurons are similar, so the neural basis for generating the same behavior from opposite activities may lie in intrinsic differences in ASEL/ASER synaptic signaling.

6) Plasticity of chemosensory behaviors

i) Olfactory adaptation

Even with its small, hardwired nervous system, *C. elegans* shows a remarkable degree of plasticity in behavior, including adaptation, sensitization, and associative learning (Colbert and Bargmann, 1995; Tomioka et al., 2006; Torayama et al., 2007; Zhang et al., 2005). In olfactory adaptation, animals exposed to high levels of an odor in the absence of food reduce their attraction to that odor (Colbert and Bargmann, 1995). Adaptation is transient because sensitivity is regained when odor is removed from adapted animals, and it is mostly odor-specific in that conditioning with one odor does not cause adaptation to another odor, even when both are sensed by the same neurons. Mutants defective for AWC olfactory adaptation include the cGMP-dependent protein kinase, *egl-4*, the transient receptor potential vanilloid (TRPV) channel *osm-9*, the arrestin homolog *arr-1*, and the uncloned mutant *adp-1* (Colbert and Bargmann, 1995; L'Etoile et al., 2002; Palmitessa et al., 2005). It is not known where *osm-9* acts for adaptation even though it is expressed in AWC. *egl-4* and *arr-1* are specifically required in AWC for adaptation.

β-arrestin has multiple roles in signaling downstream of GPCRs (reviewed in (Lefkowitz and Shenoy, 2005). The classical role of β-arrestin is binding to an activated GPCR after phosphorylation by GPCR kinase 2. This leads to termination of signaling through the GPCR and subsequent internalization of the receptor. It is now recognized that β-arrestin has a wider role in signaling, as a scaffolding protein that brings together mitogen activated kinases and other signaling molecules (Lefkowitz and Shenoy, 2005). Its role in downregulation of GPCR signaling is consistent with the inability of *C. elegans arr-1* mutants to adapt to odors, but it remains to be seen what mechanism is used in AWC olfactory adaptation.

egl-4 null mutants are defective for chemotaxis to AWC odors except for benzaldehyde, and they have an adaptation defect for benzaldehyde (L'Etoile et al., 2002). An *egl-4* hypomorph mutant with mutations in the 3' untranslated region (UTR) is proficient for AWC chemotaxis but is defective for adaptation to all AWC odors. Thus proper regulation of *egl-4* expression may be important for odor adaptation. Genetic analysis of *egl-4* suggests that the time course of adaptation can be separated genetically into a short and a long component. Short-term adaptation, which is weak and occurs after 30 minutes of conditioning, requires a putative *egl-4* phosphorylation site on *tax-2*, while long-term adaptation, occurring after one hour of conditioning, leads to strong reduction in attraction and requires a nuclear localization signal in *egl-4* (L'Etoile et al., 2002). Thus, adaptation is a dynamic response to continuous odor stimulation and may reflect the changing value associated with the conditioning odor.

ii) Olfactory sensitization

Food is an important modifier of olfactory plasticity. Animals adapt to odors when conditioned in the absence of food, and can also become sensitized to odors that are paired with food (Torayama et al., 2007). When animals are exposed to the AWC^{ON}-sensed odor butanone in the presence of food, their chemotaxis to butanone improves. The sensitization effect occurs rapidly, in as little as 30 minutes, and lasts for a few hours. Sensitization appears odor specific, but the full scope of the effect awaits further characterization. Molecularly, a specific class of cilia-defective mutants belonging to the Bardet-Biedl syndrome (BBS) genes is defective for butanone sensitization (Torayama 2007). At least one BBS gene acts in the AWC^{ON} neuron to mediate sensitization, implicating a cell-intrinsic contribution to sensitization (Torayama et al., 2007). These genes are required for specific aspects of ciliary transport and can be classified separately from other classes of cilia-defective mutants, which do not have a sensitization defect (Blacque et al., 2004; Ou et al., 2007; Torayama et al., 2007). Thus, olfactory plasticity is dynamic in both positive and negative directions, and is regulated by cell-intrinsic signaling pathways.

iii) Gustatory plasticity

Gustatory behavior in *C. elegans* is also altered by context-dependent experience (Hukema et al., 2006; Tomioka et al., 2006). When animals are starved in the absence of salt conditioning, they improve their chemotaxis to salt (Tomioka et al., 2006). However, starvation in the presence of salt causes animals to start avoiding salt. Salt-induced plasticity is generated in part by the ASER neuron, which uses an insulin/PI 3-kinase signaling pathway to regulate synaptic output. Mutations in insulin/*daf-2* or PI 3-

kinase/*age-1* abolishes gustatory plasticity, and the PTEN phosphatase/*daf-18*, which anatagonizes PI 3 kinase signaling, is defective for salt chemotaxis. Salt-evoked Ca^{2+} responses in ASER is normal in PTEN phosphatase/*daf-18* mutant animals, indicating that primary signal transduction is intact in the mutant. Because the *daf-18* chemotaxis defect can be rescued by expressing a wild-type copy of *daf-18* specifically in ASER, the defect must lie between primary signal transduction and downstream synaptic partners.

Salt avoidance behavior after salt conditioning requires sensory neurons other than ASE (Hukema et al., 2006). Genetic analysis suggests that sensory neurons that mediate avoidance behaviors, such as the polymodal nociceptive neuron ASH and hyperoxia avoidance neuron URX, are also required for salt avoidance after conditioning. Therefore, the full range of gustatory plasticity is generated by coordinated activity of attraction driving and avoidance driving gustatory neurons.

iv) Pathogen learning

C. elegans uses olfactory plasticity to change its preference between pathogenic and non-pathogenic bacteria (Zhang et al., 2005). Some strains of the soil bacteria *Pseudomonas aeruginosa* can infect and kill *C. elegans*. Animals grown on non-pathogenic *Escherichia coli* will chemotax equally well to *E. coli* and to the pathogenic *Pseudomonas* when given a choice between the two. However, if animals are grown on *Pseudomonas* and then given a choice between the two, they will choose *E. coli* over *Pseudomonas*. The switch can happen after four hours exposure to the pathogenic bacteria, and another pathogenic bacteria, *Serratia marcescens*, has the same effect as *Pseudomonas*. Pathogen learning requires serotonin signaling acting on interneurons. It

is not known which sensory neurons mediates the attraction (or avoidance) of these particular bacteria, but it is likely that the main olfactory neurons (AWA, AWC, and AWB) are involved because the assay requires long-distance sensing of bacterial cues. A surfactant produced by *Serratia*, serrawettin W2, is sensed by AWC and drives avoidance behaviors in *C. elegans* (Pradel et al., 2007). However, serrawettin W2 avoidance behavior is not required for pathogen learning. In summary, changes in internal states, such as infection, can switch the behavioral response of *C. elegans* to bacterial odor cues.

v) Chemosensory plasticity in mammals and insects

Adaptation, sensitization, and associative learning are observed in mammals and insect olfactory systems as well as in *C. elegans*. For the most part, the relationship between sensory signaling pathways and behavior has not been established in these more complex systems. Instead, studies of active brain areas have been used to localize sites of learning. In the fly, learning can be observed in functional changes as early as the antennal lobe (Sachse et al., 2007; Yu et al., 2004), and also in mushroom bodies (MBs) (Yu et al., 2006), which are essential for olfactory leaning (de Belle and Heisenberg, 1994; Heisenberg et al., 1985). In the MBs, cAMP signaling initiates the functional changes that cause changes in odor preference (Yu et al., 2006). In mammals, olfactory plasticity has been observed physiologically in OSNs, where regulation of CNGs has an important role in olfactory adaptation (Munger et al., 2001), and in the OB (Fletcher and Wilson, 2003), which is rich in modulatory inputs (Gomez et al., 2005; Kiselycznyk et al., 2006).

References

Adler, E., Hoon, M. A., Mueller, K. L., Chandrashekar, J., Ryba, N. J., and Zuker, C. S. (2000). A novel family of mammalian taste receptors. Cell *100*, 693-702.

Araneda, R. C., Kini, A. D., and Firestein, S. (2000). The molecular receptive range of an odorant receptor. Nat Neurosci *3*, 1248-1255.

Bargmann, C. I., Chemosensation in *C. elegans* (October 25, 2006), *WormBook*, ed. The *C. elegans* Research Community, WormBook, 10.1895/wormbook.1.123.1, http://www.wormbook.org

Bargmann, C. I., Hartwieg, E., and Horvitz, H. R. (1993). Odorant-selective genes and neurons mediate olfaction in *C. elegans*. Cell *74*, 515-527.

Bargmann, C. I., and Horvitz, H. R. (1991). Chemosensory neurons with overlapping functions direct chemotaxis to multiple chemicals in *C. elegans*. Neuron *7*, 729-742.

Bathellier, B., Buhl, D. L., Accolla, R., and Carleton, A. (2008). Dynamic ensemble odor coding in the mammalian olfactory bulb: sensory information at different timescales. Neuron *57*, 586-598.

Behrens, M., Brockhoff, A., Kuhn, C., Bufe, B., Winnig, M., and Meyerhof, W. (2004). The human taste receptor hTAS2R14 responds to a variety of different bitter compounds. Biochem Biophys Res Commun *319*, 479-485.

Berg, H. C., and Brown, D. A. (1972). Chemotaxis in *Escherichia coli* analysed by three-dimensional tracking. Nature *239*, 500-504.

Birnby, D. A., Link, E. M., Vowels, J. J., Tian, H., Colacurcio, P. L., and Thomas, J. H. (2000). A transmembrane guanylyl cyclase (DAF-11) and Hsp90 (DAF-21) regulate a

common set of chemosensory behaviors in *Caenorhabditis elegans*. Genetics *155*, 85-104.

Blacque, O. E., Reardon, M. J., Li, C., McCarthy, J., Mahjoub, M. R., Ansley, S. J., Badano, J. L., Mah, A. K., Beales, P. L., Davidson, W. S.*, et al.* (2004). Loss of *C. elegans* BBS-7 and BBS-8 protein function results in cilia defects and compromised intraflagellar transport. Genes Dev *18*, 1630-1642.

Broome, B. M., Jayaraman, V., and Laurent, G. (2006). Encoding and decoding of overlapping odor sequences. Neuron *51*, 467-482.

Buck, L., and Axel, R. (1991). A novel multigene family may encode odorant receptors: a molecular basis for odor recognition. Cell *65*, 175-187.

Butcher, R. A., Fujita, M., Schroeder, F. C., and Clardy, J. (2007). Small-molecule pheromones that control dauer development in *Caenorhabditis elegans*. Nat Chem Biol *3*, 420-422.

Chalasani, S. H., Chronis, N., Tsunozaki, M., Gray, J. M., Ramot, D., Goodman, M. B., and Bargmann, C. I. (2007). Dissecting a circuit for olfactory behaviour in *Caenorhabditis elegans*. Nature *450*, 63-70.

Chandrashekar, J., Hoon, M. A., Ryba, N. J., and Zuker, C. S. (2006). The receptors and cells for mammalian taste. Nature *444*, 288-294.

Chandrashekar, J., Mueller, K. L., Hoon, M. A., Adler, E., Feng, L., Guo, W., Zuker, C. S., and Ryba, N. J. (2000). T2Rs function as bitter taste receptors. Cell *100*, 703-711.

Chang, A. J., Chronis, N., Karow, D. S., Marletta, M. A., and Bargmann, C. I. (2006). A distributed chemosensory circuit for oxygen preference in *C. elegans*. PLoS Biol *4*, e274.

Chess, A., Simon, I., Cedar, H., and Axel, R. (1994). Allelic inactivation regulates olfactory receptor gene expression. Cell *78*, 823-834.

Chikuda, H., Kugimiya, F., Hoshi, K., Ikeda, T., Ogasawara, T., Shimoaka, T., Kawano, H., Kamekura, S., Tsuchida, A., Yokoi, N.*, et al.* (2004). Cyclic GMP-dependent protein kinase II is a molecular switch from proliferation to hypertrophic differentiation of chondrocytes. Genes Dev *18*, 2418-2429.

Chou, J., H. (1998). Molecular Genetic Analysis of Chemosensroy Behaviors in *C. elegans*. Ph. D. dissertation, University of California at San Francisco.

Chou, J. H., Bargmann, C. I., and Sengupta, P. (2001). The *Caenorhabditis elegans odr-2* gene encodes a novel Ly-6-related protein required for olfaction. Genetics *157*, 211-224.

Chuang, C. F., Vanhoven, M. K., Fetter, R. D., Verselis, V. K., and Bargmann, C. I. (2007). An innexin-dependent cell network establishes left-right neuronal asymmetry in *C. elegans*. Cell *129*, 787-799.

Chusho, H., Tamura, N., Ogawa, Y., Yasoda, A., Suda, M., Miyazawa, T., Nakamura, K., Nakao, K., Kurihara, T., Komatsu, Y.*, et al.* (2001). Dwarfism and early death in mice lacking C-type natriuretic peptide. Proc Natl Acad Sci U S A *98*, 4016-4021.

Clark, D. A., Gabel, C. V., Lee, T. M., and Samuel, A. D. (2007). Short-term adaptation and temporal processing in the cryophilic response of *Caenorhabditis elegans*. J Neurophysiol *97*, 1903-1910.

Coburn, C. M., and Bargmann, C. I. (1996). A putative cyclic nucleotide-gated channel is required for sensory development and function in *C. elegans*. Neuron *17*, 695-706.

Coburn, C. M., Mori, I., Ohshima, Y., and Bargmann, C. I. (1998). A cyclic nucleotide-gated channel inhibits sensory axon outgrowth in larval and adult *Caenorhabditis*

elegans: a distinct pathway for maintenance of sensory axon structure. Development *125*, 249-258.

Colbert, H. A., and Bargmann, C. I. (1995). Odorant-specific adaptation pathways generate olfactory plasticity in *C. elegans*. Neuron *14*, 803-812.

Colosimo, M. E., Brown, A., Mukhopadhyay, S., Gabel, C., Lanjuin, A. E., Samuel, A. D., and Sengupta, P. (2004). Identification of thermosensory and olfactory neuron-specific genes via expression profiling of single neuron types. Curr Biol *14*, 2245-2251.

Couto, A., Alenius, M., and Dickson, B. J. (2005). Molecular, anatomical, and functional organization of the *Drosophila* olfactory system. Curr Biol *15*, 1535-1547.

Croll, N. A. (1975) Components and patterns in the behavior of the nematode *Caenorhabditis elegans*. J Zool *176*:159 –176.

de Belle, J. S., and Heisenberg, M. (1994). Associative odor learning in *Drosophila* abolished by chemical ablation of mushroom bodies. Science *263*, 692-695.

de Bold, A. J., Borenstein, H. B., Veress, A. T., and Sonnenberg, H. (1981). A rapid and potent natriuretic response to intravenous injection of atrial myocardial extract in rats. Life Sci *28*, 89-94.

Dethier, V.G. (1976). The Hungry Fly (Cambridge, MA: Harvard University Press).

Duchamp-Viret, P., Chaput, M. A., and Duchamp, A. (1999). Odor response properties of rat olfactory receptor neurons. Science *284*, 2171-2174.

Dusenbery, D. B. (1980) Responses of the nematode *Caenorhabditis elegans* to controlled chemical stimulation. J Comp Physiol [A] *136*:327–331.

Dusenbery, D. B., Sheridan, R. E., and Russell, R. L. (1975). Chemotaxis-defective mutants of the nematode *Caenorhabditis elegans*. Genetics *80*, 297-309.

Fishilevich, E., and Vosshall, L. B. (2005). Genetic and functional subdivision of the *Drosophila* antennal lobe. Curr Biol *15*, 1548-1553.

Fletcher, M. L., and Wilson, D. A. (2003). Olfactory bulb mitral-tufted cell plasticity: odorant-specific tuning reflects previous odorant exposure. J Neurosci *23*, 6946-6955.

Fuse, M., Davey, K. G., and Sommerville, R. I. (1993). Osmoregulation in the parasitic nematode *Pseudoterranova decipiens*. J Exp Biol *175*, 127-142.

Gao, Q., Yuan, B., and Chess, A. (2000). Convergent projections of *Drosophila* olfactory neurons to specific glomeruli in the antennal lobe. Nat Neurosci *3*, 780-785.

Glendinning, J. I., Davis, A., and Ramaswamy, S. (2002a). Contribution of different taste cells and signaling pathways to the discrimination of "bitter" taste stimuli by an insect. J Neurosci *22*, 7281-7287.

Glendinning, J. I., Gresack, J., and Spector, A. C. (2002b). A high-throughput screening procedure for identifying mice with aberrant taste and oromotor function. Chem Senses *27*, 461-474.

Godfrey, P. A., Malnic, B., and Buck, L. B. (2004). The mouse olfactory receptor gene family. Proc Natl Acad Sci U S A *101*, 2156-2161.

Gomez, C., Brinon, J. G., Barbado, M. V., Weruaga, E., Valero, J., and Alonso, J. R. (2005). Heterogeneous targeting of centrifugal inputs to the glomerular layer of the main olfactory bulb. J Chem Neuroanat *29*, 238-254.

Gray, J. M., Hill, J. J., and Bargmann, C. I. (2005). A circuit for navigation in *Caenorhabditis elegans*. Proc Natl Acad Sci U S A *102*, 3184-3191.

Gray, J. M., Karow, D. S., Lu, H., Chang, A. J., Chang, J. S., Ellis, R. E., Marletta, M. A., and Bargmann, C. I. (2004). Oxygen sensation and social feeding mediated by a *C. elegans* guanylate cyclase homologue. Nature *430*, 317-322.

Hallem, E. A., and Carlson, J. R. (2006). Coding of odors by a receptor repertoire. Cell *125*, 143-160.

Hedgecock, E. M., and Russell, R. L. (1975). Normal and mutant thermotaxis in the nematode *Caenorhabditis elegans*. Proc Natl Acad Sci U S A *72*, 4061-4065.

Heisenberg, M., Borst, A., Wagner, S., and Byers, D. (1985). *Drosophila* mushroom body mutants are deficient in olfactory learning. J Neurogenet *2*, 1-30.

Holtwick, R., Gotthardt, M., Skryabin, B., Steinmetz, M., Potthast, R., Zetsche, B., Hammer, R. E., Herz, J., and Kuhn, M. (2002). Smooth muscle-selective deletion of guanylyl cyclase-A prevents the acute but not chronic effects of ANP on blood pressure. Proc Natl Acad Sci U S A *99*, 7142-7147.

Huang, A. L., Chen, X., Hoon, M. A., Chandrashekar, J., Guo, W., Trankner, D., Ryba, N. J., and Zuker, C. S. (2006). The cells and logic for mammalian sour taste detection. Nature *442*, 934-938.

Hubel, D. H., and Wiesel, T. N. (1962). Receptive fields, binocular interaction and functional architecture in the cat's visual cortex. J Physiol *160*, 106-154.

Hudspeth, A. J. (1989). How the ear's works work. Nature *341*, 397-404.

Hukema, R. K., Rademakers, S., Dekkers, M. P., Burghoorn, J., and Jansen, G. (2006). Antagonistic sensory cues generate gustatory plasticity in *Caenorhabditis elegans*. Embo J *25*, 312-322.

Inada, H., Ito, H., Satterlee, J., Sengupta, P., Matsumoto, K., and Mori, I. (2006). Identification of guanylyl cyclases that function in thermosensory neurons of *Caenorhabditis elegans*. Genetics *172*, 2239-2252.

Jeong, P. Y., Jung, M., Yim, Y. H., Kim, H., Park, M., Hong, E., Lee, W., Kim, Y. H., Kim, K., and Paik, Y. K. (2005). Chemical structure and biological activity of the *Caenorhabditis elegans* dauer-inducing pheromone. Nature *433*, 541-545.

Jiao, Y., Moon, S. J., and Montell, C. (2007). A *Drosophila* gustatory receptor required for the responses to sucrose, glucose, and maltose identified by mRNA tagging. Proc Natl Acad Sci U S A *104*, 14110-14115.

Kaplan, J. M., and Horvitz, H. R. (1993). A dual mechanosensory and chemosensory neuron in *Caenorhabditis elegans*. Proc Natl Acad Sci U S A *90*, 2227-2231.

Kaupp, U. B., and Seifert, R. (2002). Cyclic nucleotide-gated ion channels. Physiol Rev *82*, 769-824.

Kiselycznyk, C. L., Zhang, S., and Linster, C. (2006). Role of centrifugal projections to the olfactory bulb in olfactory processing. Learn Mem *13*, 575-579.

Kishimoto, I., Dubois, S. K., and Garbers, D. L. (1996). The heart communicates with the kidney exclusively through the guanylyl cyclase-A receptor: acute handling of sodium and water in response to volume expansion. Proc Natl Acad Sci U S A *93*, 6215-6219.

Komatsu, H., Jin, Y. H., L'Etoile, N., Mori, I., Bargmann, C. I., Akaike, N., and Ohshima, Y. (1999). Functional reconstitution of a heteromeric cyclic nucleotide-gated channel of *Caenorhabditis elegans* in cultured cells. Brain Res *821*, 160-168.

Komatsu, H., Mori, I., Rhee, J. S., Akaike, N., and Ohshima, Y. (1996). Mutations in a cyclic nucleotide-gated channel lead to abnormal thermosensation and chemosensation in *C. elegans*. Neuron *17*, 707-718.

L'Etoile, N. D., and Bargmann, C. I. (2000). Olfaction and odor discrimination are mediated by the *C. elegans* guanylyl cyclase ODR-1. Neuron *25*, 575-586.

L'Etoile, N. D., Coburn, C. M., Eastham, J., Kistler, A., Gallegos, G., and Bargmann, C. I. (2002). The cyclic GMP-dependent protein kinase EGL-4 regulates olfactory adaptation in *C. elegans*. Neuron *36*, 1079-1089.

Larsson, M. C., Domingos, A. I., Jones, W. D., Chiappe, M. E., Amrein, H., and Vosshall, L. B. (2004). Or83b encodes a broadly expressed odorant receptor essential for *Drosophila* olfaction. Neuron *43*, 703-714.

Laurent, G., and Davidowitz, H. (1994). Encoding of Olfactory Information with Oscillating Neural Assemblies. Science *265*, 1872-1875.

Lefkowitz, R. J., and Shenoy, S. K. (2005). Transduction of receptor signals by beta-arrestins. Science *308*, 512-517.

Li, X., Staszewski, L., Xu, H., Durick, K., Zoller, M., and Adler, E. (2002). Human receptors for sweet and umami taste. Proc Natl Acad Sci U S A *99*, 4692-4696.

Lopez, M. J., Wong, S. K., Kishimoto, I., Dubois, S., Mach, V., Friesen, J., Garbers, D. L., and Beuve, A. (1995). Salt-resistant hypertension in mice lacking the guanylyl cyclase-A receptor for atrial natriuretic peptide. Nature *378*, 65-68.

Lucas, K. A., Pitari, G. M., Kazerounian, S., Ruiz-Stewart, I., Park, J., Schulz, S., Chepenik, K. P., and Waldman, S. A. (2000). Guanylyl cyclases and signaling by cyclic GMP. Pharmacol Rev *52*, 375-414.

Luo, L., Gabel, C. V., Ha, H. I., Zhang, Y., and Samuel, A. D. (2008). Olfactory behavior of swimming *C. elegans* analyzed by measuring motile responses to temporal variations of odorants. J Neurophysiol.

Malnic, B., Godfrey, P. A., and Buck, L. B. (2004). The human olfactory receptor gene family. Proc Natl Acad Sci U S A *101*, 2584-2589.

Malnic, B., Hirono, J., Sato, T., and Buck, L. B. (1999). Combinatorial receptor codes for odors. Cell *96*, 713-723.

Marella, S., Fischler, W., Kong, P., Asgarian, S., Rueckert, E., and Scott, K. (2006). Imaging taste responses in the fly brain reveals a functional map of taste category and behavior. Neuron *49*, 285-295.

Marin, E. C., Jefferis, G. S., Komiyama, T., Zhu, H., and Luo, L. (2002). Representation of the glomerular olfactory map in the *Drosophila* brain. Cell *109*, 243-255.

Miller, A. C., Thiele, T. R., Faumont, S., Moravec, M. L., and Lockery, S. R. (2005). Step-response analysis of chemotaxis in *Caenorhabditis elegans*. J Neurosci *25*, 3369-3378.

Miyazawa, T., Ogawa, Y., Chusho, H., Yasoda, A., Tamura, N., Komatsu, Y., Pfeifer, A., Hofmann, F., and Nakao, K. (2002). Cyclic GMP-dependent protein kinase II plays a critical role in C-type natriuretic peptide-mediated endochondral ossification. Endocrinology *143*, 3604-3610.

Mori, K., Nagao, H., and Yoshihara, Y. (1999). The olfactory bulb: coding and processing of odor molecule information. Science *286*, 711-715.

Mueller, K. L., Hoon, M. A., Erlenbach, I., Chandrashekar, J., Zuker, C. S., and Ryba, N. J. (2005). The receptors and coding logic for bitter taste. Nature *434*, 225-229.

Munger, S. D., Lane, A. P., Zhong, H., Leinders-Zufall, T., Yau, K. W., Zufall, F., and Reed, R. R. (2001). Central role of the CNGA4 channel subunit in Ca2+-calmodulin-dependent odor adaptation. Science *294*, 2172-2175.

Nelson, F. K., and Riddle, D. L. (1984). Functional study of the *Caenorhabditis elegans* secretory-excretory system using laser microsurgery. J Exp Zool *231*, 45-56.

Nelson, G., Chandrashekar, J., Hoon, M. A., Feng, L., Zhao, G., Ryba, N. J., and Zuker, C. S. (2002). An amino-acid taste receptor. Nature *416*, 199-202.

Nelson, G., Hoon, M. A., Chandrashekar, J., Zhang, Y., Ryba, N. J., and Zuker, C. S. (2001). Mammalian sweet taste receptors. Cell *106*, 381-390.

Ortiz, C. O., Etchberger, J. F., Posy, S. L., Frokjaer-Jensen, C., Lockery, S., Honig, B., and Hobert, O. (2006). Searching for neuronal left/right asymmetry: genomewide analysis of nematode receptor-type guanylyl cyclases. Genetics *173*, 131-149.

Ou, G., Koga, M., Blacque, O. E., Murayama, T., Ohshima, Y., Schafer, J. C., Li, C., Yoder, B. K., Leroux, M. R., and Scholey, J. M. (2007). Sensory ciliogenesis in *Caenorhabditis elegans*: assignment of IFT components into distinct modules based on transport and phenotypic profiles. Mol Biol Cell *18*, 1554-1569.

Palmitessa, A., Hess, H. A., Bany, I. A., Kim, Y. M., Koelle, M. R., and Benovic, J. L. (2005). *Caenorhabditis elegans* arrestin regulates neural G protein signaling and olfactory adaptation and recovery. J Biol Chem *280*, 24649-24662.

Pfeifer, A., Aszodi, A., Seidler, U., Ruth, P., Hofmann, F., and Fassler, R. (1996). Intestinal secretory defects and dwarfism in mice lacking cGMP-dependent protein kinase II. Science *274*, 2082-2086.

Pfeifer, A., Klatt, P., Massberg, S., Ny, L., Sausbier, M., Hirneiss, C., Wang, G. X., Korth, M., Aszodi, A., Andersson, K. E*., et al.* (1998). Defective smooth muscle regulation in cGMP kinase I-deficient mice. Embo J *17*, 3045-3051.

Pierce-Shimomura, J. T., Faumont, S., Gaston, M. R., Pearson, B. J., and Lockery, S. R. (2001). The homeobox gene *lim-6* is required for distinct chemosensory representations in *C. elegans*. Nature *410*, 694-698.

Pierce-Shimomura, J. T., Morse, T. M., and Lockery, S. R. (1999). The fundamental role of pirouettes in *Caenorhabditis elegans* chemotaxis. J Neurosci *19*, 9557-9569.

Pradel, E., Zhang, Y., Pujol, N., Matsuyama, T., Bargmann, C. I., and Ewbank, J. J. (2007). Detection and avoidance of a natural product from the pathogenic bacterium Serratia marcescens by *Caenorhabditis elegans*. Proc Natl Acad Sci U S A *104*, 2295-2300.

Ramot, D., Macinnis, B. L., and Goodman, M. B. (2008). Bidirectional temperature-sensing by a single thermosensory neuron in *C. elegans*. Nat Neurosci.

Ressler, K. J., Sullivan, S. L., and Buck, L. B. (1994). Information coding in the olfactory system: evidence for a stereotyped and highly organized epitope map in the olfactory bulb. Cell *79*, 1245-1255.

Roayaie, K., Crump, J. G., Sagasti, A., and Bargmann, C. I. (1998). The G alpha protein ODR-3 mediates olfactory and nociceptive function and controls cilium morphogenesis in *C. elegans* olfactory neurons. Neuron *20*, 55-67.

Robertson, H. M., and Thomas, J. H., The putative chemoreceptor families of *C. elegans* (January 06, 2006), *WormBook*, ed. The *C. elegans* Research Community, WormBook, 10.1895/wormbook.1.66.1, http://www.wormbook.org.

Rubin, B. D., and Katz, L. C. (1999). Optical imaging of odorant representations in the mammalian olfactory bulb. Neuron *23*, 499-511.

Sachse, S., Rueckert, E., Keller, A., Okada, R., Tanaka, N. K., Ito, K., and Vosshall, L. B. (2007). Activity-dependent plasticity in an olfactory circuit. Neuron *56*, 838-850.

Sagasti, A., Hisamoto, N., Hyodo, J., Tanaka-Hino, M., Matsumoto, K., and Bargmann, C. I. (2001). The CaMKII UNC-43 activates the MAPKKK NSY-1 to execute a lateral signaling decision required for asymmetric olfactory neuron fates. Cell *105*, 221-232.

Sato, K., Pellegrino, M., Nakagawa, T., Nakagawa, T., Vosshall, L. B., and Touhara, K. (2008). Insect olfactory receptors are heteromeric ligand-gated ion channels. Nature *452*, 1002-1006.

Schild, D., and Restrepo, D. (1998). Transduction mechanisms in vertebrate olfactory receptor cells. Physiol Rev *78*, 429-466.

Schlief, M. L., and Wilson, R. I. (2007). Olfactory processing and behavior downstream from highly selective receptor neurons. Nat Neurosci *10*, 623-630.

Scott, K. (2005). Taste recognition: food for thought. Neuron *48*, 455-464.

Scott, K., Brady, R., Jr., Cravchik, A., Morozov, P., Rzhetsky, A., Zuker, C., and Axel, R. (2001). A chemosensory gene family encoding candidate gustatory and olfactory receptors in *Drosophila*. Cell *104*, 661-673.

Sengupta, P., Chou, J. H., and Bargmann, C. I. (1996). *odr-10* encodes a seven transmembrane domain olfactory receptor required for responses to the odorant diacetyl. Cell *84*, 899-909.

Shang, Y., Claridge-Chang, A., Sjulson, L., Pypaert, M., and Miesenbock, G. (2007). Excitatory local circuits and their implications for olfactory processing in the fly antennal lobe. Cell *128*, 601-612.

Slone, J., Daniels, J., and Amrein, H. (2007). Sugar receptors in *Drosophila*. Curr Biol *17*, 1809-1816.

Srinivasan, J., Kaplan, F., Ajredini, R., Zachariah, C., Alborn, H. T., Teal, P. E., Malik, R. U., Edison, A. S., Sternberg, P. W., and Schroeder, F. C. (2008). A blend of small molecules regulates both mating and development in *Caenorhabditis elegans*. Nature.

Stopfer, M., Bhagavan, S., Smith, B. H., and Laurent, G. (1997). Impaired odour discrimination on desynchronization of odour-encoding neural assemblies. Nature *390*, 70-74.

Stopfer, M., Jayaraman, V., and Laurent, G. (2003). Intensity versus identity coding in an olfactory system. Neuron *39*, 991-1004.

Stryer, L. (1986). Cyclic GMP cascade of vision. Annu Rev Neurosci *9*, 87-119.

Suzuki, H., Thiele, T. R., Faumont, S., Ezcurra, M., Lockery, S. R., and Schafer, W. R. (2008). Functional asymmetry in *Caenorhabditis elegans* taste neurons and its computational role in chemotaxis. Nature *454*, 114-117.

Tamura, N., Doolittle, L. K., Hammer, R. E., Shelton, J. M., Richardson, J. A., and Garbers, D. L. (2004). Critical roles of the guanylyl cyclase B receptor in endochondral ossification and development of female reproductive organs. Proc Natl Acad Sci U S A *101*, 17300-17305.

Tomioka, M., Adachi, T., Suzuki, H., Kunitomo, H., Schafer, W. R., and Iino, Y. (2006). The insulin/PI 3-kinase pathway regulates salt chemotaxis learning in *Caenorhabditis elegans*. Neuron *51*, 613-625.

Torayama, I., Ishihara, T., and Katsura, I. (2007). *Caenorhabditis elegans* integrates the signals of butanone and food to enhance chemotaxis to butanone. J Neurosci *27*, 741-750.

Touhara, K., Sengoku, S., Inaki, K., Tsuboi, A., Hirono, J., Sato, T., Sakano, H., and Haga, T. (1999). Functional identification and reconstitution of an odorant receptor in single olfactory neurons. Proc Natl Acad Sci U S A *96*, 4040-4045.

Troemel, E. R., Chou, J. H., Dwyer, N. D., Colbert, H. A., and Bargmann, C. I. (1995). Divergent seven transmembrane receptors are candidate chemosensory receptors in *C. elegans*. Cell *83*, 207-218.

Troemel, E. R., Kimmel, B. E., Bargmann, C. I., Hartwieg, E., and Horvitz, H. R. (1997). Reprogramming chemotaxis responses: sensory neurons define olfactory preferences in *C. elegans*. Cell *91*, 161-169.

Troemel, E. R., Sagasti, A., and Bargmann, C. I. (1999). Lateral signaling mediated by axon contact and calcium entry regulates asymmetric odorant receptor expression in *C. elegans*. Cell *99*, 387-398.

Tsalik, E. L., and Hobert, O. (2003). Functional mapping of neurons that control locomotory behavior in *Caenorhabditis elegans*. J Neurobiol *56*, 178-197.

Uchida, N., Takahashi, Y. K., Tanifuji, M., and Mori, K. (2000). Odor maps in the mammalian olfactory bulb: domain organization and odorant structural features. Nat Neurosci *3*, 1035-1043.

Vassar, R., Chao, S. K., Sitcheran, R., Nunez, J. M., Vosshall, L. B., and Axel, R. (1994). Topographic organization of sensory projections to the olfactory bulb. Cell *79*, 981-991.

Vosshall, L. B., Wong, A. M., and Axel, R. (2000). An olfactory sensory map in the fly brain. Cell *102*, 147-159.

Wachowiak, M., and Cohen, L. B. (2001). Representation of odorants by receptor neuron input to the mouse olfactory bulb. Neuron *32*, 723-735.

Wakabayashi, T., Kitagawa, I., and Shingai, R. (2004). Neurons regulating the duration of forward locomotion in *Caenorhabditis elegans*. Neurosci Res *50*, 103-111.

Wang, J. W., Wong, A. M., Flores, J., Vosshall, L. B., and Axel, R. (2003). Two-photon calcium imaging reveals an odor-evoked map of activity in the fly brain. Cell *112*, 271-282.

Wang, Z., Singhvi, A., Kong, P., and Scott, K. (2004). Taste representations in the *Drosophila* brain. Cell *117*, 981-991.

Ward, A., Liu, J., Feng, Z., and Xu, X. Z. (2008). Light-sensitive neurons and channels mediate phototaxis in *C. elegans*. Nat Neurosci *11*, 916-922.

Ward, S. (1973). Chemotaxis by the nematode *Caenorhabditis elegans*: identification of attractants and analysis of the response by use of mutants. Proc Natl Acad Sci U S A *70*, 817-821.

Wehr, M., and Laurent, G. (1996). Odour encoding by temporal sequences of firing in oscillating neural assemblies. Nature *384*, 162-166.

Wes, P. D., and Bargmann, C. I. (2001). *C. elegans* odour discrimination requires asymmetric diversity in olfactory neurons. Nature *410*, 698-701.

White, J. G., Southgate, E., Thomson, J. N., and Brenner, S. (1986). The structure of the nervous system of the nematode *Caenorhabditis elegans*. Phil Trans R Soc Lond B *314*, 1-340.

White, J. Q., Nicholas, T. J., Gritton, J., Truong, L., Davidson, E. R., and Jorgensen, E. M. (2007). The sensory circuitry for sexual attraction in *C. elegans* males. Curr Biol *17*, 1847-1857.

Wicher, D., Schafer, R., Bauernfeind, R., Stensmyr, M. C., Heller, R., Heinemann, S. H., and Hansson, B. S. (2008). *Drosophila* odorant receptors are both ligand-gated and cyclic-nucleotide-activated cation channels. Nature *452*, 1007-1011.

Wilson, R. I., Turner, G. C., and Laurent, G. (2004). Transformation of olfactory representations in the *Drosophila* antennal lobe. Science *303*, 366-370.

Wong, A. M., Wang, J. W., and Axel, R. (2002). Spatial representation of the glomerular map in the *Drosophila* protocerebrum. Cell *109*, 229-241.

Yu, D., Akalal, D. B., and Davis, R. L. (2006). *Drosophila* alpha/beta mushroom body neurons form a branch-specific, long-term cellular memory trace after spaced olfactory conditioning. Neuron *52*, 845-855.

Yu, D., Ponomarev, A., and Davis, R. L. (2004). Altered representation of the spatial code for odors after olfactory classical conditioning; memory trace formation by synaptic recruitment. Neuron *42*, 437-449.

Yu, S., Avery, L., Baude, E., and Garbers, D. L. (1997). Guanylyl cyclase expression in specific sensory neurons: a new family of chemosensory receptors. Proc Natl Acad Sci U S A *94*, 3384-3387.

Zariwala, H. A., Miller, A. C., Faumont, S., and Lockery, S. R. (2003). Step response analysis of thermotaxis in *Caenorhabditis elegans*. J Neurosci *23*, 4369-4377.

Zhang, Y., Chou, J. H., Bradley, J., Bargmann, C. I., and Zinn, K. (1997). The *Caenorhabditis elegans* seven-transmembrane protein ODR-10 functions as an odorant receptor in mammalian cells. Proc Natl Acad Sci U S A *94*, 12162-12167.

Zhang, Y., Hoon, M. A., Chandrashekar, J., Mueller, K. L., Cook, B., Wu, D., Zuker, C. S., and Ryba, N. J. (2003). Coding of sweet, bitter, and umami tastes: different receptor cells sharing similar signaling pathways. Cell *112*, 293-301.

Zhang, Y., Lu, H., and Bargmann, C. I. (2005). Pathogenic bacteria induce aversive olfactory learning in *Caenorhabditis elegans*. Nature *438*, 179-184.

Zhao, G. Q., Zhang, Y., Hoon, M. A., Chandrashekar, J., Erlenbach, I., Ryba, N. J., and Zuker, C. S. (2003). The receptors for mammalian sweet and umami taste. Cell *115*, 255-266.

CHAPTER 2

The role of olfactory neuron diversity in *C. elegans* odor discrimination

Summary

The olfactory system detects and discriminates between a diverse array of chemicals. In the nematode *C. elegans*, many attractive food-related odors are sensed by a pair of AWC olfactory neurons. AWC neurons are further separated functionally into two types, AWC^{ON} and AWC^{OFF}. Using these two types of neurons, *C. elegans* can discriminate between four odors and AWC neuronal diversity is required for discrimination between some odors. This study shows that AWC neuronal diversity is not required for discrimination between other pairs of odors. In particular, AWC^{ON} alone can discriminate between the odors 2,4,5-trimethylthiazole and benzaldehyde, and AWC^{OFF} alone can discriminate between 2,4,5-trimethylthiazole and 2,3-pentanedione. These results suggest that cell autonomous mechanisms are sufficient for odor discrimination. The TRPV channel mutants *osm-9* and *ocr-2* have mild defects in odor discrimination in AWC. *ocr-2* is not expressed in AWC, so the *ocr-2* defect suggests that cell non-autonomous mechanisms may play a role in AWC odor discrimination.

Background

Sensory discrimination reflects an animal's ability to separate complex sensory inputs into distinct neural representations. For an organism like the nematode *C. elegans*, this poses a problem because of its relatively small nervous system. We would like to know the mechanisms by which a limited nervous system allows for discrimination between sensory stimuli.

In the *C. elegans* olfactory system, two pairs of olfactory sensory neurons, called AWA and AWC, sense attractive food-related odors (Bargmann et al., 1993). Odors are most likely detected by numerous G protein-coupled receptors (GPCRs) expressed in each neuron (Bargmann, 2006). The odor specificities of AWA and AWC are distinct but overlapping, and specificity of some odors is concentration dependent (Table 1). For example, only AWA senses diacetyl at low concentrations but both AWA and AWC can sense diacetyl at higher concentrations (Chou et al., 2001). The two AWC neurons can be further subdivided into two classes based on expression of the GPCR *str-2* (Troemel et al., 1999). A *str-2::gfp* reporter is expressed asymmetrically in either one or the other AWC neuron; the *str-2*-expressing neuron is called AWC^{ON} and the other is called AWC^{OFF}. The AWC^{ON} and AWC^{OFF} neurons have distinct odor specificity (Wes and Bargmann, 2001), so AWC asymmetry increases olfactory neuron diversity to three neuron types (AWA, AWC^{ON} and AWC^{OFF}) and expands the coding capacity of the olfactory system (Table 1). Even so, the vastly smaller number of olfactory neurons compared to the number of distinct odors raises questions about how well *C. elegans* discriminates between them.

Olfactory discrimination in *C. elegans* has been tested in two ways: cross-saturation and cross-adaptation. In adaptation, animals are conditioned by exposing them to an odor for an extended time in the absence of food. Animals tested for chemotaxis following conditioning attenuate their response to the conditioning odor (Colbert and Bargmann, 1995). During cross-adaptation, animals are conditioned with one odor and tested for chemotaxis to a different odor. If adapted animals can chemotax to the test odor better than to the adapted odor, they are able to discriminate between the two odors. This phenomenon has not been studied extensively, but *C. elegans* discriminates between at least two classes of AWC-sensed odors, and discriminates between AWA- and AWC-sensed odors (Colbert and Bargmann, 1995).

During saturation, the animal's chemotaxis response to a point source of odor is attenuated when the same odor is uniformly mixed in the assay plate at high enough levels (Bargmann et al., 1993). In cross-saturation, animals are tested for chemotaxis to one odor in the presence of saturating amounts of another odor in the assay plate. If animals chemotax better in cross-saturation than in self-saturation, they are able to discriminate between the two odors. This form of discrimination has been studied more extensively. In the rest of this chapter, discrimination will refer to the ability of animals to distinguish between two odors as determined by the cross-saturation assay.

Wild-type *C. elegans* discriminates between at least six odors sensed by the two pairs of olfactory neurons (Bargmann et al., 1993). In a genetic background that leaves only the two AWC neurons out of all the amphid sensory neurons functional, animals can discriminate between at least four odors (Chou, 1998). Discrimination between two of these four odors, butanone and benzaldehyde, requires AWC asymmetry (Wes and

Bargmann, 2001). Genetic or laser ablation of AWC^{OFF} neurons causes defects in sensing a benzaldehyde gradient in the presence of a saturating background of butanone. Thus at least in one case, sensory neuron diversity contributes directly to odor discrimination. This study shows that AWC asymmetry is not necessary for some forms of odor discrimination. A candidate approach testing various signaling and odor adaptation mutants identified the TRPV channels, *osm-9* and *ocr-2*, as being defect for odor discrimination. Olfactory discrimination may rely on both diversity of sensory neurons as well as cell autonomous mechanisms.

Results

The 2 AWC^{ON} mutant *nsy-1* is defective for butanone/benzaldehyde discrimination

nsy-1 mutants lack AWC^{OFF} neurons and have a defect in sensing benzaldehyde in a background of butanone (Troemel et al., 1997; Wes and Bargmann, 2001) (Tables 1 and 2). To understand the extent to which AWC asymmetry contributes to odor discrimination, *nsy-1* mutants were tested for chemotaxis to butanone in the presence of saturating and non-saturating amounts of benzaldehyde in the assay plate. Benzaldehyde chemotaxis was saturated at levels of benzaldehyde above 0.1 µL/plate (Fig. 1A). *nsy-1* mutant animals showed reduced chemotaxis to butanone compared to wild-type animals across a wide range of benzaldehyde levels in the plate (Fig. 1B and C). At the highest amount of benzaldehyde in the plates (0.5 µL/plate), wild-type animals showed a mild reduction in butanone chemotaxis (Fig. 1B), but the reduction in chemotaxis in *nsy-1* mutants was more severe (Fig. 1C). This result suggests that *nsy-1* may have a broader defect in discrimination of odors, even at sub-saturating amounts of the background odor.

AWC^{ON} can discriminate between some odors

2,4,5-trimethylthiazole is an attractive odor sensed by the AWA and AWC olfactory neurons (Bargmann et al., 1993) (Table 1). *C. elegans* mutants that are defective for all amphid sensory neuron function except for AWC are able to sense 2,4,5-trimethylthiazole in a uniform background of another AWC-sensed odor (Chou, 1998). However, discrimination between 2,4,5-trimethylthiazole and other AWC odors may require AWC asymmetry. To test this, *nsy-1* was crossed with *odr-7*, which is equivalent to a genetic ablation of the AWA neurons (Sengupta et al., 1994). In *nsy-1; odr-7* double mutants the only functional class of olfactory neurons is AWC^{ON} (Table 2). The *nsy-1; odr-7* double mutant was slightly defective but still capable of sensing 2,4,5-trimethylthiazole (Fig. 2A), suggesting that AWC^{ON} can sense this odor. A uniform background of butanone slightly affects chemotaxis to 2,4,5-trimethylthiazole in wild-type, *nsy-1* and *odr-7* single mutant animals (Fig. 2A). However, the *nsy-1; odr-7* double mutants were strongly defective in discriminating 2,4,5-trimethylthiazole from butanone (Fig. 2A). These results suggest that olfactory diversity is important for discriminating between the two odors. The result also suggests that 2,4,5-trimethylthiazole sensing is distributed among AWA, AWC^{ON} and AWC^{OFF} neurons.

To test if the discrimination defect was unique to butanone, *nsy-1; odr-7* double mutants were tested for discrimination with benzaldehyde and isoamylalcohol as the background odor. In the presence of a uniform background of benzaldehyde or isoamyl alcohol, *nys-1* and *odr-7* single mutants as well as *nsy-1; odr-7* double mutant animals had either normal or slightly reduced chemotaxis to 2,4,5-trimethylthiazole compared to

the no background odor control (Fig. 2B). This result suggests that AWA and AWC^{OFF} have a slight role in discrimination between these sets of odors, but that AWC^{ON} is capable of odor discrimination between some pairs of odors.

AWC^{OFF} can discriminate between odors

Because 2,4,5-trimethylthiazole is sensed by AWA and AWC neurons, it is suitable to use as the background odor in discrimination assays. A uniform background of 0.5 µL/plate of 2,4,5-trimethylthiazole attenuates chemotaxis to the same odor (Fig. 3A), suggesting that high levels of 2,4,5-trimethylthiazole can saturate self-responses in both AWA and AWC neurons. Under saturating 2,4,5-trimethylthiazole levels, wild-type animals were able to chemotax to 2,3-pentanedione, an AWC^{OFF}-sensed odor at the dilution tested (Fig. 3B, Table 1). To test if olfactory neuron diversity could explain this discrimination, the AWA-defective *odr-7* mutant was combined with the 2 AWC^{OFF} mutants *nsy-4* or *nsy*-5 (Chuang et al., 2007; Vanhoven et al., 2006) (Table 2). AWC^{ON} does not sense 2,3-pentanedione (Wes and Bargmann, 2001).

nsy-4; odr-7 and *nsy-5; odr-7* double mutants were both able to chemotax to 2,4,5-trimethylthiazole, although they were slightly defective compared to wild-type (Fig. 4A). These results suggest that AWC^{OFF} can sense this odor. In discrimination, *odr-7* animals were slightly defective for sensing 2,3-pentanedione in the presence of 2,4,5-trimethylthiazole (Fig. 4B). Thus there may be a small contribution of AWA for discrimination between these two odors. *nsy-4; odr-7* double mutants were also slightly defective, but were still mostly capable of sensing 2,3-pentanedione in the presence of 2,4,5-trimethylthiazole (Fig. 4B). *nsy-5; odr-7* double mutants also discriminated

between 2,3-pentanedione and 2,3,5-trimethylthiazole to a similar extent(Fig. 4B). The mild defects seen in the *nsy-4; odr*-7 and *nsy-5; odr-7* doubles mutants are likely to be due to the *odr-7* mutation. Therefore, olfactory neuron diversity plays only a minor role in 2,3-pentanedione and 2,3,5-trimethylthiazole discrimination.

Candidate signaling mutants are not defective for odor discrimination

Because the AWC^{OFF} neuron is capable of discriminating between 2,3-pentanedione and 2,4,5-trimethylthiazole, potential discrimination genes were sought by two approaches: a mutant screen and a candidate gene approach. For the candidate approach, mutants known to function in G-protein signaling as well as mutants in olfactory adaptation were tested. The Gα and Gβ subunit mutants *gpa-5* and *gpb-2* (Chase et al., 2001; Jansen et al., 1999; Robatzek et al., 2001) were not defective for discrimination (Fig. 5A). Preliminary results suggest that the Gα subunit mutant *gpa-2* is also not defective for discrimination (data not shown). Regulator of G-protein signaling (RGS) proteins stimulate GTPase activity of ATP-bound Gα (He et al., 1998). *eat-16* encodes one of many *C. elegans* RGS proteins and *eat-16* mutants were not defective for discrimination either (Fig. 5A).

TRPV channel mutants are defective for odor discrimination

Discrimination between odors may require specific desensitization to the background odor while maintaining sensitivity to the test odor gradient. *adp-1* is a mutant defective for adaptation to most AWC sensed odors after prolonged conditioning (Colbert and Bargmann, 1995). This mutant discriminated between 2,3-pentanedione and 2,4,5-

trimethylthiazole as well as wild type (Fig. 5B). Another adaptation mutant *egl-4*, which encodes a cGMP-dependent kinase (L'Etoile et al., 2002), could also discriminate between odors (Fig 5B). These results indicate that rapid desensitization and slower adaptation are at least partly genetically distinct.

osm-9, which encodes a TRPV cation channel and has AWC adaptation defects (Colbert and Bargmann, 1995), showed a mild defect in discrimination between 2,3-pentanedione and 2,4,5-trimethylthiazole (Fig. 5B). However, the defect was observed only in the *osm-9(ky10)* allele, which is predicted to lead to premature truncation of the protein, whereas the point mutant allele *osm-9(n2743)* did not show a discrimination defect. Both alleles share defects in AWA odor chemotaxis as well as AWC adaptation (Colbert et al., 1997), so the *osm-9(ky10)* discrimination defect cannot be attributed only to a defect in AWA function as was seen in the *odr-7* mutant (Fig. 4B), or a defect in AWC adaptation. *osm-9* may have a function in olfactory discrimination independent of its role in sensory transduction and odor adaptation. Another TRPV homolog mutant, *ocr-2*, is also defective for discrimination between 2,3-pentanedione and 2,4,5-trimethylthiazole (Fig. 5B).

A screen for discrimination mutants was carried out by mutagenizing animals and isolating those that fail to sense 2,3-pentanedione in the presence of 2,4,5-trimethylthiazole. Potential candidates underwent a secondary screen to identify mutants that could sense 2,3-pentanedione in the absence of 2,4,5-trimethylthiazole. Unfortunately, the mutants isolated in this screen were defective for sensing 2,3-pentanedione both in the presence and absence of 2,4,5-trimethylthiazole.

Discussion

This study sought to dissect the role of olfactory neuron diversity in *C. elegans* odor discrimination behavior. The AWC^{ON} neuron cannot discriminate between a background of benzaldehyde and a point source of butanone, or between a background of butanone and a point source of 2,4,5-trimethylthiazole. However, AWC^{ON} is capable of discriminating between a background of benzaldehyde or isoamylalcohol and a point source of 2,4,5-trimethylthiazole. The AWC^{OFF} neuron can discriminate between a background of 2,4,5-trimethylthiazole and a point source of 2,3-pentanedione. Thus, neuronal diversity, as determined by *str-2* expression, is not necessary for odor discrimination in some contexts. These results suggest that single olfactory neuron classes can distinguish different odors using cell-intrinsic mechanisms. Alternatively, there may be other forms of asymmetry between the two AWC neurons that are independent of mechanisms determining *str-2* asymmetry, or hidden contributions from neurons that are not sufficient for chemotaxis in the absence of AWA and AWC.

Cell-autonomous mechanisms for odor discrimination may involve odor-specific segregation of signaling pathways. Olfactory sensory transduction is mediated by a GPCR signaling pathway (Bargmann, 2006) and there are many regulators of the pathway (Pierce and Lefkowitz, 2001; Pitcher et al., 1998; Ross and Wilkie, 2000). None of the tested GPCR signaling regulators were defective for odor discrimination. A mutant in the *C. elegans* homolog of the GPCR kinase (GRK), *grk-2*, has defects in olfactory chemotaxis (Fukuto et al., 2004) and was not tested for discrimination in this study. AWC expresses multiple Gα subunits, of which only one, ODR-3, is necessary for olfactory chemotaxis (Bargmann, 2006). The other Gα subunits play modulatory

roles in chemotaxis (Lans et al., 2004), and may still play a role in odor discrimination. The RGS homolog e*at-16* has been implicated in AWC thermotaxis signaling (Kuhara et al., 2008), but it is not known if it regulates olfactory chemotaxis.

AWC adaptation mutants were mostly normal for odor discrimination, except for the TRPV channel mutant, *osm-9*, which had mild discrimination defects. *osm-9* is expressed in many sensory neurons, including AWC, and *osm-9* mutants have a wide range of sensory defects (Chang et al., 2006; Colbert and Bargmann, 1995; Colbert et al., 1997). *osm-9* mutants are defective for chemotaxis to AWA-sensed odors and even though they chemotax normally to AWC-sensed odors, they have specific adaptation defects in AWC (Colbert and Bargmann, 1995). It is not known if they have a defect for adaptation to 2,4,5-trimethylthiazole, which was used as the background odor in the discrimination assays. One allele of *osm-9*, *osm-9(ky10)*, had a discrimination defect, whereas another allele, *osm-9(n2743)*, did not show a defect. The two alleles have similar phenotypes in most assays, and the discrimination assay represents the first example in which the two alleles show separate phenotypes. *osm-9(ky10)* is an early stop mutation that is likely to be a null, whereas *osm-9(n2743)* is a missense mutation in a conserved amino acid in the ankyrin domain. Allele-specific defects of TRP channels is seen in *ocr-2* (Sokolchik et al., 2005). The N-terminal domain of *ocr-2* is specifically required for regulation of gene expression and osmotic avoidance behaviors but not for chemotaxis. Analogously, the ankyrin domain of *osm-9* may be important for most *osm-9* functions, but may be dispensable for AWC odor discrimination.

A deletion allele of *ocr-2* also had a discrimination defect, confirming a role for TRP channel signaling in odor discrimination. *ocr-2* is expressed in a smaller subset of

sensory neurons that also express *osm-9*, including AWA and some nociceptive sensory neurons, but it is not expressed in AWC (Tobin et al., 2002). *ocr-2(ak47)* mutants exhibit defects in some sensory behaviors and share AWA chemotaxis defects with *osm-9* mutants. *osm-9* and *ocr-2* are mutually dependent on each other for proper localization to the sensory cilia in sensory neurons that express both of them.

The shared discrimination defect of *osm-9(ky10)* and *ocr-2* mutants suggests that cells that expresses both TRP channels are important for discrimination, which excludes AWC as the site of action. AWA is a potential neuron where *osm-9* and *ocr-2* may function to regulate odor discrimination. A genetic ablation of AWA using an *odr-7* mutation also had a mild effect on odor discrimination. However, the AWC discrimination defect is allele-specific, whereas the AWA sensory defect is not, so the two defects are genetically separable. AWA may not be necessary for odor discrimination, but a specific disruption of TRP channel signaling in AWA may disrupt AWC discrimination. Alternatively, *osm-9* and *ocr-2* may be acting in other neurons (ASH, ADF, ADL) to provide modulatory inputs to the AWC chemotaxis circuit.

The *osm-9* and *ocr-2* mutant defects in odor discrimination were relatively mild, suggesting that there are other mechanisms for discrimination. This may include other signaling pathways that have not been tested, such as phosphodiesterases. However, a screen to isolate discrimination mutants yielded no candidates and a larger screen may be necessary to isolate mutants. It is also possible that there are redundant signaling pathways as well as redundancy between mechanisms that rely on olfactory neuron diversity and those that rely on cell-intrinsic signaling pathways.

Materials and methods

Strains and reagents

The following strains were used in this study: wild-type Bristol (N2), CX4731 *nsy-1(ky542) II*, CX3030 *odr-7(ky4) X*, CX5966 *nsy-1(ky542) II; odr-7(ky4) X*, CX6332 *nsy-4(ky616) IV*, CX6333 *nsy-4(ky616) IV; odr-7(ky4) X*, CX6161 *nsy-5(ky634) I*, CX6334 *nsy-5(ky634) I; odr-7(ky4) X*, NL1137 *gpa-5(pk326) X*, DA541 *gpb-2(ad541) I*, JT609 *eat-16(sa609) I*, CX2345 *adp-1(ky20) I*, CX2960 *egl-4(ky95) IV*, CX10 *osm-9(ky10) IV*, MT6317 *osm-9(n2743) IV*, VM384 *ocr-2 (ak47) IV*.

All odors were obtained from Sigma-Aldrich (St. Louis, MO). Dilutions of odors in ethanol used for the point source were as follows: 2-butanone 1:1,000; benzaldehyde 1:200; 2,4,5-trimehtylthiazole 1:1,000; 2,3-pentanedione 1:10,000.

Behavioral assays

Population chemotaxis assays were performed on assay agar (1.6 % agar, 1 mM $MgSO_4$, 1 mM $MgCl_2$, 5 mM phosphate buffer, pH 6.0) essentially as descried (Bargmann et al., 1993). Discrimination assays were performed as described (Wes and Bargmann, 2001). Briefly, agar was dissolved in water by boiling, salts and buffer were added to the agar solution after cooling to less than 65ºC, then 1 mL assay buffer (1 mM $MgSO_4$, 1 mM $MgCl_2$, 5 mM phosphate buffer, pH 6.0) with or without the background odor diluted to the appropriate concentration was added after cooling to < 55ºC and assay plates were poured immediately. Assays were performed between one and eight hours after pouring the plates. Amounts of odors used in the plates were as follows, unless noted otherwise:

butanone 1.2 μL/plate, benzaldehyde 0.1 μL/plate, isoamyl alchohol 0.5 μL/plate, 2,4,5-trimethylthiazole 0.2 μL/plate.

Discrimination Screen

N2 animals were mutagenized with EMS following standard protocols (Anderson, 1995). Approximately 10,000 F2 animals were tested for 2,3-pentatnedione chemotaxis (1:10,000 dilution) in the presence of 0.2 μL/plate of 2,4,5-trimethylthiazole, and those animals that failed to discriminate for three rounds of assays were kept for further analysis. In the secondary screen, candidates from the first screen were tested for chemotaxis to 2,3-pentanedione chemotaxis in the absence of 2,4,5-trimethylthiazole. Most candidates isolated from the primary screen had a 2,3-pentanedione chemotaxis defect in the secondary screen.

References

Anderson, P. (1995). Mutagenesis. Methods Cell Biol *48*, 31-58.

Bargmann, C. I., Chemosensation in *C. elegans* (October 25, 2006), *WormBook*, ed. The *C. elegans* Research Community, WormBook, 10.1895/wormbook.1.123.1, http://www.wormbook.org

Bargmann, C. I., Hartwieg, E., and Horvitz, H. R. (1993). Odorant-selective genes and neurons mediate olfaction in *C. elegans*. Cell *74*, 515-527.

Chang, A. J., Chronis, N., Karow, D. S., Marletta, M. A., and Bargmann, C. I. (2006). A distributed chemosensory circuit for oxygen preference in *C. elegans*. PLoS Biol *4*, e274.

Chase, D. L., Patikoglou, G. A., and Koelle, M. R. (2001). Two RGS proteins that inhibit Galpha(o) and Galpha(q) signaling in C. elegans neurons require a Gbeta(5)-like subunit for function. Curr Biol *11*, 222-231.

Chou, J., H. (1998). Molecular Genetic Analysis of Chemosensroy Behaviors in *C. elegans*. Ph. D. dissertation, University of California at San Francisco.

Chou, J. H., Bargmann, C. I., and Sengupta, P. (2001). The *Caenorhabditis elegans odr-2* gene encodes a novel Ly-6-related protein required for olfaction. Genetics *157*, 211-224.

Chuang, C. F., Vanhoven, M. K., Fetter, R. D., Verselis, V. K., and Bargmann, C. I. (2007). An innexin-dependent cell network establishes left-right neuronal asymmetry in *C. elegans*. Cell *129*, 787-799.

Colbert, H. A., and Bargmann, C. I. (1995). Odorant-specific adaptation pathways generate olfactory plasticity in *C. elegans*. Neuron *14*, 803-812.

Colbert, H. A., Smith, T. L., and Bargmann, C. I. (1997). OSM-9, a novel protein with structural similarity to channels, is required for olfaction, mechanosensation, and olfactory adaptation in *Caenorhabditis elegans*. J Neurosci *17*, 8259-8269.

Fukuto, H. S., Ferkey, D. M., Apicella, A. J., Lans, H., Sharmeen, T., Chen, W., Lefkowitz, R. J., Jansen, G., Schafer, W. R., and Hart, A. C. (2004). G protein-coupled receptor kinase function is essential for chemosensation in *C. elegans*. Neuron *42*, 581-593.

He, W., Cowan, C. W., and Wensel, T. G. (1998). RGS9, a GTPase accelerator for phototransduction. Neuron *20*, 95-102.

Jansen, G., Thijssen, K. L., Werner, P., van der Horst, M., Hazendonk, E., and Plasterk, R. H. (1999). The complete family of genes encoding G proteins of *Caenorhabditis elegans*. Nat Genet *21*, 414-419.

Kuhara, A., Okumura, M., Kimata, T., Tanizawa, Y., Takano, R., Kimura, K. D., Inada, H., Matsumoto, K., and Mori, I. (2008). Temperature Sensing by an Olfactory Neuron in a Circuit Controlling Behavior of *C. elegans*. Science *320*, 803-807.

L'Etoile, N. D., Coburn, C. M., Eastham, J., Kistler, A., Gallegos, G., and Bargmann, C. I. (2002). The cyclic GMP-dependent protein kinase EGL-4 regulates olfactory adaptation in *C. elegans*. Neuron *36*, 1079-1089.

Lans, H., Rademakers, S., and Jansen, G. (2004). A network of stimulatory and inhibitory Galpha-subunits regulates olfaction in *Caenorhabditis elegans*. Genetics *167*, 1677-1687.

Pierce, K. L., and Lefkowitz, R. J. (2001). Classical and new roles of beta-arrestins in the regulation of G-protein-coupled receptors. Nat Rev Neurosci *2*, 727-733.

Pitcher, J. A., Freedman, N. J., and Lefkowitz, R. J. (1998). G protein-coupled receptor kinases. Annu Rev Biochem *67*, 653-692.

Robatzek, M., Niacaris, T., Steger, K., Avery, L., and Thomas, J. H. (2001). *eat-11* encodes GPB-2, a Gbeta(5) ortholog that interacts with G(o)alpha and G(q)alpha to regulate *C. elegans* behavior. Curr Biol *11*, 288-293.

Ross, E. M., and Wilkie, T. M. (2000). GTPase-activating proteins for heterotrimeric G proteins: regulators of G protein signaling (RGS) and RGS-like proteins. Annu Rev Biochem *69*, 795-827.

Sengupta, P., Colbert, H. A., and Bargmann, C. I. (1994). The *C. elegans* gene *odr-7* encodes an olfactory-specific member of the nuclear receptor superfamily. Cell *79*, 971-980.

Sokolchik, I., Tanabe, T., Baldi, P. F., and Sze, J. Y. (2005). Polymodal sensory function of the *Caenorhabditis elegans* OCR-2 channel arises from distinct intrinsic determinants within the protein and is selectively conserved in mammalian TRPV proteins. J Neurosci *25*, 1015-1023.

Tobin, D., Madsen, D., Kahn-Kirby, A., Peckol, E., Moulder, G., Barstead, R., Maricq, A., and Bargmann, C. (2002). Combinatorial expression of TRPV channel proteins defines their sensory functions and subcellular localization in *C. elegans* neurons. Neuron *35*, 307-318.

Troemel, E. R., Kimmel, B. E., Bargmann, C. I., Hartwieg, E., and Horvitz, H. R. (1997). Reprogramming chemotaxis responses: sensory neurons define olfactory preferences in *C. elegans*. Cell *91*, 161-169.

Troemel, E. R., Sagasti, A., and Bargmann, C. I. (1999). Lateral signaling mediated by axon contact and calcium entry regulates asymmetric odorant receptor expression in *C. elegans*. Cell *99*, 387-398.

Vanhoven, M. K., Bauer Huang, S. L., Albin, S. D., and Bargmann, C. I. (2006). The claudin superfamily protein *nsy-4* biases lateral signaling to generate left-right asymmetry in *C. elegans* olfactory neurons. Neuron *51*, 291-302.

Wes, P. D., and Bargmann, C. I. (2001). *C. elegans* odour discrimination requires asymmetric diversity in olfactory neurons. Nature *410*, 698-701.

<table>
<tr><th></th><th colspan="3">Olfactory neuron</th></tr>
<tr><th></th><th>AWA</th><th>AWC^{ON}</th><th>AWC^{OFF}</th></tr>
<tr><td rowspan="4">Odor</td><td rowspan="3">pyrazine
diacetyl (low conc.)
2,3-pentanedione (high conc.)</td><td>butanone</td><td>2,3-pentanedione (low conc.)</td></tr>
<tr><td colspan="2">benzaldehyde
isoamylalcohol
diacetyl (high conc.)</td></tr>
<tr><td colspan="3">2,4,5-trimethylthiazole</td></tr>
</table>

Table 2-1. Odor specificity of olfactory neurons
Data from: Bargmann et al. 1993; Chou et al., 2001; Wes and Bargmann, 2001.

	Olfactory neuron		
Genotype	AWA	AWC^{ON}	AWC^{OFF}
WT	√	√	√
nsy-1	√	√	—
nsy-4/nsy-5	√	—	√
odr-7	—	√	√
nsy-1; odr-7	—	√	—
nsy-4; odr-7/ nsy-5;odr-7	—	—	√

Table 2-2. Cell-fate mutants that reduce olfactory neuron diversity
√ = present, — = absent. Data from: Chuang et al., 2007; Sengupta et al., 1994; Vanhoven et al., 2006; Wes and Bargmann, 2001.

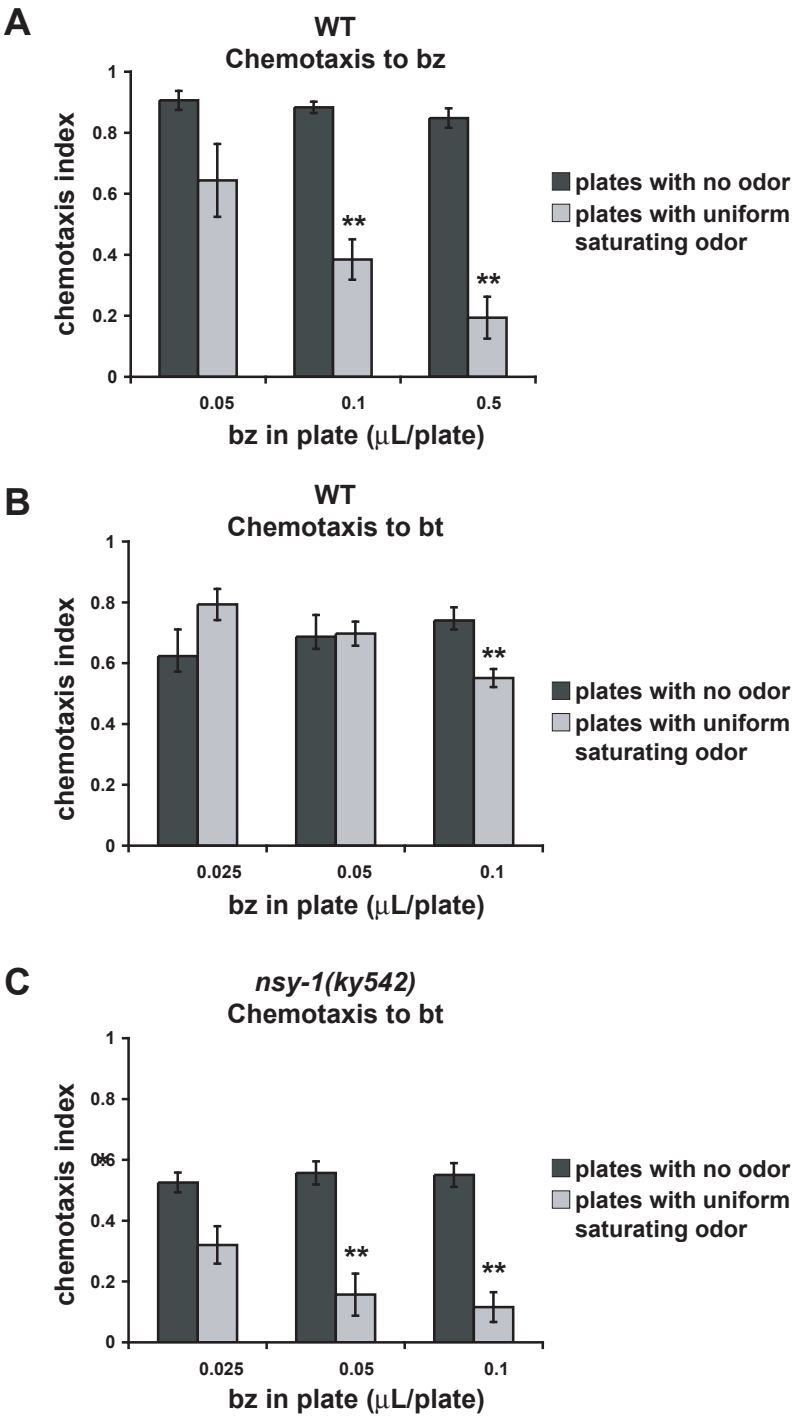


Figure 2-1. Discrimination defect of *nsy-1* mutants

(A) Benzaldehyde self-saturation in wild-type animals. Indicated amounts of benzaldehyde were put into the assay plates. (B and C) Discrimination between a point source of butanone and background benzaldehyde in wild-type (B) and *nsy-1(ky542)* mutant (C) animals. Abbreviations: WT wild-type, bz benzaldehyde, bt butanone. Dilutions (in ethnol) of attractants were: bz 1:200, bt 1:1000. * $p < 0.05$, ** $p < 0.01$ Student's *t*-test. Error bars indicate SEM.

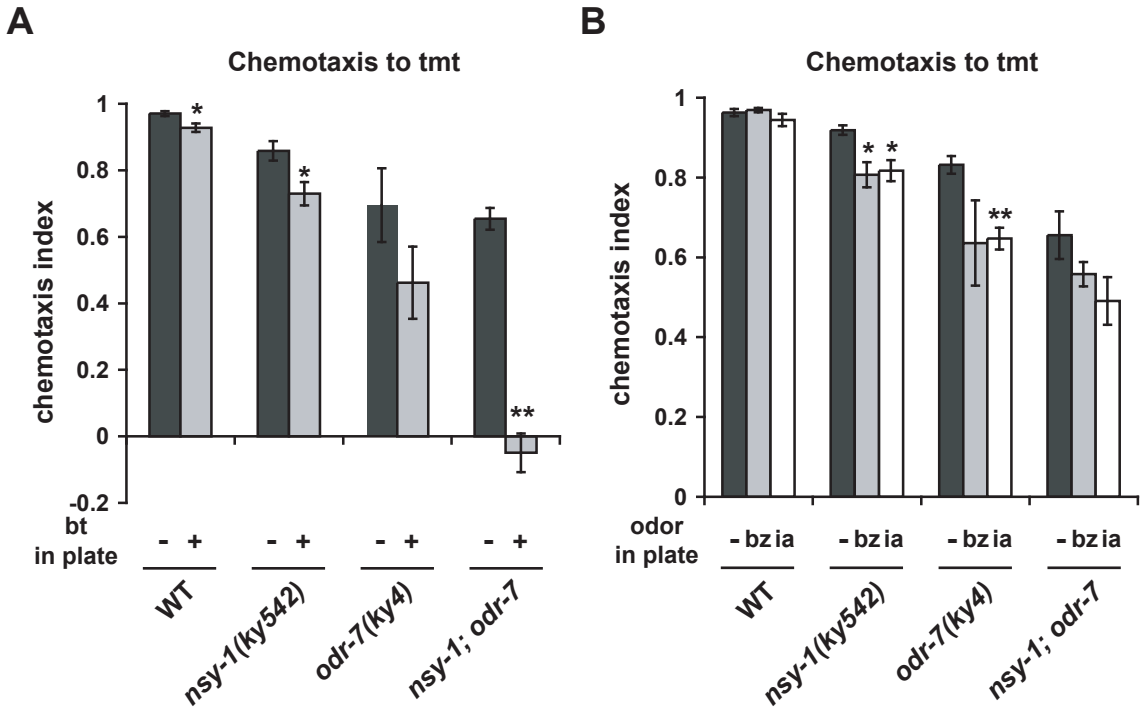


Figure 2-2. AWC^{ON} can discriminate between some odors, but cannot discriminate between butanone and 2,4,5-trimethylthiazole

Discrimination in AWA and AWC^{OFF} cell-fate mutants (A) Discrimination between a point source of 2,4,5-trimethylthiazole (1:1,000) and background butanone (1.2 µL/plate). (B) Discrimination between a point source of 2,4,5-trimethylthiazole and background isoamylalcohol (0.5 µL/plate) or benzaldehyde (0.1 µL/plate). Abbreviations: tmt 2,4,5-trimethylthiazole, ia isoamylalcohol. * $p < 0.05$, ** $p < 0.01$ Student's *t*-test. Error bars indicate SEM.

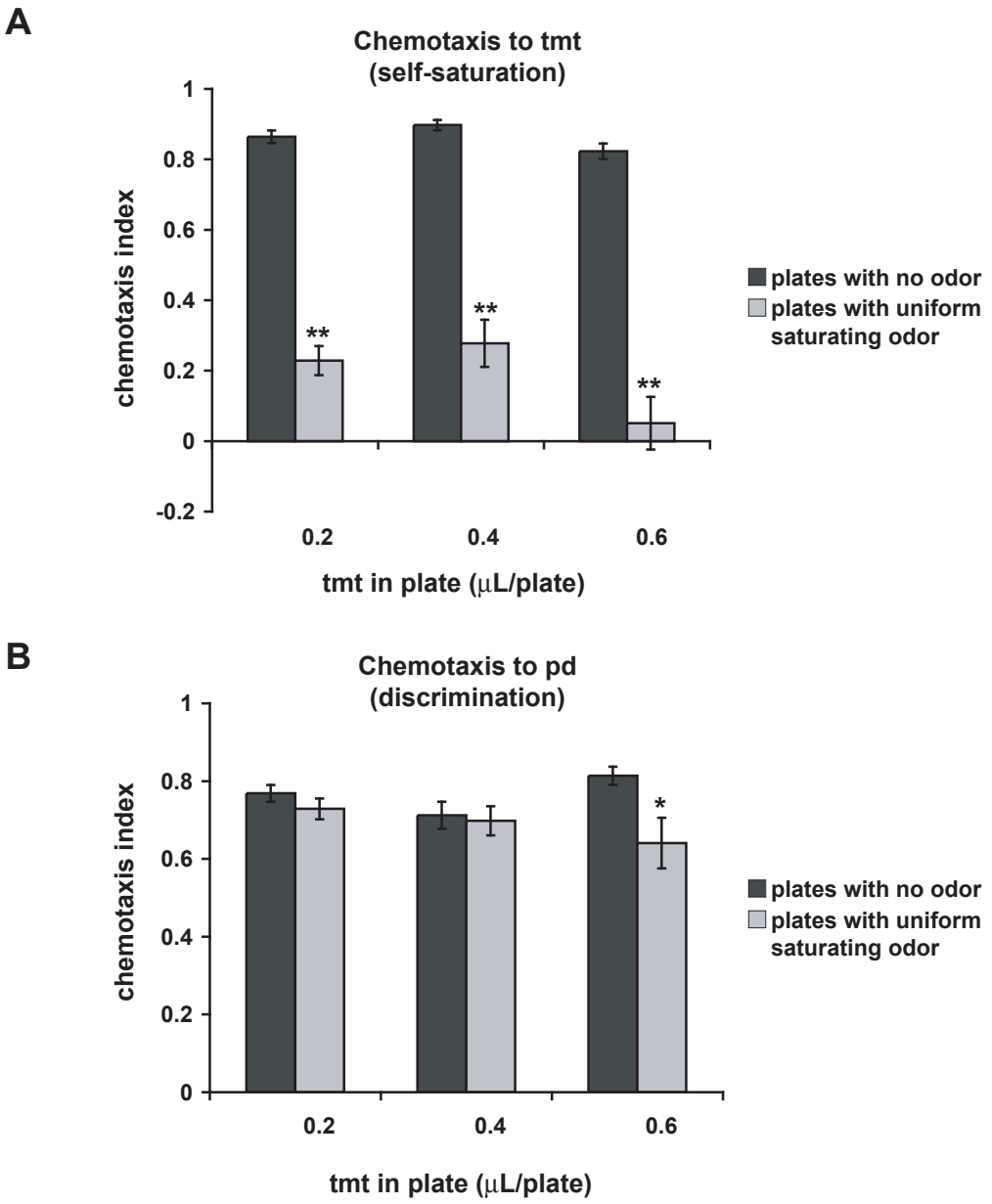


Figure 2-3. Discrimination between 2,3-pentanedione and 2,4,5-trimethylthiazole
(A) Self-saturation of 2,4,5-trimethylthiazole (1:1,000) chemotaxis in wild-type animals. (B) Discrimination between a point source of 2,3-pentanedione (1:10,000) and background 2,4,5-trimethylthiazole in wild-type animals. Abbreviations: pd 2,3-pentanedione. * $p < 0.05$, ** $p < 0.01$ Student's *t*-test. Error bars indicate SEM.

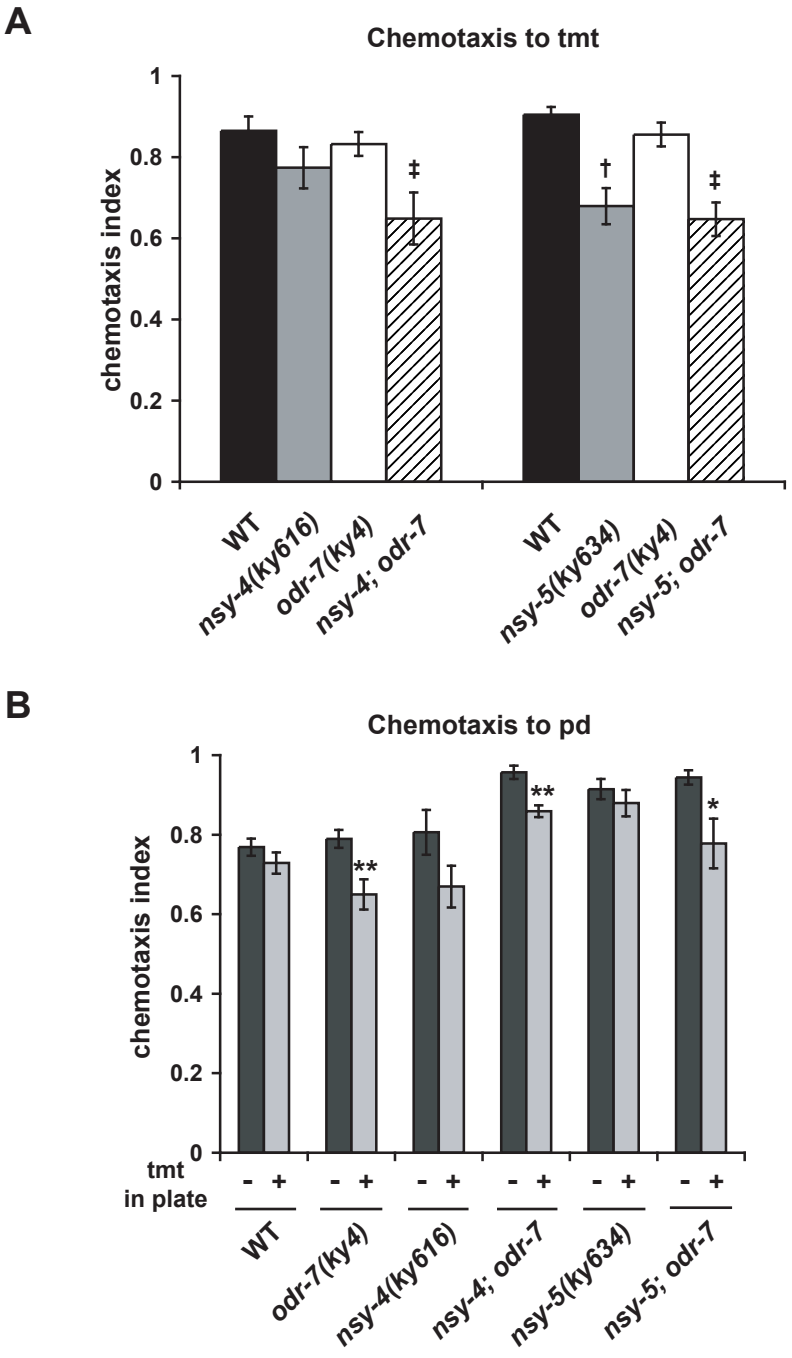


Figure 2-4. AWC^{OFF} can discriminate between odors
Chemotaxis and discrimination in AWA and AWC^{ON} cell-fate mutants. (A) Chemotaxis to 2,4,5-trimethylthiazole (1:1,000). † $p < 0.05$ relative to wild-type, ‡ $p < 0.05$ relative to both wild-type and *odr-7* mutants, Bonferroni *t*-test. (B) Discrimination between a point source of 2,3-pentanedione (1:10,000) and background 2,4,5-trimethylthiazole (0.2 µL/plate). * $p < 0.05$, ** $p < 0.01$ Student's *t*-test. Error bars indicate SEM.

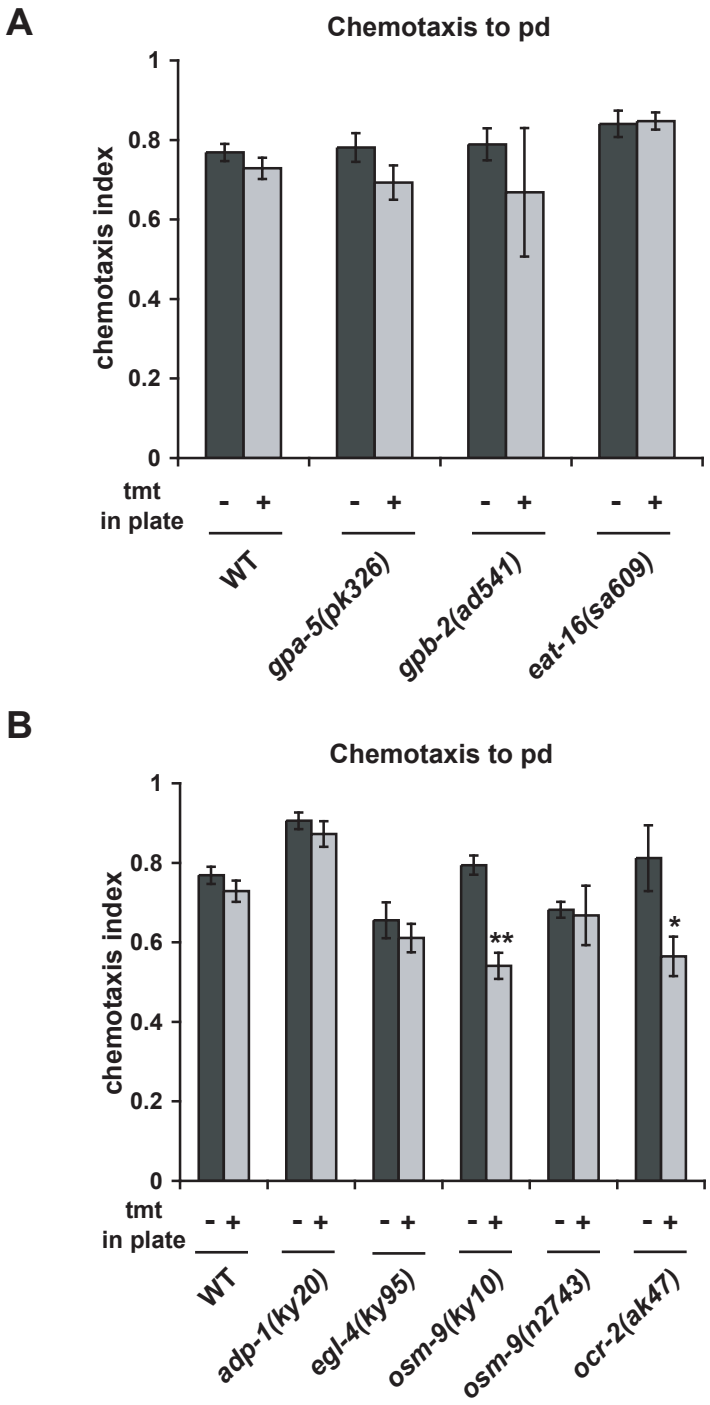


Figure 2-5. Odor discrimination in candidate mutants

Discrimination between a point source of 2,3-pentanedione (1:10,000) and background 2,4,5-trimethylthiazole (0.2 µL/plate) in various mutant backgorunds. (A) G-protein signaling mutants. (B) Adptation and TRPV channel mutants. * $p < 0.05$ One-tailed Student's *t*-test, ** $p < 0.01$ Two-tailed Student's *t*-test. Error bars indicate SEM.

CHAPTER 3

A behavioral switch: cGMP and PKC signaling in olfactory neurons reverses odor preference in *C. elegans*

(Neuron 2008, in press)

Summary

Innate chemosensory preferences are often encoded by sensory neurons that are specialized for attractive or avoidance behaviors. Here we show that one olfactory neuron in *Caenorhabditis elegans,* AWC^{ON}, has the potential to direct both attraction and repulsion. Attraction, the typical AWC^{ON} behavior, requires a receptor-like guanylate cyclase GCY-28 that acts in adults and localizes to AWC^{ON} axons. *gcy-28* mutants avoid AWC^{ON}–sensed odors; they have normal odor-evoked calcium responses in AWC^{ON}, but reversed turning biases in odor gradients. In addition to *gcy-28,* a diacylglycerol/protein kinase C pathway that regulates neurotransmission switches AWC^{ON} odor preferences. A behavioral switch in AWC^{ON} may be part of normal olfactory plasticity, as odor conditioning can induce odor avoidance in wild-type animals. Genetic interactions, acute rescue, and calcium imaging suggest that the behavioral reversal results from presynaptic changes in AWC^{ON}. These results suggest that alternative modes of neurotransmission can couple one sensory neuron to opposite behavioral outputs.

Introduction

Animals of many species are born with innate odor and taste preferences that cause them to approach food-related odors and avoid toxic substances. Experiments in nematodes, fruit flies, and mice have demonstrated that innate preferences are encoded, at least in part, by dedicated sensory neurons. In each animal, certain sensory neurons are preferentially coupled to attraction or food acceptance, while others drive aversion (Marella et al., 2006; Mueller et al., 2005; Tobin et al., 2002; Troemel et al., 1997; Zhao et al., 2003). Downstream of sensory neurons, the anatomical or physiological pathways for behavioral preference are largely undefined. At one extreme, there could be a complete labeled-line segregation of sensory projections, as proposed in *Drosophila,* where sweet and bitter taste fibers project to different target regions in the brain (Thorne et al., 2004; Wang et al., 2004). The flexibility of animal behavior, however, suggests that even innate sensory pathways may be sensitive to modification.

Chemosensory preference can be examined in detail in the nematode *C. elegans,* whose compact nervous system with 302 neurons allows functions to be mapped to specific cell types. *C. elegans* is attracted to chemicals sensed by two pairs of olfactory neurons called AWC and AWA and a pair of gustatory neurons called ASE (reviewed in Bargmann, 2006). It avoids repulsive chemicals sensed by neurons called AWB, ASH and ADL. The sensory neurons detect environmental chemicals using G protein-coupled receptors (GPCRs) encoded by ~1700 chemoreceptor genes, as well as other receptors (Robertson and Thomas, 2006). Each sensory neuron expresses many chemoreceptor genes and detects many chemicals, an organization distinct from the one receptor-one neuron organization of the mammalian olfactory system. Sensory transduction

downstream of *C. elegans* GPCRs is mediated either by cyclic guanosine monophosphate (cGMP) signaling through guanylate cyclases and cGMP-gated channels, or by signaling through transient receptor potential V (TRPV) channels, depending on the cell type (Bargmann, 2006).

In addition to the sensory properties defined by GPCRs, each sensory neuron is associated with a preferred behavioral output: attraction for AWC, AWA and ASE, and avoidance for AWB, ASH, and ADL. The strength of neuron-behavior coupling was demonstrated by expressing one receptor, the diacetyl-sensing GPCR ODR-10, in different sensory neurons (Troemel et al., 1997). Expression of ODR-10 in AWA or AWC neurons leads to attraction to diacetyl, whereas expression of ODR-10 in AWB leads to diacetyl avoidance (Sengupta et al., 1996; Troemel et al., 1997; Wes and Bargmann, 2001). The mechanisms by which AWA and AWC specify attraction and AWB specifies avoidance are not obvious, as these sensory neurons have largely overlapping synaptic targets (White et al., 1986).

Despite strong innate preferences, chemosensory behaviors of *C. elegans* can be altered by adaptation, sensitization, and associative learning. A striking change in behavior is caused by starving animals in the presence of NaCl, which is normally an attractive taste. Starvation/salt pairing for as little as ten minutes leads to salt avoidance, a reversal of normal behavior (Tomioka et al., 2006). In salt chemotaxis learning, an insulin signal from a downstream neuron activates an insulin receptor/PI 3-kinase signaling pathway within the ASER salt-sensing neuron to suppress its attractive activity (Tomioka et al., 2006). Mutation of the PI 3-kinase pathway eliminates salt chemotaxis learning, and constitutive activation by a mutation in the PTEN lipid phosphatase *daf-18*

suppresses salt attraction. The ASER sensory neuron has a normal NaCl-evoked sensory response in calcium imaging of PI 3-kinase/*age-1* or PTEN/*daf-18* mutants, indicating that the PI 3-kinase pathway acts downstream of ASER sensory transduction, probably at the level of synaptic modulation (Tomioka et al., 2006). While ASER accounts for the loss of attraction after conditioning, the cellular mechanism of avoidance is less clear. One possibility is that ASER itself can direct attraction or repulsion depending on prior sensory experience (Tomioka et al., 2006). Alternatively, other sensory neurons may drive avoidance of NaCl when ASER's attractive role is silenced after conditioning. Several results support the second, multicellular model for avoidance. For example, if the ASH avoidance neurons are killed or inactivated, animals subjected to starvation/salt conditioning are no longer attracted to salt, but they do not avoid it (Hukema et al., 2006).

Here we examine a switch in olfactory preference in *C. elegans* and provide evidence that a single olfactory neuron can switch between attractive and avoidance behaviors, in violation of the pure labeled-line model. At a behavioral level, alternative chemosensory preferences are associated with reversed biases in turning frequency during odor chemotaxis. At a molecular level, two components of the behavioral switch are axonal cGMP signaling and a DAG/PKC signaling pathway that affects synaptic transmission. Specific sensory experiences alter the balance between attractive and repulsive behavioral states. These results suggest that axonal signaling pathways can rapidly respecify the connections between sensory neurons and behavioral outputs.

Results

gcy-28 mutations switch AWC^{ON} odor preference from attraction to avoidance

The two AWC sensory neurons sense partly overlapping groups of odors. The AWC^{ON} neuron senses butanone, the contralateral AWC^{OFF} neuron senses 2,3-pentanedione, and both AWC neurons sense benzaldehyde and isoamyl alcohol (Troemel et al., 1999; Wes and Bargmann, 2001). A screen for mutants defective in butanone chemotaxis yielded a notable mutant, *gcy-28(ky713),* that avoided butanone instead of approaching it (Fig. 1A, see Experimental Procedures). *gcy-28(ky713)* mutants avoided butanone across a range of concentrations that were attractive to wild-type animals (Fig. S1A). They showed reduced attraction, but not repulsion, to other odors sensed by AWC neurons, and were proficient in chemotaxis to odors sensed by AWA neurons (Fig. 1A). A deletion mutation in the *gcy-28* gene, *gcy-28(tm2411)*, had behavioral defects similar to those of *gcy-28(ky713)*.

The butanone avoidance defect in *gcy-28* mutants could be due to altered activity of AWC^{ON}, or due to altered function of other cells such as avoidance neurons. To distinguish between these possibilities, we examined mutants with defects in known cell types. *ceh-36* mutants lack AWC neurons due to a mutation in an Otx-type homeobox gene (Koga and Ohshima, 2004; Lanjuin et al., 2003). *gcy-28; ceh-36* mutants were not repelled by butanone, suggesting that AWC causes butanone avoidance in *gcy-28* mutants (Fig. 1B). Consistent with a defect in AWC, mutations in the AWC signal transduction genes *odr-1* and *tax-4,* which encode a ciliary guanylate cylase and a cyclic nucleotide-gated channel, respectively, also suppressed butanone avoidance of *gcy-28* mutants (Fig. S1B, data not shown). *gcy-28* butanone avoidance was not affected by a *lim-4* mutation that inactivates AWB avoidance neurons and ADF neurons, by an *osm-9* mutation that

inactivates ASH and ADL avoidance neurons, or by a transgene that kills URX, AQR, and PQR oxygen-sensing neurons (Fig. S1C, S1D, and data not shown).

A marker for AWC^{ON}, *str-2*::GFP, was appropriately expressed in one AWC per animal in *gcy-28* mutants, suggesting that both AWC^{ON} and AWC^{OFF} were specified correctly (data not shown). To examine AWC^{ON} and AWC^{OFF} function independently, we used mutants that eliminated each cell type. *nsy-5* mutants have no AWC^{ON} cells but instead have two AWC^{OFF} cells (Fig. 1C) (Chuang et al., 2007), and *nsy-5 gcy-28* double mutants, like *nsy-5* mutants, were neither attracted to nor repelled by butanone (Fig. 1D). *nsy-1* mutants have two AWC^{ON} neurons and no AWC^{OFF} neurons (Fig. 1C) (Sagasti et al., 2001), and *gcy-28; nsy-1* double mutants showed enhanced avoidance of butanone compared to the *gcy-28* single mutants (Fig. 1E). These results suggest that AWC^{ON} is responsible for butanone avoidance in *gcy-28* mutants. To ask whether the *gcy-28* defect was butanone-specific or more general to AWC^{ON}, the double mutants were examined for benzaldehyde chemotaxis. *gcy-28; nsy-1* double mutants with two AWC^{ON} neurons avoided benzaldehyde (Fig. 1E). This result suggests that the AWC^{ON} neuron is systematically switched to an avoidance function in *gcy-28* mutants.

The AWC^{OFF} neuron is specifically required for chemotaxis to 2,3-pentanedione. *nsy-5, nsy-5 gcy-28* and *gcy-28; nsy-1* mutants all showed diminished attraction to 2,3-pentanedione, but not avoidance (Fig. 1D and E, Fig. S1E). Therefore, AWC^{OFF} function is reduced but not reversed by the *gcy-28* mutation. Reduced, but normal activity of AWC^{OFF} is also suggested by the partial recovery of benzaldehyde chemotaxis in *nsy-5 gcy-28* mutants with two AWC^{OFF} neurons (Fig. 1D), in contrast with the benzaldehyde avoidance of *gcy-28; nsy-1* mutants (Fig. 1E). Benzaldehyde chemotaxis in *gcy-28* single

mutants was variable, as might be expected from an interaction of antagonistic signals from (repulsive) AWC^{ON} and (weakly attractive) AWC^{OFF} neurons.

As a further test of AWC^{ON} function in *gcy-28* mutants, we expressed the diacetyl receptor, ODR-10, in AWC^{ON} (Fig. 1F). In an *odr-10* mutant, expression of *odr-10* in AWC^{ON} restores attraction to diacetyl (Wes and Bargmann, 2001) (Fig. 1F). By contrast, in a *gcy-28;odr-10* double mutant, *odr-10* expression in AWC^{ON} causes animals to avoid diacetyl (Fig. 1F). Thus AWC^{ON} drives odor avoidance in *gcy-28* mutants.

gcy-28 mutants reverse the turning bias in AWC-mediated chemotaxis

To better understand both normal chemotaxis and the behavioral basis of the olfactory defects in *gcy-28* mutants, we analyzed olfactory chemotaxis using the framework of the biased random walk or "pirouette" model that was first developed for taste chemotaxis (Pierce-Shimomura et al., 1999). In the presence of attractive tastes, animals bias their turning frequency as a function of the concentration gradient, turning less when the concentration of an attractant is increasing and turning more when attractant concentration is decreasing (Pierce-Shimomura et al., 1999). This behavioral strategy results in eventual accumulation at an attractant source through a biased random walk, the mechanism of bacterial chemotaxis (Berg and Brown, 1972). Step changes in the concentration of the attractive odor isoamyl alcohol can regulate the turning rates of freely moving animals (Chalasani et al., 2007), or the turning of animals in liquid drops (Luo et al., 2008), but the turning response in odor gradients has not been examined.

Turning responses of *C. elegans* in odor gradients were observed by video microscopy of animals placed between a spot of odor and a spot of diluent (Fig. 2A and

B). The frequency of turns was measured and classified as a function of the angle θ, where θ is the difference between the average direction of the animal's motion in a five-second window before the turn and the direction of the odor source (Fig. 2C). This angle approximates the concentration change the animal had been experiencing, with $\theta < 90°$ corresponding to increasing odor and $\theta > 90°$ corresponding to decreasing odor. Wild-type animals showed net movement toward the odor source (Fig. $2D_1$), increased their turning frequency when heading down the odor gradient, and reduced their turning frequency when heading up the gradient (Fig. $2D_2$, Fig. S2A). In the absence of odor, animals showed neither net migration nor turning bias (Fig. $2E_1$ and E_2). Wild-type animals had a similar turning bias in gradients of several attractive odors sensed by AWC neurons (Fig. 2G-I), and an opposite turning bias to the repulsive odor 2-nonanone, which is sensed by AWB neurons (Fig. S2C and D). These turning behaviors in odor gradients are consistent with a biased random walk model for positive and negative chemotaxis.

A similar analysis with *gcy-28* mutants revealed significant alterations of their turning bias. *gcy-28* mutants showed net movement away from a butanone source (Fig. $2F_1$), increased their turning frequency when heading up the odor gradient, and reduced their turning frequency when heading down the gradient (Fig. $2F_2$, Fig. S2B). In gradients of 2,3-pentanedione or benzaldehyde, *gcy-28* mutants showed little bias in turning frequency with respect to the odor gradient (Fig. 2H and I). Thus the regulated turning response of *gcy-28* mutants to different odors matched their accumulation in chemotaxis assays, with a reversed bias to butanone and no bias to benzaldehyde and 2,3-pentanedione.

To determine whether the turning bias was generated by AWC^{ON}, we used a laser microbeam to kill the AWC^{ON} neuron in wild-type animals and *gcy-28* mutants. Killing AWC^{ON} in wild-type animals abolished the net migration toward butanone (Fig. 3A)(Wes and Bargmann, 2001), and AWC^{ON}-ablated animals in a butanone gradient showed no turning bias going up or down the gradient (Fig. 3B). Killing AWC^{ON} in *gcy-28* animals abolished butanone avoidance (Fig. 3C) and eliminated the butanone-evoked turning bias (Fig. 3D). Overall rates of turning were unchanged after killing AWC^{ON}; only odor regulation was altered. These results indicate that AWC^{ON} is necessary for butanone avoidance in *gcy-28* mutants.

***gcy-28* encodes a receptor-type guanylate cyclase**

gcy-28(ky713) was mapped to the left arm of chromosome I using standard methods, and determined to affect the predicted gene T01A4.1 (*gcy-28*) (Fig 4A, Supplementary Material). *gcy-28* encodes several related receptor-type guanylate cyclases (rGCs), single-spanning transmembrane proteins with an extracellular ligand-binding domain and intracellular kinase-like and guanylate cyclase domains (Fig. 4B). Consistent with its sequence, the cyclase domain of *gcy-28* has guanylate cyclase activity when expressed in heterologous cells (Baude et al., 1997). Three splice forms of *gcy-28* were predicted from the genome sequence (T01A4.1a-c). We confirmed two of three forms by isolation of cDNAs (*gcy-28.a* and *gcy-28.c*, corresponding to T01A4.1a and T01A4.1c, respectively), and identified a fourth splice form, T01A4.1d (*gcy-28.d*), which fuses the upstream predicted gene T01A4.2 to T01A4.1 (Fig. 4A). The three confirmed *gcy-28* isoforms share predicted intracellular domains, but have alternative exons encoding the

N-terminal extracellular domain. The *gcy-28(ky713)* mutation is a C to G transversion predicted to substitute a conserved phenylalanine for a leucine in the cyclase domain (Fig. 4C).

We subsequently obtained *gcy-28(tm2411)* (Shohei Mitani, National Bioresource Project, Japan), a deletion allele that results in a predicted frameshift upstream of the cyclase domain (Fig. 4A and B). The similar phenotypes of *gcy-28(ky713)* and *gcy-28(tm2411)* (Fig. 1A) suggest that strong loss-of-function mutations in *gcy-28* cause AWC chemotaxis defects.

The genome sequence of *C. elegans* predicts 27 genes for rGCs and seven soluble GCs (Morton, 2004; Ortiz et al., 2006). Many of the nematode cyclases result from unique expansions within the nematode clade, but some are shared by nematodes and other invertebrates (Fitzpatrick et al., 2006). *gcy-28* belongs to the natriuretic peptide receptor family of rGCs shared by both vertebrates and invertebrates (Fig. 4D). In mammals, natriuretic peptide signaling is important for proper regulation of blood pressure, cardiac myocyte growth, and bone development (Lopez et al., 1995; Oliver et al., 1997; Tamura et al., 2004; Tsuji and Kunieda, 2005). Although they are expressed in neurons in vertebrates, the role of natriuretic peptide receptors in the nervous system is largely unexplored.

GCY-28 can act in AWC to mediate chemotaxis

A reporter transgene driven by regions upstream of the *gcy-28.c* isoform has widespread expression in neurons and other tissues (Ortiz et al., 2006). We confirmed these results with additional reporters and found expression in almost all neurons, including AWC, as

well as body wall muscle, gut, and hypodermis. The *gcy-28.a* upstream region was expressed in many, but not all, neurons, and the *gcy-28.d* upstream region was expressed in some neurons and in the gut.

A *gcy-28.c* cDNA expressed from its own promoter rescued the chemotaxis defects of *gcy-28* mutants, but failed to rescue when it included the *ky713* mutation (Fig. 5A). Heat-shock expression of *gcy-28.c* in adults resulted in behavioral rescue within two hours, indicating that the gene acts in mature neurons and not during nervous system development (Fig. 5B). The *gcy-28.c* isoform had high rescuing activity when expressed broadly (Fig. 5A-C) but incomplete rescuing activity when expressed only in AWC (Fig. 5D). By contrast, a *gcy-28.d* cDNA rescued chemotaxis when expressed under a pan-neuronal promoter (Fig. 5C), under the AWC-selective *odr-3* promoter (Fig. 5D), or under the AWC^{ON}-selective *str-2* promoter (Fig. 5E). The results with *gcy-28.c* suggest that *gcy-28* may have roles in multiple neurons; nevertheless, the full rescue with *gcy-28.d* suggests that *gcy-28* can function cell-autonomously in AWC^{ON}.

GFP-tagged isoforms of GCY-28.c and GCY-28.d had different subcellular localization in AWC. GCY-28.d, the more active isoform, was enriched in the axonal process, whereas GCY-28.c was present at equivalent levels in dendrites and axons (Fig. 5F). Both isoforms were present in the cell body and excluded from sensory cilia, in contrast with the cilia-localized rGCs ODR-1 and DAF-11, which function in sensory transduction (Birnby et al., 2000; L'Etoile and Bargmann, 2000). The axonal localization of GCY-28 suggests that it does not mediate primary sensory transduction in AWC.

To ask directly whether sensory transduction was affected in *gcy-28* mutants, we measured odor-evoked calcium transients in AWC^{ON} neurons expressing the genetically

encoded calcium indicator G-CaMP. In both wild-type animals and *gcy-28* mutants, removing animals from butanone resulted in a strong increase in AWC^{ON} calcium levels, reported as an increase in G-CaMP fluorescence (Fig. 5G). These results are consistent with prior studies that suggest a hyperpolarizing, or inhibitory, mode of sensory transduction in AWC (Chalasani et al., 2007). Wild type and *gcy-28* showed similar AWC^{ON} responses across a range of butanone concentrations, and similar responses to other AWC-sensed odors (Fig. S3). In both wild-type and *gcy-28* mutant animals, calcium levels in AWC^{ON} were unchanged or decreased upon odor addition (Fig. 5G, Fig. S3). Thus *gcy-28* is not essential for the first steps of sensory transduction in AWC^{ON}.

***gcy-28* interacts with axonal diacylglycerol and protein kinase C signaling**

To establish a potential mechanism for cGMP effects on behavioral preference, we searched for mutations that resembled or suppressed *gcy-28*. A major effector of mammalian natriuretic peptide receptors is the cGMP-dependent kinase (PKG) (Potter et al., 2006). In *C. elegans* a PKG mutant, *egl-4*, has AWC chemotaxis and adaptation defects, as well as defects in other sensory behaviors (Daniels et al., 2000; Fujiwara et al., 2002; L'Etoile et al., 2002). However, close examination suggested that *egl-4* is not the primary target of cGMP from GCY-28: *egl-4* loss-of-function mutants had chemotaxis defects that were qualitatively different from *gcy-28* mutants, and the double mutant had defects different from either single mutant (Fig. S4A). Moreover, a gain-of-function mutation in *egl-4* did not suppress *gcy-28* butanone avoidance or other chemotaxis defects (Fig. S4B).

The presence of GCY-28 protein in axons suggested a possible role in regulation of synaptic function. To investigate this possibility, we examined mutations that alter synaptic transmission. *dgk-1* encodes a diacylglycerol (DAG) kinase that hydrolyzes DAG to phosphatidic acid (PA), and loss-of-function mutations in *dgk-1* increase DAG signaling and enhance cholinergic neurotransmission at the *C. elegans* neuromuscular junction (Lackner et al., 1999; Nurrish et al., 1999). A mutation in *dgk-1* strongly suppressed *gcy-28* chemotaxis defects (Fig. 6A), and this suppression was partially rescued by expressing a *dgk-1* cDNA in AWC (Fig. 6A). To ask whether this effect was due to increased DAG signaling or decreased PA signaling, we used a pharmacological agonist of DAG signaling, the synthetic β-phorbol ester phorbol 12-myristate 13-acetate (PMA) (Colon-Gonzalez and Kazanietz, 2006). Treating *gcy-28* mutants with PMA for two hours rescued their chemotaxis defects (Fig. 6B). Thus increased DAG signaling suppresses *gcy-28,* perhaps by affecting synaptic release.

One of the targets of DAG signaling is protein kinase C (PKC); previous work has shown that AWC chemotaxis requires the function of the *C. elegans* PKC *pkc-1/ttx-4* in AWC (Okochi et al., 2005). We found that the chemotaxis defect in *pkc-1* is similar to that of *gcy-28* (Fig. 6C): *pkc-1* mutants avoided butanone, while showing little preference for benzaldehyde. Functional Ca^{2+} imaging of AWC^{ON} cells in *pkc-1* mutants revealed normal butanone responses, suggesting that the *pkc-1* defect, like the *gcy-28* defect, is not in primary sensory transduction (Fig S5). *gcy-28; pkc-1* double mutants avoided butanone as much as *pkc-1* single mutants, suggesting that these two genes have related functions in AWC chemotaxis (Fig. 6C).

To further explore the similarity between *gcy-28* and *pkc-1,* we asked whether activation of PKC-1 in AWC might rescue *gcy-28* mutants. PKCs can be made constitutively active by an A160E mutation in the autoinhibitory pseudosubstrate motif (Dekker et al., 1993). Expression of PKC-1(A160E) in AWC fully rescued the chemotaxis defects of *gcy-28* mutants (Fig. 6D). Thus synaptic DAG signaling through PKC-1 may act downstream of or in parallel to GCY-28 to regulate the behavioral preference encoded by AWC^{ON}.

AWC sensory neurons synapse onto three classes of interneurons called AIB, AIY, and AIA (White et al., 1986). To ask whether the predicted change in AWC synaptic function might be observed in target neurons, we monitored butanone-evoked calcium responses in the AIB interneurons using G-CaMP. In wild-type animals, AWC has an excitatory connection with AIB, so AIB, like AWC, is activated by odor removal and inhibited by odor addition (Chalasani et al., 2007). AIB had a small but significant increase in calcium after butanone removal in wild-type animals, and a weaker but similar increase in *gcy-28* mutants (Fig. 6E). A difference between wild type and *gcy-28* was observed upon butanone addition: wild-type AIB neurons were inhibited by butanone, but *gcy-28* AIB neurons were not (Fig. 6E).

AWC olfactory preference changes with odor history

Certain odor conditioning protocols can lead to context-dependent, bidirectional modifications in AWC olfactory behavior. Odor conditioning in the absence of food causes adaptation, a reduction in chemotaxis (Colbert and Bargmann, 1995). Odor conditioning in the presence of food causes sensitization, or enhanced chemotaxis

(Torayama et al., 2007). Previous studies have viewed these changes as increases or decreases in odor-specific AWC activity; we hypothesized that these context-dependent behaviors might, instead, affect the competing attractive and repulsive activities of AWC.

In the absence of food, conditioning wild-type animals with butanone for up to 90 minutes causes a butanone-specific reduction in chemotaxis (Colbert and Bargmann, 1995). We found that extending the conditioning to two hours led to butanone avoidance by wild-type animals (Fig. 7A). Long-term butanone conditioning also reduced benzaldehyde chemotaxis in wild-type animals, but did not affect chemotaxis to the AWC^{OFF} odor 2,3-pentanedione, suggesting a broader reduction of AWC^{ON} activity (Fig. 7A). The AWC^{ON} behaviors of butanone-adapted wild-type animals thus resembled the AWC^{ON} behaviors of naïve *gcy-28* mutants. In a *gcy-28* mutant, butanone adaptation did not cause stronger avoidance of butanone or reduced attraction to benzaldehyde, but instead reduced butanone avoidance (Fig. 7A; see also Fig. S7). These results suggest that *gcy-28* mutants occupy a behavioral state that wild-type animals enter after butanone adaptation.

Wild-type animals conditioned with butanone and food increase their chemotaxis to butanone (Fig. 7B). The sensitization response was intact in g*cy-28* mutants; in fact, conditioned *gcy-28* mutants were actually rescued, with levels of chemotaxis comparable to sensitized wild-type animals (Fig. 7B; see also Fig. S7). To determine if sensitization extended to all AWC^{ON} odors, animals were first conditioned with butanone and food, then tested for chemotaxis to benzaldehyde. Wild-type animals showed a small but consistent enhancement of benzaldehyde chemotaxis, and *gcy-28* animals showed striking rescue of their benzaldehyde chemotaxis defect (Fig. 7B). Butanone-induced

sensitization did not affect 2,3-pentanedione chemotaxis (Fig. 7B). The pattern of odor responses suggests that butanone-induced sensitization caused a systematic enhancement of AWC^{ON}-mediated chemotaxis in both wild-type and *gcy-28* animals. The adaptation and sensitization experiments show that specific olfactory experiences can either mimic the *gcy-28* mutation, or rescue it.

Its widespread expression in the nervous system suggests that GCY-28 may have a role in other *C. elegans* behaviors. Indeed, *gcy-28* mutants had subtle defects in salt chemotaxis learning, and they also had strong defects in the regulation of thermotaxis by starvation (Fig. S6) (Mohri et al., 2005; Tomioka et al., 2006). Although neither of these changes is as dramatic as the effect on AWC, they suggest that *gcy-28* signaling regulates multiple forms of sensory plasticity in *C. elegans*.

Discussion

A single-neuron switch between attraction and repulsion

Mutations in the receptor-type guanylate cyclase *gcy-28* lead to an avoidance behavior in place of the attractive behavior normally directed by the AWC^{ON} neuron. The behavioral defect in *gcy-28* mutants can be rapidly rescued by heat shock expression of *gcy-28,* by treatment with the DAG analog PMA, or, most strikingly, by conditioning animals briefly with butanone and food. These results suggest that AWC^{ON} neurons can switch rapidly between attractive and repulsive signaling modes.

A switch between attractive and repulsive signaling may contribute to wild-type behavior after odor adaptation or sensitization (Fig. 7C). The behavior of butanone-adapted animals resembles that of *gcy-28* mutants, and an analogy between the adapted state and the *gcy-28* mutant is suggested by the analysis of DAG signaling: genetic or pharmacological activation of DAG signaling in AWC neurons prevents adaptation in wild-type animals (Matsuki et al., 2006), and reverses the behavioral defects in *gcy-28* mutants. As a potential receptor, GCY-28 could transmit an internal signal about food or another cue to AWC. We suggest that the repulsive drive after adaptation is associated with low *gcy-28* activity and low DAG signaling, and the attractive drive from normal or sensitized AWC neurons is associated with high *gcy-28* activity, DAG signaling, and active *pkc-1*.

Many aspects of AWC^{ON} olfactory neurons revealed by this and other studies parallel those of the ASER gustatory neurons. Based on calcium imaging, both AWC^{ON} and ASER are OFF-sensing cells whose activity rises after decreases in attractive odors or tastes (Chalasani et al., 2007; Suzuki et al., 2008). In their normal attractive modes,

both AWC^{ON} and ASER promote turning behavior when active. Finally, both AWC^{ON} and ASER are subject to plasticity that can reverse the polarity of sensory behavior (Hukema et al., 2006; Tomioka et al., 2006). In each case, the behavioral change is observed despite a normal or near-normal sensory OFF-response. Moreover, both switches involve molecules that regulate lipid signaling and possibly synaptic function -- *dgk-1*and *pkc-1* in AWC^{ON}, and $G_q\alpha$/*egl-30*, PI 3-kinase/*age-1*, and PTEN/*daf-18* in ASER (Tomioka et al., 2006).

For ASER, the behavioral switch after salt conditioning is regulated by a secreted insulin signal made by AIA interneurons (Tomioka et al., 2006). Several other neurons also contribute to salt plasticity, suggesting that conditioning affects multiple cell types. Although plasticity of the ASER neurons can fully explain the loss of attraction after conditioning, the switch to repulsion requires ASH avoidance neurons, ADF neurons, and URX, AQR, and PQR oxygen-avoidance neurons (Hukema et al., 2006). It is possible that ASER switches to an avoidance function, but it is not clear whether it does so. By contrast, our results show that repulsion directed by AWC^{ON} does not require any of the known avoidance neurons (AWB, ASH, ADL, URX, AQR, PQR) or ADF. Instead, AWC^{ON} appears to reverse its behavioral strategy directly, by changing its regulation of turning behavior during chemotaxis..

The gustatory ASE neurons and olfactory AWC neurons each have bilaterally asymmetric gene expression, and in each case the left-right pairs detect overlapping, but distinct, chemicals (Hobert et al., 2002). However, the functional asymmetry of these neurons is manifested differently in behavior. ASEL and ASER have reciprocal sensory and behavioral properties: unlike ASER, ASEL is an ON-sensing cell whose activity

rises when attractive tastes appear, and ASEL inhibits turning when active (Suzuki et al., 2008). AWC^{ON} and AWC^{OFF} are more similar; they are both OFF-sensing cells that stimulate turning when active (Chalasani et al., 2007). The AWCs differ, however, in their apparent sensitivity to the *gcy-28* and *pkc-1* signaling pathways, which reverse odor preference in AWC^{ON} but not in AWC^{OFF}. One interesting possibility suggested by the behavioral analysis of *gcy-28* turning behavior is that *gcy-28* switches AWC^{ON} between an ASER-like behavioral output that stimulates turning, and an ASEL-like behavioral output that inhibits turning.

Modulation of synaptic transmission may modify sensory preference

The similar chemotaxis phenotypes of *gcy-28* and *pkc-1* mutants and the genetic interactions between *gcy-28* and the DAG/PKC pathway suggest that these two signaling pathways regulate a common process in AWC^{ON}. The most likely possibilities are excitability or synaptic release. The most active GCY-28 isoform resides in axons, and while subject to the potential artifacts of GFP-tagged proteins, its localization suggests an interaction with the synaptic machinery. Synaptic transmission in vertebrate neurons can be regulated by cGMP-regulated protein kinases, cGMP-gated channels, and cGMP-regulated phosphodiesterases (Herring et al., 2001; Murphy and Isaacson, 2003; Richard and Bourque, 1996; Savchenko et al., 1997; Yu et al., 2006). DAG and phorbol esters modulate synaptic transmission by activating PKCs and Munc13/UNC-13 (Betz et al., 1998; Lackner et al., 1999; Shapira et al., 1987); in *C. elegans*, genetic or pharmacological manipulations that increase DAG enhance synaptic transmission, and PKC-1 regulates neuropeptide release (Nurrish et al., 1999; Lackner et al., 1999; Sieburth

et al., 2007). The DAG/PKC synaptic signaling pathway is implicated in thermal behavioral plasticity, where DAG signaling affects the synaptic output of AFD thermosensory neurons (Okochi et al., 2005; Biron et al., 2006).

The altered butanone-evoked calcium signals in AIB are consistent with a change in synaptic function in *gcy-28* mutants. It is interesting that the defect appears mainly upon odor addition, which normally suppresses AIB activity, because it suggests that suppression and activation of AIB could each convey unique information. Electrophysiology in *Ascaris* has demonstrated that nematode motor neurons have graded neurotransmission; they release tonic transmitter at rest, increase release upon depolarization, and decrease it upon hyperpolarization (Davis and Stretton, 1989). If AWC^{ON} has similar synaptic properties, the altered AIB response in *gcy-28* could result from changes in tonic AWC^{ON} transmission, changes in hyperpolarization suppression of release, or an altered resting potential. These results should be interpreted with caution; the effects of *gcy-28* on AIB are subtle, and the cellular site of action has not been determined, so they could be direct or indirect.

There are several mechanisms by which *gcy-28* could alter turning behavior. AWC neurons use glutamate as a transmitter and also express neuropeptides, either of which could be regulated by *gcy-28* (Chalasani et al., 2007; Nathoo et al., 2001). *gcy-28* could redistribute the weights of AWC connections with its functionally distinct synaptic partners, AIA, AIB, and AIY (White et al., 1986; Chalasani et al., 2007). *gcy-28* could also alter the quality of AWC connection with individual synaptic partners: AWC normally activates the AIB target neuron and inhibits the AIY target neuron, but can activate AIY in certain receptor mutants (Chalasani et al., 2007). The biased random walk

strategy for chemotaxis is intrinsically probabilistic and variable. Through relatively simple changes in synaptic weights or dynamics, the probabilistic circuit may have more flexibility to change its properties than deterministic circuits with fixed behavioral outputs.

GCY-28 is the sole *C. elegans* member of the natriuretic peptide receptor family, corresponding to vertebrate guanylate cyclase A (GC-A) and guanylate cyclase B (GC-B)(Potter et al., 2006). The natriuretic peptides do not have obvious homologs in the *C. elegans* genome; if there is a peptide ligand for GCY-28, it may have a distinct structure. Both GC-A and GC-B are expressed in the vertebrate brain, and in the rat olfactory bulb (Gutkowska et al., 1997; Potter et al., 2006); it will be interesting to ask whether they have a role in olfactory behavior.

Context and experience modify sensory preferences in all animals. In *C. elegans,* we find that modulatory pathways acting in single sensory neurons can transform behaviors, allowing behavioral changes to emerge from changes in peripheral neurons. *C. elegans* has a small nervous system, but more complex animals also have anatomical pathways that support peripheral modulation. The mammalian olfactory bulb receives central innervation from adrenergic, serotonergic, and cholinergic fibers that could act as early as the presynaptic terminal of olfactory sensory neurons (Gomez et al., 2005). Our results suggest that modulatory information at this first synapse might generate qualitative differences in olfactory signaling, not just increases or decreases in sensory activity. Rapid behavioral switching provides a new view of the functional plasticity that can be generated within a fixed neuroanatomy.

Experimental Procedures

Standard techniques were used for nematode culture and molecular biology. A complete strain list, description of *gcy-28* cloning, detailed molecular biology, and sequence analysis methods are in Supplementary Material.

Behavioral assays

Population chemotaxis assays were performed on assay agar (1.6 % agar, 1 mM $MgSO_4$, 1 mM $MgCl_2$, 5 mM phosphate buffer, pH 6.0) in 10 cm square plates, which are better for detecting avoidance behavior than round assay plates (Troemel et al., 1997). Unless otherwise indicated, odor dilutions in ethanol were 2-butanone 1:1,000; 2,3-pentanedione 1:10,000; benzaldehyde 1:200; diacetyl 1:1,000; 2-methylpyrazine 1:1,000; 2-nonanone 1:10. 2 µl of diluted odor was placed on one side of the plate, and 2 µl of ethanol at the other side, with azide to anaesthetize animals that reached odor or ethanol sources. Washed adult animals were placed in the center of the plate, and the distribution of animals counted after 1-2 hours. A score of 1.0 represents perfect attraction, -1.0 perfect repulsion, and 0 random behavior. All data points are averages of ≥ 4 assays, with ≥ 50 animals each, repeated on at least two different days.

For tracking assays (Fig. 2, 3), about 50 animals were picked onto an NGM plate without bacteria, washed with S-basal and assay buffer, and placed on round 10 cm plates with assay agar. Excess liquid was wicked off, and recording was started after a spot of odor and diluent were placed on the agar surface. Unlike standard chemotaxis assays, no sodium azide was added. Tracking assays were performed under a dissecting scope

(Stemi 2000; Zeiss, Thornwood, NY) with a custom-modified base that illuminates a wide field (Serco Technical Services, Livermore, CA). The field was captured by a digital camera (MacroFire; Optronics, Goleta, CA) with 1240x1240 pixel resolution at 2 frames per second. Captured movies were analyzed using MATLAB (MathWorks, Natick, MA) scripts (Ramot et al., 2008; http://wormsense.stanford.edu/). Tracks were segmented into turns and runs, essentially as described (Pierce-Shimomura et al., 1999). Runs were analyzed in 5-second bins, and an average bearing relative to the odor was obtained for each bin. Absolute angles were binned in 30° intervals.

PMA treatment was performed as described (Okochi et al., 2005). Briefly, adult animals were washed onto culture plates with 1 μg/ml PMA (PMA+) or DMSO solvent (PMA-) in the agar, incubated at room temperature for two hours, and then tested for chemotaxis in drug-free assay plates.

Heat shock treatment was performed as described (L'Etoile et al., 2002). Animals were incubated at 33°C for two hours, and then incubated for another two hours at 20°C before testing for chemotaxis.

Butanone sensitization assays were performed as described, with some modifications (Torayama et al., 2007). Animals on their NGM growth plate were exposed to butanone vapor by spotting 12 μL of butanone on agar plugs on the plate lid and sealing the plate with parafilm. After 90 minutes animals were washed and tested for chemotaxis on square plates. The butanone dilution used for chemotaxis was 1:1000. Adaptation assays were performed essentially as described (Colbert and Bargmann, 1995). Animals were washed and placed on 3% assay agar plates. 20 μL butanone was placed on agar plugs on the plate lid and the plates were sealed with parafilm. After two

hours animals were washed off and tested for chemotaxis on square plates. Controls were treated identically except that butanone was omitted from the conditioning plate.

Laser ablations were performed on L1 animals as described (Bargmann and Avery, 1995). The AWC^{ON} cell was identified by expression of *str-2::GFP* in the integrated strain CX6343. About 20 animals were ablated for each tracking assay, and some animals were tested twice on two different days.

Calcium imaging

Calcium imaging was performed as described (Chalasani et al., 2007; Chronis et al., 2007). For AWC^{ON} imaging, the strain CX10281 expresses the calcium indicator G-CaMP2.0 (Tallini et al., 2006) in AWC^{ON} under the *str-2* promoter. *gcy-28(tm2411)* and *pkc-1(nj1)* were crossed into CX10281 to generate the strains CX10223 and CX10784, respectively. For AIB imaging, the strain CX7469 expressing G-CaMP1.0 in AIB neurons (Chalasani et al., 2007) was crossed with *gcy-28(tm2411)* to generate the strain CX8994. Animals were washed in buffer without food for ~20 minutes prior to imaging, a protocol designed to mimic the washes before chemotaxis assays. This brief washing step enhances the reliability of chemotaxis and of AWC calcium imaging. Imaging was conducted in a polydimethylsiloxane (PDMS) chamber in which an animal's nose was exposed to a stream of buffer that could be switched between odor-containing and odor-free solutions using an electronically gated valve. The standard stimulus protocol consisted of a 5-minute step pulse of the indicated dilution of odor in S-basal (without cholesterol) followed by odor removal. G-CaMP fluorescence intensity was measured for 10 seconds before and 50 seconds after the onset or offset of the odor stimulus; the

same animals were imaged for odor onset and offset. All G-CaMP strains had the appropriate olfactory behaviors for their respective genetic backgrounds.

Acknowledgments

We thank the late David Garbers, Norio Suzuki, Isao Katsura, Loren Looger, the National Bioresource Project, and the *Caenorhabditis* Genetic Center (CGC) for strains and reagents; Daniel Ramot, Miriam Goodman, Jennifer Garrison, Carl Procko, and Shai Shaham for methods and advice; and members of the Bargmann lab for comments and discussions. MT designed and conducted genetic and behavioral experiments; MT and CHS conducted imaging experiments; MT and CIB interpreted results and wrote the paper. This work was funded by NIDCD and by the G. Harold and Leila Y. Mathers Charitable Foundation. CIB is an Investigator of the Howard Hughes Medical Institute.

References

Bargmann, C.I., Chemosensation in *C. elegans* (October 25, 2006), *WormBook*, ed. The *C. elegans* Research Community, WormBook, 10.1895/wormbook.1.123.1, http://www.wormbook.org

Bargmann, C.I., and Avery, L. (1995). Laser killing of cells in *Caenorhabditis elegans*. Methods Cell Biol *48*, 225-250.

Baude, E.J., Arora, V.K., Yu, S., Garbers, D.L., and Wedel, B.J. (1997). The cloning of a *Caenorhabditis elegans* guanylyl cyclase and the construction of a ligand-sensitive mammalian/nematode chimeric receptor. J Biol Chem *272*, 16035-16039.

Berg, H.C., and Brown, D.A. (1972). Chemotaxis in *Escherichia coli* analysed by three-dimensional tracking. Nature *239*, 500-504.

Betz, A., Ashery, U., Rickmann, M., Augustin, I., Neher, E., Sudhof, T.C., Rettig, J., and Brose, N. (1998). Munc13-1 is a presynaptic phorbol ester receptor that enhances neurotransmitter release. Neuron *21*, 123-136.

Biron, D., Shibuya, M., Gabel, C., Wasserman, S.M., Clark, D.A., Brown, A., Sengupta, P., and Samuel, A.D. (2006). A diacylglycerol kinase modulates long-term thermotactic behavioral plasticity in *C. elegans*. Nat Neurosci *9*, 1499-1505.

Birnby, D.A., Link, E.M., Vowels, J.J., Tian, H., Colacurcio, P.L., and Thomas, J.H. (2000). A transmembrane guanylyl cyclase (DAF-11) and Hsp90 (DAF-21) regulate a common set of chemosensory behaviors in *Caenorhabditis elegans*. Genetics *155*, 85-104.

Chalasani, S.H., Chronis, N., Tsunozaki, M., Gray, J.M., Ramot, D., Goodman, M.B., and Bargmann, C.I. (2007). Dissecting a circuit for olfactory behaviour in *Caenorhabditis elegans*. Nature *450*, 63-70.

Chronis, N., Zimmer, M., and Bargmann, C.I. (2007). Microfluidics for in vivo imaging of neuronal and behavioral activity in *Caenorhabditis elegans*. Nat Methods *4*, 727-731.

Chuang, C.F., Vanhoven, M.K., Fetter, R.D., Verselis, V.K., and Bargmann, C.I. (2007). An innexin-dependent cell network establishes left-right neuronal asymmetry in *C. elegans*. Cell *129*, 787-799.

Colbert, H.A., and Bargmann, C.I. (1995). Odorant-specific adaptation pathways generate olfactory plasticity in *C. elegans*. Neuron *14*, 803-812.

Colon-Gonzalez, F., and Kazanietz, M.G. (2006). C1 domains exposed: from diacylglycerol binding to protein-protein interactions. Biochim Biophys Acta *1761*, 827-837.

Daniels, S.A., Ailion, M., Thomas, J.H., and Sengupta, P. (2000). *egl-4* acts through a transforming growth factor-beta/SMAD pathway in *Caenorhabditis elegans* to regulate multiple neuronal circuits in response to sensory cues. Genetics *156*, 123-141.

Davis, R.E., and Stretton, A.O. (1989). Signaling properties of *Ascaris* motorneurons: graded active responses, graded synaptic transmission, and tonic transmitter release. J Neurosci *9,* 415-425.

Dekker, L.V., McIntyre, P., and Parker, P.J. (1993). Mutagenesis of the regulatory domain of rat protein kinase C-eta. A molecular basis for restricted histone kinase activity. J Biol Chem *268*, 19498-19504.

Fitzpatrick, D.A., O'Halloran, D.M., and Burnell, A.M. (2006). Multiple lineage specific expansions within the guanylyl cyclase gene family. BMC Evol Biol *6*, 26.

Fujiwara, M., Sengupta, P., and McIntire, S.L. (2002). Regulation of body size and behavioral state of *C. elegans* by sensory perception and the EGL-4 cGMP-dependent protein kinase. Neuron *36*, 1091-1102.

Gomez, C., Brinon, J.G., Barbado, M.V., Weruaga, E., Valero, J., and Alonso, J.R. (2005). Heterogeneous targeting of centrifugal inputs to the glomerular layer of the main olfactory bulb. J Chem Neuroanat *29,* 238-254.

Gutkowska, J., Antunes-Rodrigues, J., and McCann, S.M. (1997). Atrial natriuretic peptide in brain and pituitary gland. Physiol Rev *77*, 465-515.

Herring, N., Zaman, J.A., and Paterson, D.J. (2001). Natriuretic peptides like NO facilitate cardiac vagal neurotransmission and bradycardia via a cGMP pathway. Am J Physiol Heart Circ Physiol *281*, H2318-2327.

Hobert, O., Johnston, R.J., Jr., and Chang, S. (2002). Left-right asymmetry in the nervous system: the *Caenorhabditis elegans* model. Nat Rev Neurosci *3,* 629-640.

Hukema, R.K., Rademakers. S., Dekkers, M.P.J., Burghoorn, J., and Jansen, G. (2006). Antagonistic sensory cues generate gustatory plasticity in *Caenorhabditis elegans.* EMBO J 25, 312-322.

Koga, M., and Ohshima, Y. (2004). The *C. elegans ceh-36* gene encodes a putative homemodomain transcription factor involved in chemosensory functions of ASE and AWC neurons. J Mol Biol *336*, 579-587.

L'Etoile, N.D., and Bargmann, C.I. (2000). Olfaction and odor discrimination are mediated by the *C. elegans* guanylyl cyclase ODR-1. Neuron *25*, 575-586.

L'Etoile, N.D., Coburn, C.M., Eastham, J., Kistler, A., Gallegos, G., and Bargmann, C.I. (2002). The cyclic GMP-dependent protein kinase EGL-4 regulates olfactory adaptation in *C. elegans*. Neuron *36*, 1079-1089.

Lackner, M.R., Nurrish, S.J., and Kaplan, J.M. (1999). Facilitation of synaptic transmission by EGL-30 Gqalpha and EGL-8 PLCbeta: DAG binding to UNC-13 is required to stimulate acetylcholine release. Neuron *24*, 335-346.

Lanjuin, A., VanHoven, M.K., Bargmann, C.I., Thompson, J.K., and Sengupta, P. (2003). Otx/otd homeobox genes specify distinct sensory neuron identities in *C. elegans*. Dev Cell *5*, 621-633.

Lopez, M.J., Wong, S. K., Kishimoto, I., Dubois, S., Mach, V., Friesen, J., Garbers, D. L., and Beuve, A. (1995). Salt-resistant hypertension in mice lacking the guanylyl cyclase-A receptor for atrial natriuretic peptide. Nature *378*, 65-68.

Luo, L., Gabel, C.V., Ha, H. ., Zhang, Y., and Samuel, A.D. (2008). Olfactory behavior of swimming *C. elegans* analyzed by measuring motile responses to temporal variations of odorants. J Neurophysiol *9,* 2617-2625.

Marella, S., Fischler, W., Kong, P., Asgarian, S., Rueckert, E., and Scott, K. (2006). Imaging taste responses in the fly brain reveals a functional map of taste category and behavior. Neuron *49*, 285-295.

Matsuki, M., Kunitomo, H., and Iino, Y. (2006). Goalpha regulates olfactory adaptation by antagonizing Gqalpha-DAG signaling in *Caenorhabditis elegans*. Proc Natl Acad Sci USA *103*, 1112-1117.

Mohri, A., Kodama, E., Kimura, K.D., Koike, M., Mizuno, T., and Mori, I. (2005). Genetic control of temperature preference in the nematode *Caenorhabditis elegans*. Genetics *169*, 1437-1450.

Morton, D.B. (2004). Invertebrates yield a plethora of atypical guanylyl cyclases. Mol Neurobiol *29*, 97-116.

Mueller, K.L., Hoon, M.A., Erlenbach, I., Chandrashekar, J., Zuker, C.S., and Ryba, N.J. (2005). The receptors and coding logic for bitter taste. Nature *434*, 225-229.

Murphy, G.J., and Isaacson, J.S. (2003). Presynaptic cyclic nucleotide-gated ion channels modulate neurotransmission in the mammalian olfactory bulb. Neuron *37*, 639-647.

Nathoo, A.N., Moeller, R.A., Westlund, B.A., and Hart, A.C. (2001). Identification of neuropeptide-like protein gene families in *Caenorhabditis elegans* and other species. Proc Natl Acad Sci USA *98*, 14000-14005.

Nurrish, S., Segalat, L., and Kaplan, J.M. (1999). Serotonin inhibition of synaptic transmission: Galpha(0) decreases the abundance of UNC-13 at release sites. Neuron *24*, 231-242.

Okochi, Y., Kimura, K.D., Ohta, A., and Mori, I. (2005). Diverse regulation of sensory signaling by *C. elegans* nPKC-epsilon/eta TTX-4. Embo J *24*, 2127-2137.

Oliver, P.M., Fox, J.E., Kim, R., Rockman, H.A., Kim, H.S., Reddick, R.L., Pandey, K.N., Milgram, S.L., Smithies, O., and Maeda, N. (1997). Hypertension, cardiac hypertrophy, and sudden death in mice lacking natriuretic peptide receptor A. Proc Natl Acad Sci USA *94*, 14730-14735.

Ortiz, C.O., Etchberger, J.F., Posy, S.L., Frokjaer-Jensen, C., Lockery, S., Honig, B., and Hobert, O. (2006). Searching for neuronal left/right asymmetry: genomewide analysis of nematode receptor-type guanylyl cyclases. Genetics *173*, 131-149.

Pierce-Shimomura, J.T., Morse, T.M., and Lockery, S.R. (1999). The fundamental role of pirouettes in *Caenorhabditis elegans* chemotaxis. J Neurosci *19*, 9557-9569.

Potter, L.R., Abbey-Hosch, S., and Dickey, D.M. (2006). Natriuretic peptides, their receptors, and cyclic guanosine monophosphate-dependent signaling functions. Endocr Rev *27*, 47-72.

Ramot, D., Johnson, B.E., Berry, T.L., Jr., Carnell, L., and Goodman, M.B. (2008). The Parallel Worm Tracker: a platform for measuring average speed and drug-induced paralysis in nematodes. PLoS ONE *3,* e2208.

Richard, D., and Bourque, C.W. (1996). Atrial natriuretic peptide modulates synaptic transmission from osmoreceptor afferents to the supraoptic nucleus. J Neurosci *16*, 7526-7532.

Robertson, H.M., and Thomas, J.H., The putative chemoreceptor families of *C. elegans* (January 06, 2006), *WormBook*, ed. The *C. elegans* Research Community, WormBook, 10.1895/wormbook.1.66.1, http://www.wormbook.org.

Sagasti, A., Hisamoto, N., Hyodo, J., Tanaka-Hino, M., Matsumoto, K., and Bargmann, C.I. (2001). The CaMKII UNC-43 activates the MAPKKK NSY-1 to execute a lateral signaling decision required for asymmetric olfactory neuron fates. Cell *105*, 221-232.

Savchenko, A., Barnes, S., and Kramer, R.H. (1997). Cyclic-nucleotide-gated channels mediate synaptic feedback by nitric oxide. Nature *390*, 694-698.

Sengupta, P., Chou, J.H., and Bargmann, C.I. (1996). *odr-10* encodes a seven transmembrane domain olfactory receptor required for responses to the odorant diacetyl. Cell *84*, 899-909.

Shapira, R., Silberberg, S.D., Ginsburg, S., and Rahamimoff, R. (1987). Activation of protein kinase C augments evoked transmitter release. Nature *325*, 58-60.

Sieburth, D., Madison, J.M., and Kaplan, J.M. (2007). PKC-1 regulates secretion of neuropeptides. Nat Neurosci *10*, 49-57.

Suzuki, H., Thiele, T.R., Faumont, S., Ezcurra, M., Lockery, S.R., and Schafer, W.R. (2008). Functional asymmetry in *Caenorhabditis elegans* taste neurons and its computational role in chemotaxis. Nature *454,* 114-117.

Tallini, Y.N., Ohkura, M., Choi, B.R., Ji, G., Imoto, K., Doran, R., Lee, J., Plan, P., Wilson, J., Xin, H.B., et al. (2006). Imaging cellular signals in the heart in vivo:

Cardiac expression of the high-signal Ca2+ indicator GCaMP2. Proc Natl Acad Sci USA *103,* 4753-4758.

Tamura, N., Doolittle, L.K., Hammer, R.E., Shelton, J.M., Richardson, J.A., and Garbers, D.L. (2004). Critical roles of the guanylyl cyclase B receptor in endochondral ossification and development of female reproductive organs. Proc Natl Acad Sci USA *101*, 17300-17305.

Thorne, N., Chromey, C., Bray, S., and Amrein, H. (2004). Taste perception and coding in *Drosophila*. Curr Biol *14*, 1065-1079.

Tobin, D., Madsen, D., Kahn-Kirby, A., Peckol, E., Moulder, G., Barstead, R., Maricq, A., and Bargmann, C.I. (2002). Combinatorial expression of TRPV channel proteins defines their sensory functions and subcellular localization in *C. elegans* neurons. Neuron *35*, 307-318.

Tomioka, M., Adachi, T., Suzuki, H., Kunitomo, H., Schafer, W.R., and Iino, Y. (2006). The insulin/PI 3-kinase pathway regulates salt chemotaxis learning in *Caenorhabditis elegans*. Neuron *51*, 613-625.

Torayama, I., Ishihara, T., and Katsura, I. (2007). *Caenorhabditis elegans* integrates the signals of butanone and food to enhance chemotaxis to butanone. J Neurosci *27*, 741-750.

Troemel, E.R., Kimmel, B.E., Bargmann, C.I., (1997). Reprogramming chemotaxis responses: sensory neurons define olfactory preferences in *C. elegans*. Cell *91*, 161-169.

Troemel, E.R., Sagasti, A., and Bargmann, C.I. (1999). Lateral signaling mediated by axon contact and calcium entry regulates asymmetric odorant receptor expression in *C. elegans*. Cell *99*, 387-398.

Tsuji, T., and Kunieda, T. (2005). A loss-of-function mutation in natriuretic peptide receptor 2 (Npr2) gene is responsible for disproportionate dwarfism in *cn/cn* mouse. J Biol Chem *280*, 14288-14292.

Wang, Z., Singhvi, A., Kong, P., and Scott, K. (2004). Taste representations in the *Drosophila* brain. Cell *117*, 981-991.

Wes, P.D., and Bargmann, C.I. (2001). *C. elegans* odour discrimination requires asymmetric diversity in olfactory neurons. Nature *410*, 698-701.

White, J.G., Southgate, E., Thomson, J.N., and Brenner, S. (1986). The structure of the nervous system of the nematode *Caenorhabditis elegans*. Phil Trans R Soc Lond B *314*, 1-340.

Yu, Y.C., Cao, L.H., and Yang, X.L. (2006). Modulation by brain natriuretic peptide of GABA receptors on rat retinal ON-type bipolar cells. J Neurosci *26*, 696-707.

Zhao, G.Q., Zhang, Y., Hoon, M.A., Chandrashekar, J., Erlenbach, I., Ryba, N.J., and Zuker, C.S. (2003). The receptors for mammalian sweet and umami taste. Cell *115*, 255-266.

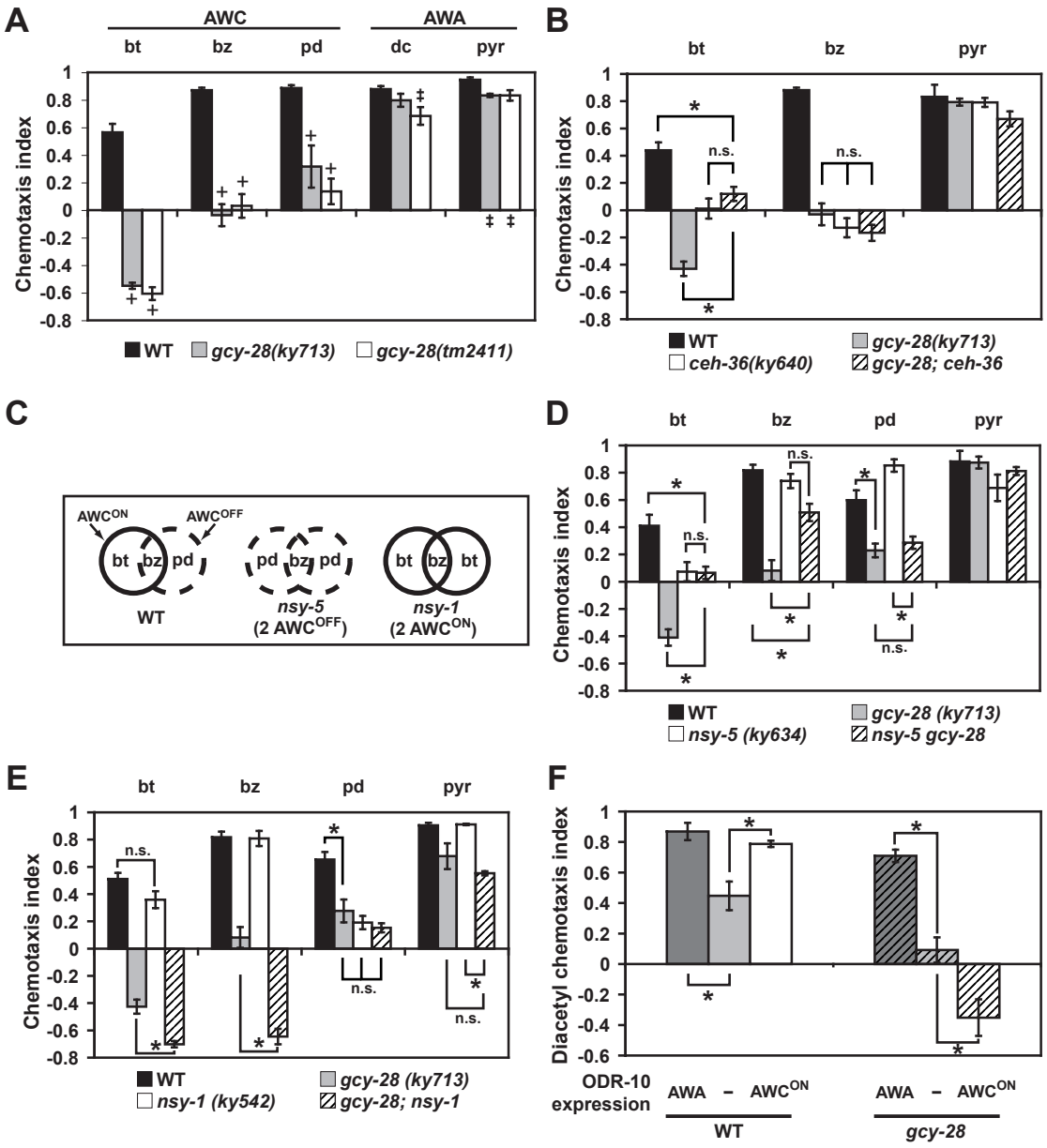

A
AWC
AWA
bt
bz
pd
dc
pyr
Chemotaxis index
WT
gcy-28(ky713)
gcy-28(tm2411)
B
bt
bz
pyr
n.s.
WT
gcy-28(ky713)
ceh-36(ky640)
gcy-28; ceh-36
C
AWC^ON
AWC^OFF
WT
nsy-5
(2 AWC^OFF)
nsy-1
(2 AWC^ON)
D
bt
bz
pd
pyr
n.s.
WT
gcy-28 (ky713)
nsy-5 (ky634)
nsy-5 gcy-28
E
bt
bz
pd
pyr
n.s.
WT
gcy-28 (ky713)
nsy-1 (ky542)
gcy-28; nsy-1
F
Diacetyl chemotaxis index
ODR-10
expression
AWA – AWC^ON
WT
gcy-28

Figure 3-1

Figure 3-1. AWC^{ON} mediates odor avoidance instead of attraction in *gcy-28* mutants

(A) Chemotaxis of wild-type and *gcy-28* mutant animals to AWC- and AWA-sensed odors. (B) Effect of a *ceh-36* mutation on *gcy-28* chemotaxis. *ceh-36* mutants lack functional AWC and ASEL neurons. (C) Venn diagram representation of odor specificity in the AWC^{ON} (solid-line) and AWC^{OFF} (dashed-line) neurons. (D) Effect of a *nsy-5* mutation (2 AWC^{OFF} neurons) on *gcy-28* chemotaxis. (E) Effect of a *nsy-1* mutation (2 AWC^{ON} neurons) on *gcy-28* chemotaxis. (F) Diacetyl chemotaxis in strains misexpressing ODR-10 using the AWC^{ON}-selective *str-2* promoter. *odr-10* is normally expressed in AWA. + $p < 0.01$, ‡ $p < 0.05$ compared to wild type by Dunnett test. * $p < 0.05$, Bonferroni t-test. Error bars represent standard error of the mean (SEM). Abbreviations: WT, wild type; bt, 2-butanone; bz, benzaldehyde; pd, 2,3-pentanedione; dc, diacetyl; pyr, 2-methylpyrazine; n.s., not significant.

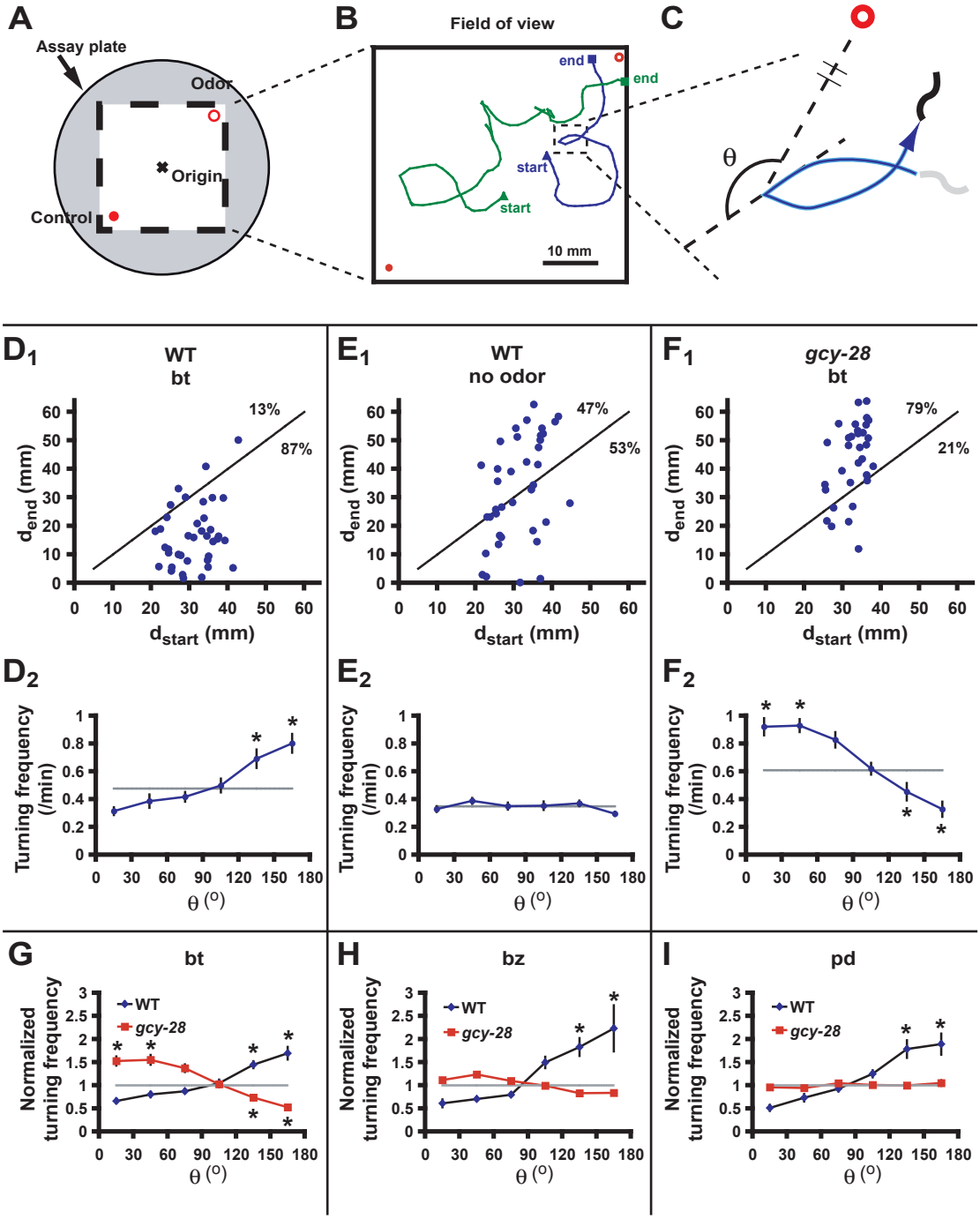

A
Assay plate
Odor
Origin
Control
B
Field of view
end
end
start
start
10 mm
C
θ
D1
WT
bt
13%
87%
dend (mm)
dstart (mm)
E1
WT
no odor
47%
53%
F1
gcy-28
bt
79%
21%
D2
E2
F2
Turning frequency (/min)
θ (°)
G
bt
H
bz
I
pd
Normalized turning frequency
WT
gcy-28

Figure 3-2

Figure 3-2. Regulated turning during chemotaxis to odors

(A) Chemotaxis tracking assay. The odor (open circle) and control (closed circle) spots were spaced 64 mm apart, and animals were placed at the origin. Behavior of animals was recorded for 15 minutes. (B) Representative tracks made by two wild-type animals migrating up a butanone gradient. The beginning and end of the tracks are marked. A track ends when the animal either exits the field of view or reaches within ~5 mm of the odor or the control spot. (C) A section of a track before and after a turning event. Angle θ represents the difference between the animal's direction of motion during a five-second interval before the turn and the direction to the odor. (D, E and F) Chemotaxis and regulated turning. (D_1, E_1, F_1) d_{start} and d_{end} represent the distance between the animal and the odor at the beginning and the end, respectively, of an animal's track. Points below the diagonal are animals showing net migration toward the source; point above the diagonal, animals showing net migration away from the source. The percentages of animals above and below the diagonal are indicated. In the absence of odor (E), one control source was chosen arbitrarily as the reference point. Scatter plots are representative data from one assay each. (D_2, E_2 and F_2) Turning frequency plots representing averages of at least five assays each. The grey line represents the mean turning frequency over all assays for each condition. Wild-type animals showed no turning bias in the absence of odor (one-way ANOVA, $p > 0.1$). Similar turning biases were observed throughout the 15-minute assay (Fig. S2A and B). (G, H and I) Turning in gradients of different odors. Turning frequencies were normalized to the mean frequency of each individual assay. * $p < 0.05$ relative to the mean by Dunnett test. *gcy-28* animals showed no turning bias toward pd (one-way ANOVA, $p = 0.96$). *gcy-28* animals

had a significant bias in response to bz by one-way ANOVA ($p = 0.003$) but a post-hoc Dunnett test showed no significant deviations from the average ($p > 0.05$). *gcy-28; nsy-1* double mutants, which avoid benzaldehyde (Fig. 1E), had a small but significant reversal in turning bias compared to wild-type (Fig. S2E and F). Error bars show SEM.

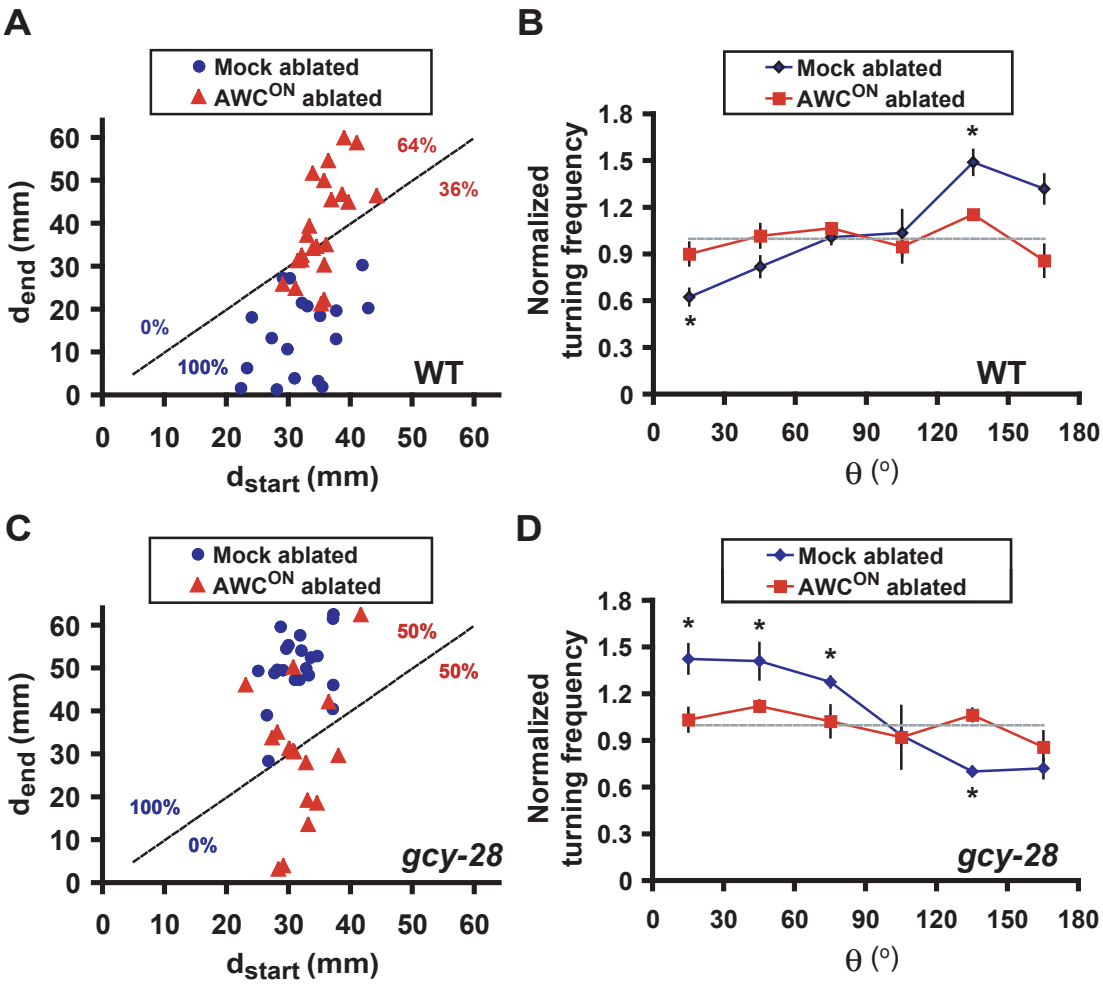

A
Mock ablated
AWC^ON ablated
64%
36%
0%
100%
WT
d_end (mm)
d_start (mm)
B
Mock ablated
AWC^ON ablated
Normalized turning frequency
WT
θ (°)
C
Mock ablated
AWC^ON ablated
50%
50%
100%
0%
gcy-28
d_end (mm)
d_start (mm)
D
Mock ablated
AWC^ON ablated
Normalized turning frequency
gcy-28
θ (°)

Figure 3-3

Figure 3-3. Ablation of AWC^{ON} abolishes turning bias in wild type and *gcy-28* animals

Tracking analysis of chemotaxis and turning bias in AWC^{ON}-ablated and control mock-ablated animals. (A and B) Wild-type animals. (C and D) *gcy-28(ky713)* mutants. In the scatter plots, the percentages of animals falling above or below the diagonal for mock-ablated and AWC^{ON}-ablated animals are indicated in blue and red, respectively. Net displacement ($d_{end} - d_{start}$) between mock and AWC^{ON}-ablated animals is significantly different for both wild-type and *gcy-28* animals (Mann-Whitney test, $p < 0.01$). Turning frequency is normalized to the mean frequency of each condition. Ablated animals do not show any significant turning bias (one-way ANOVA, WT: $p = 0.36$, *gcy-28*: $p = 0.85$). Turning frequencies are an average of three assays. Error bars represent SEM. * $p < 0.05$ relative to the mean by Dunnett test.

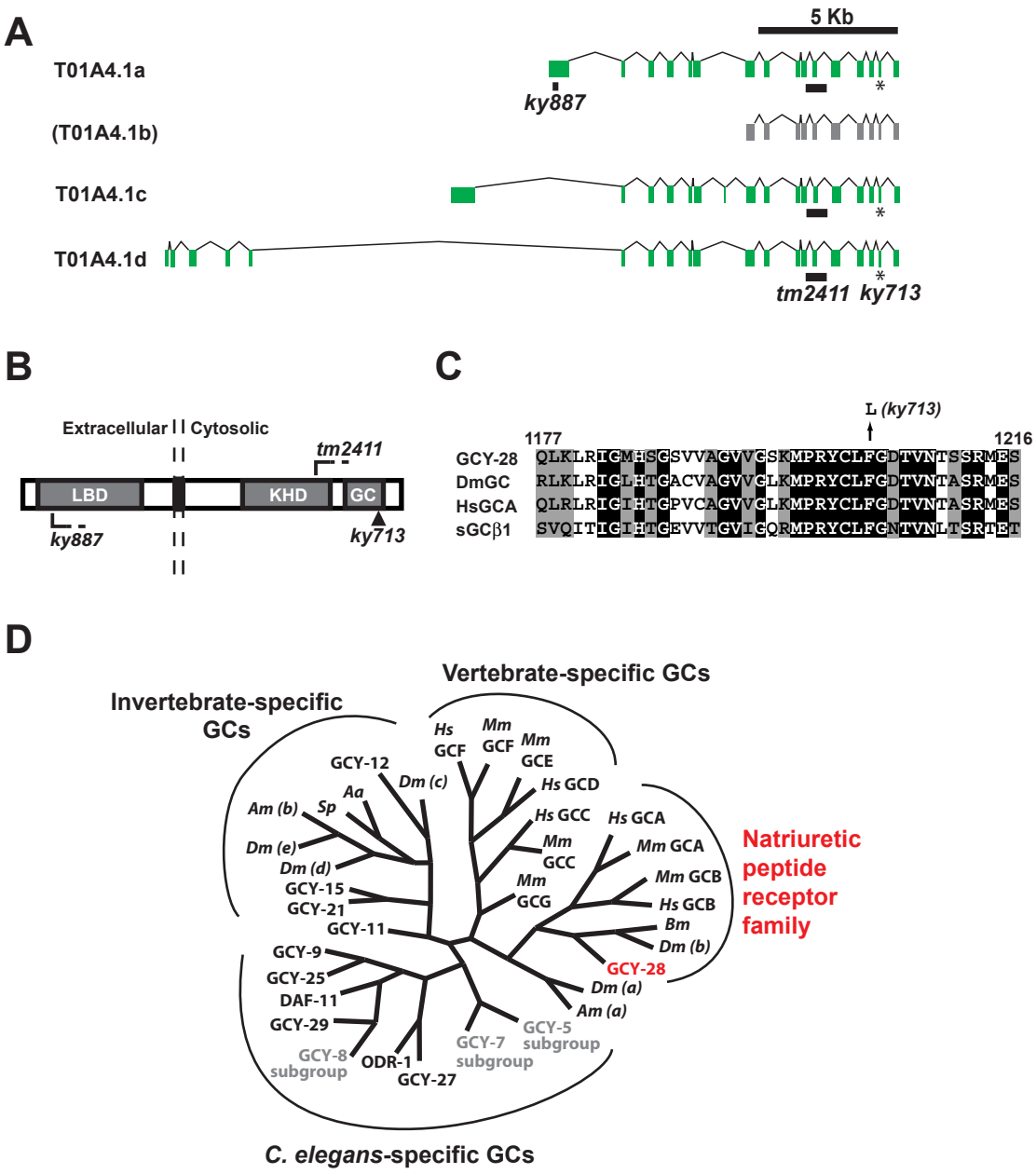
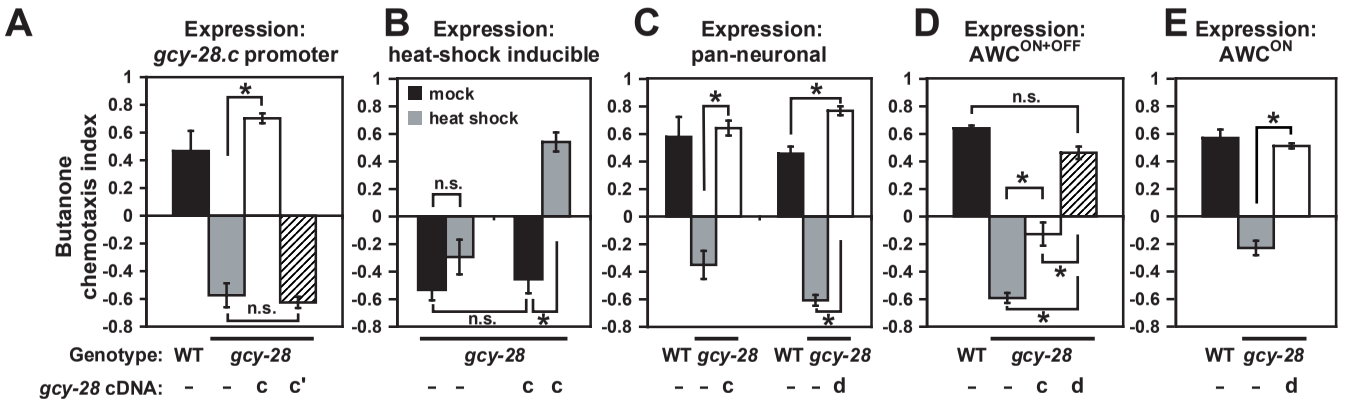
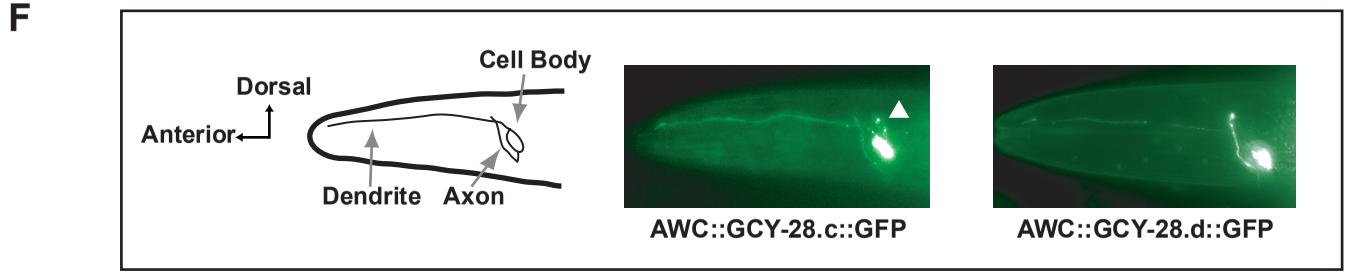

A
5 Kb
T01A4.1a
ky887
(T01A4.1b)
T01A4.1c
T01A4.1d
tm2411 ky713
B
Extracellular
Cytosolic
tm2411
LBD
KHD
GC
ky887
ky713
C
L (ky713)
1177
1216
GCY-28 QLKLRIGMHSGSVVAGVVGSKMPRYCLFGDTVNTSSRMES
DmGC RLKLRIGLHTGACVAGVVGLKMPRYCLFGDTVNTASRMES
HsGCA QLRLRIGIHTGPVCAGVVGLKMPRYCLFGDTVNTASRMES
sGCβ1 SVQITIGIHTGEVVTGVIGQRMPRYCLFGNTVNLTSRIET
D
Vertebrate-specific GCs
Invertebrate-specific GCs
Hs GCF
Mm GCF
Mm GCE
Hs GCD
Hs GCC
Hs GCA
Mm GCC
Mm GCA
Mm GCG
Mm GCB
Hs GCB
Bm
Dm (b)
GCY-28
Dm (a)
Am (a)
GCY-5 subgroup
GCY-7 subgroup
ODR-1
GCY-27
GCY-8 subgroup
GCY-29
DAF-11
GCY-25
GCY-9
GCY-11
GCY-21
GCY-15
Dm (d)
Dm (e)
Am (b)
Sp
Aa
GCY-12
Dm (c)
Natriuretic peptide receptor family
C. elegans-specific GCs

Figure 3-4

Figure 3-4. Sequence analysis of *gcy-28*

(A) Genomic organization of the *gcy-28* locus. Isoforms confirmed by cDNAs are shown in green. The first five exons of T01A4.1d were previously annotated in WormBase as a separate ORF, T01A4.2. Some T01A4.1c cDNAs lack the small exon 7 and some T01A4.1a cDNAs contain this exon. The *ky713* missense mutation is indicated by an asterisk, and two deletions (*tm2411* and *ky887*) are indicated by a line. *ky887* affects only T01A4.1a and has no chemotaxis defects (see Supplementary Methods). (B) Schematic of the domain structures of GCY-28 isoforms a, c and d. The approximate positions of the mutations are indicated. The alleles *tm2411* and *ky887* are deletions predicted to cause a frameshift. LBD – ligand-binding domain; KHD – kinase homology domain; GC – guanylate cyclase domain. (C) Alignment of part of the guanylate cyclase domains from different species. Conserved residues are shaded in black, similar residues are shaded in grey. The *ky713* mutation is F1204L. Numbers are relative to GCY-28.c. Abbreviations are: DmGC *Drosophila melanogaster* transmembrane guanylate cyclase; HsGCA *Homo sapiens* guanylate cyclase A; sGCβ1 *Homo sapiens* soluble guanylate cyclase β subunit. (D) Consensus tree of tmGCs. *C. elegans* tmGCs are GCYs, ODR-1 and DAF-11. The GCY-5 subgroup includes GCY-1, 2, 3, 4, 5, and 19; GCY-7 subgroup includes GCY-6, 7, 14, 17, 20, and 22; GCY-8 subgroup includes GCY-8, 18, and 23 (Ortiz et al., 2006). Other species are abbreviated as follows: *Hs, Homo sapiens*; *Mm, Mus musculus*; *Dm, Drosophila melanogaster*; *Am, Apis mellifera*; *Bm, Bombyx mori*; *Aa, Asterias amurensis*; *Sp, Strongylocentrotus purpuratus*.


A
Expression:
gcy-28.c promoter
B
Expression:
heat-shock inducible
C
Expression:
pan-neuronal
D
Expression:
AWC^ON+OFF
E
Expression:
AWC^ON
Butanone chemotaxis index
mock
heat shock
n.s.
Genotype: WT gcy-28
gcy-28 cDNA: - - c c'
gcy-28 - - c c
WT gcy-28 WT gcy-28
- - c - - d
WT gcy-28
- - c d
WT gcy-28
- - d


F
Dorsal
Anterior
Cell Body
Dendrite
Axon
AWC::GCY-28.c::GFP
AWC::GCY-28.d::GFP

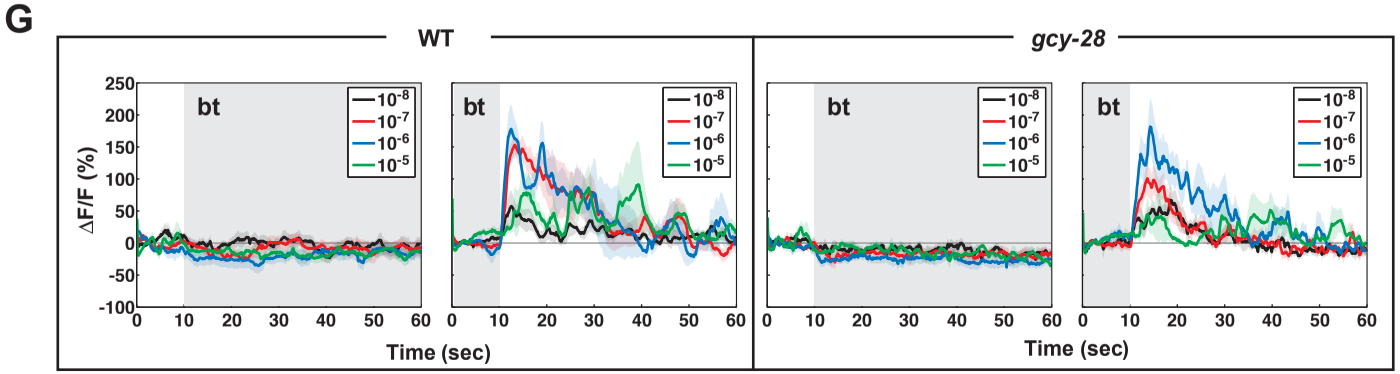

G
WT
gcy-28
bt
10^-8
10^-7
10^-6
10^-5
ΔF/F (%)
Time (sec)

Figure 3-5

Figure 3-5. Spatial and temporal sites of GCY-28 action

(A-E) Butanone chemotaxis of *gcy-28(ky713)* mutants expressing different isoforms of *gcy-28* cDNAs under various promoters. Error bars represent SEM. * $p < 0.05$, Bonferroni t-test. (A) 3.2 Kb regulatory region upstream of *gcy-28.c* driving *gcy-28.c* cDNA. A cDNA with the *ky713* mutation is denoted c'. (B) Heat-shock inducible *hsp16-41* promoter driving *gcy-28.c* cDNA. (C) Pan-neural *H20* promoter driving *gcy-28.c* and *gcy-28.d* cDNAs. (D) AWC-selective *odr-3* promoter driving *gcy-28.c* and *gcy-28.d* cDNAs. (E) AWC^{ON}-selective *str-2* promoter driving *gcy-28.d* cDNA. (F) Subcellular localization of GFP-tagged GCY-28 expressed in AWC using the *odr-3* promoter. This promoter is expressed weakly in another olfactory neuron, AWB (arrowhead). (G) Average Ca^{2+} responses of AWC^{ON} neurons measured by changes in G-CaMP fluorescence in wild type and *gcy-28(tm2411)* animals. Grey shading indicates the presence of butanone. Legend indicates the dilution of butanone used as the stimulus. The left panels for each genotype show responses at the onset of the stimulus; the right panels show responses after removal of the stimulus. The shaded area around each trace represents the SEM. n = 7-11 animals for each condition.

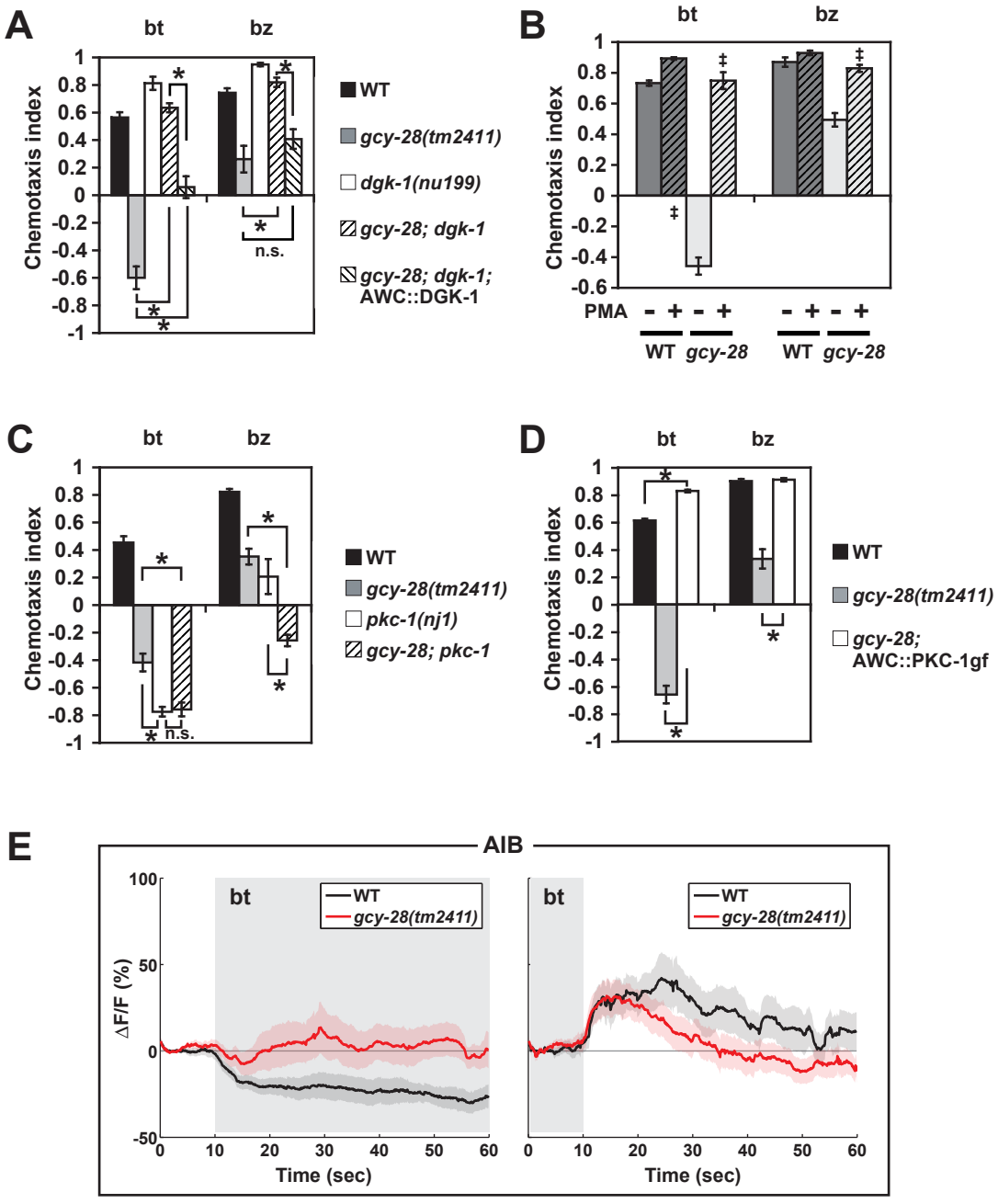

A
bt
bz
Chemotaxis index
WT
gcy-28(tm2411)
dgk-1(nu199)
gcy-28; dgk-1
gcy-28; dgk-1; AWC::DGK-1
n.s.
B
PMA
WT
gcy-28
C
pkc-1(nj1)
gcy-28; pkc-1
D
gcy-28; AWC::PKC-1gf
E
AIB
ΔF/F (%)
Time (sec)

Figure 3-6

Figure 3-6. *gcy-28* and DAG/PKC signaling interact to transform behavior

(A) Effect of a *dgk-1* mutation on chemotaxis of *gcy-28* mutants. For AWC-specific rescue of *dgk-1*, a *dgk-1.a* cDNA was expressed under the *odr-3* promoter. *dgk-1* single mutants carrying the rescuing array had chemotaxis indices comparable to wild-type animals (data not shown). (B) Chemotaxis of *gcy-28(tm2411)* mutants after treatment with 1μg/ml PMA for 2 hours. (C) Chemotaxis of *pkc-1* and *gcy-28; pkc-1* double mutants. (D) Effect of expressing PKC-1(A160E), a gain-of-function form of PKC-1, in AWC under the *odr-3* promoter. Expression in AWC^{ON} under the *str-2* promoter also rescued chemotaxis (data not shown). Error bars represent SEM. * $p < 0.05$, Bonferroni t-test, ‡ $p < 0.01$ relative to mock treated control, Student's t-test. (E) Average Ca^{2+} responses of AIB neurons measured by changes in G-CaMP fluorescence in wild type (n = 29) and *gcy-28(tm2411)* mutants (n = 27). Grey shading indicates the presence of butanone (10^{-6} dilution). Left panel, butanone onset; right panel, butanone offset after five minutes, in the same animals. The shaded area around each trace represents the SEM.

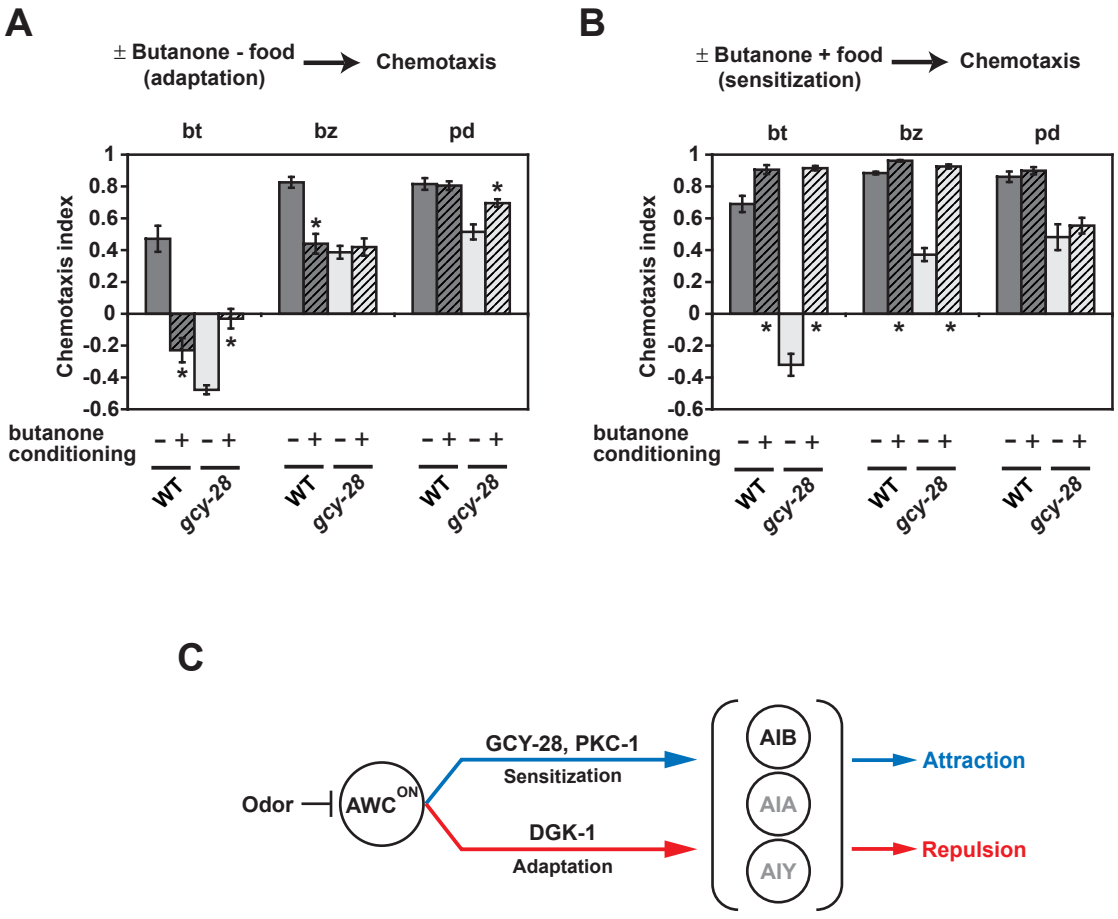
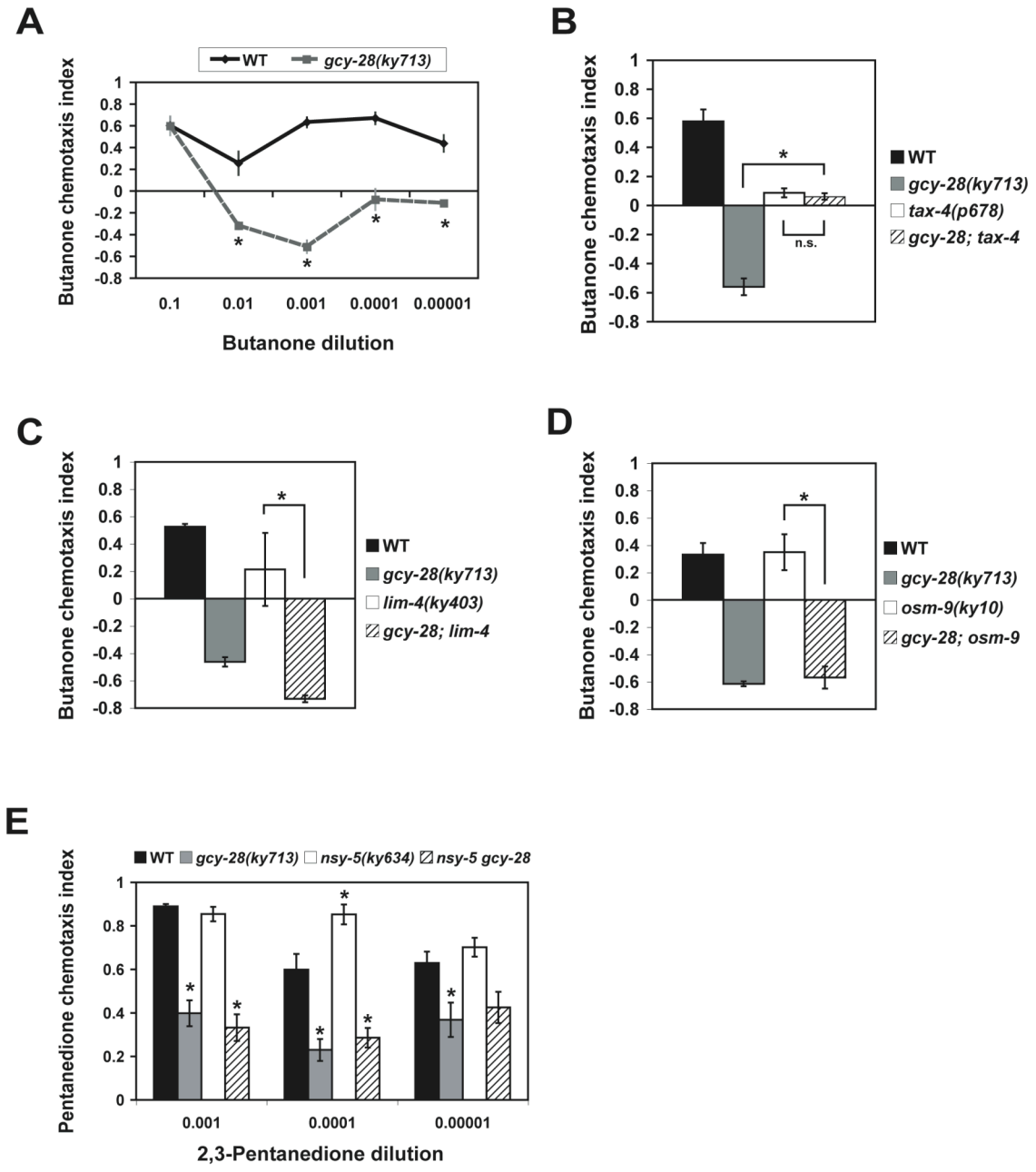

A
± Butanone - food
(adaptation)
Chemotaxis
bt
bz
pd
Chemotaxis index
1
0.8
0.6
0.4
0.2
0
-0.2
-0.4
-0.6
butanone
conditioning
- + - +
WT
gcy-28
B
± Butanone + food
(sensitization)
Chemotaxis
C
Odor
AWC ON
GCY-28, PKC-1
Sensitization
DGK-1
Adaptation
AIB
AIA
AIY
Attraction
Repulsion

Figure 3-7

Figure 3-7. Olfactory plasticity is altered in *gcy-28* mutants

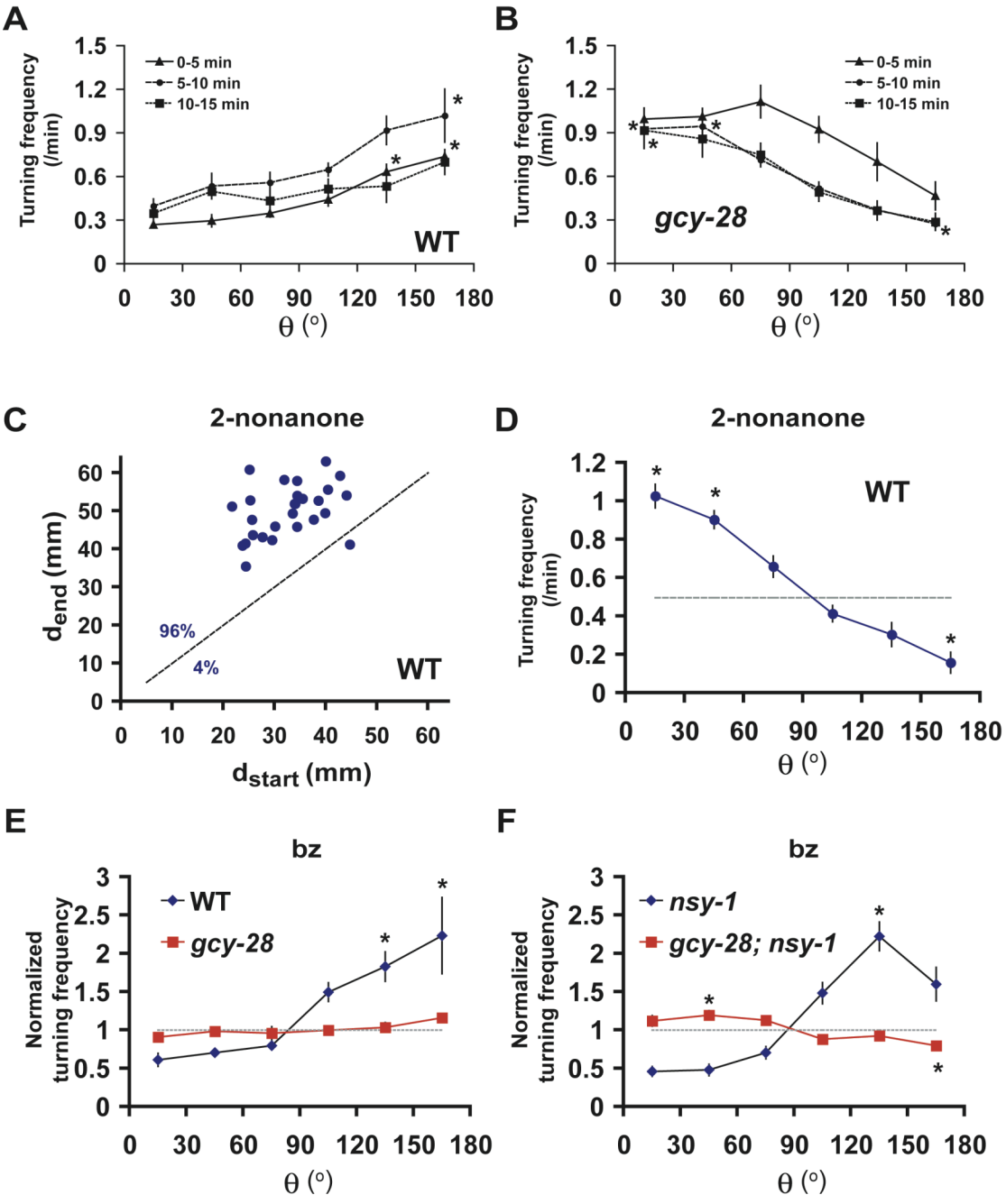
(A) Butanone adaptation in wild-type and *gcy-28(ky713)* mutant animals. Animals were incubated without food for 120 minutes, with or without butanone vapor (20 μL), then tested for chemotaxis to the indicated odors. Shorter adaptation protocols caused sensitization (rescue) of *gcy-28* mutants, consistent with a defect in starvation-odor integration (Fig. S7). (B) Butanone sensitization in wild-type and *gcy-28(tm2411)* mutant animals. Animals were incubated with food for 90 minutes, with or without butanone vapor (12 μL), then tested for chemotaxis to the indicated odors. Error bars represent SEM. * $p < 0.01$ relative to the respective control condition, Student's t-test. (C) Model for GCY-28 and DAG/PKC-1 signaling in AWC^{ON}. AWC^{ON} has two classes of synaptic outputs onto downstream interneurons (AIB, AIA, AIY), one driving attraction to odors and another driving avoidance of odors. GCY-28 and PKC-1 promote attraction in naïve animals, and DGK-1 promotes repulsion. Sensitization and adaptation favor attraction and repulsion, respectively.



Supplementary Figure 1

Supplementary Figure 1. Characterization of *gcy-28* mutants.

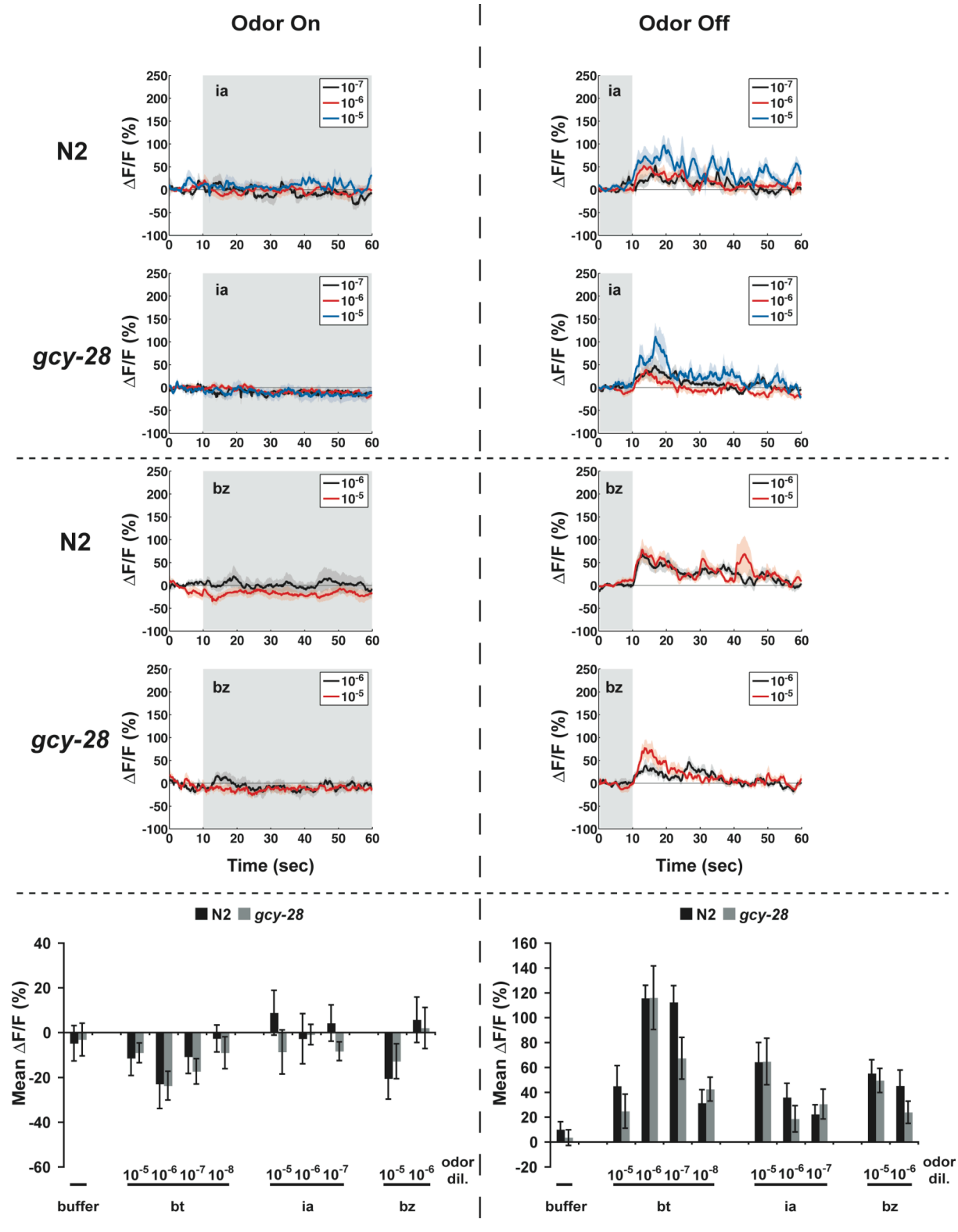
(A) Butanone dose-response. * $p < 0.01$, Student's t-test, relative to wild-type. (B) Effect of a *tax-4* cGMP-gated channel mutation on *gcy-28* butanone chemotaxis. * $p < 0.05$, n.s. not significant, Bonferroni t-test. (C) Effect of a *lim-4* mutation that disrupts AWB and ADF cell fate on *gcy-28* butanone chemotaxis. * $p < 0.05$, Bonferroni t-test. (D) Effect of an *osm-9* TRPV channel mutation that disrupts ASH and ADL signaling on *gcy-28* butanone chemotaxis. * $p < 0.05$, Bonferroni t-test. (E) 2,3-pentanedione dose-response of *nsy-5* (2 AWC^{OFF}) mutants. * $p < 0.05$, Bonferroni t-test, relative to wild-type. Error bars represent SEM.



Supplementary Figure 2

Supplementary Figure 2. Turning biases during chemotaxis.

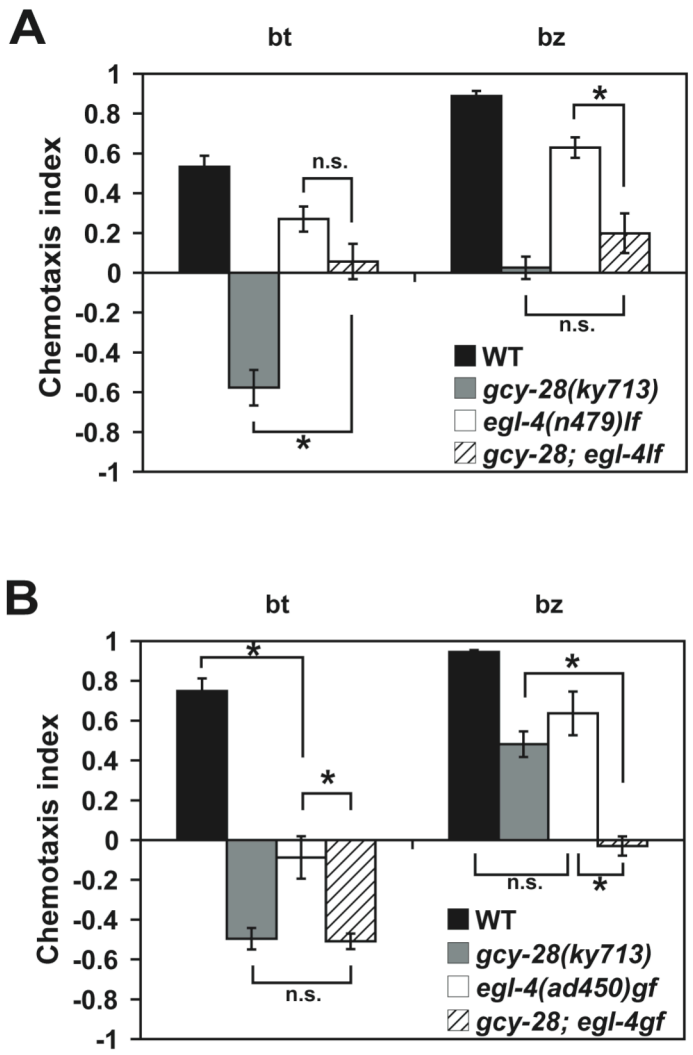
(A and B) Movies of (A) wild-type animals, Fig. 2D, and (B) *gcy-28* mutants, Fig. 2E, were segmented into five-minute intervals and turning biases were determined for each interval. Similar trends were observed at all times although wild-type was not statistically significant at 10-15 minutes and *gcy-28* was not statistically significant at 0-5 minutes by the Dunnett test. (C and D) Tracking analysis of wild-type animals in a gradient of 2-nonanone, a repellent sensed by the AWB olfactory neurons. (E and F) Effects of *gcy-28* and *nsy-1* mutations on turning bias in response to benzaldehyde. The double mutant shows a positive turning bias ($p < 0.05$). *gcy-28(ky713)* shows no bias (one-way ANOVA, $p = 0.44$). Error bars represent SEM. * $p < 0.05$ relative to the mean by the Dunnett test.



Supplementary Figure 3

Supplementary Figure 3. Ca^{2+} responses of AWC^{ON} neurons in *gcy-28* animals.

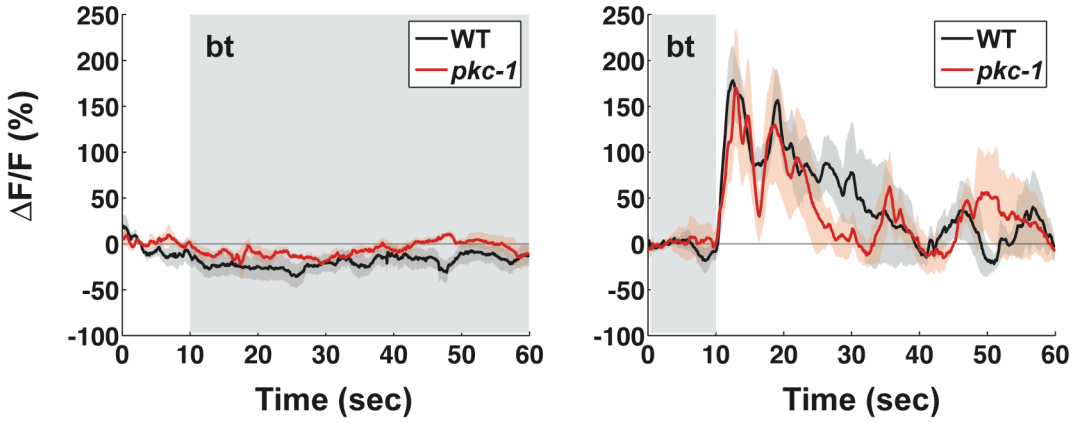
Left and right panels show responses at the onset and offset, respectively, of the indicated odor. Grey shading indicates the presence of odor. Traces are averages of responses from 6-8 animals each, with the SEM indicated by the shading around the curve. Bar graphs represent the average ΔF/F during ten seconds after the switch in stimulus. Note the different scales between the onset and offset graphs. Odor dilution are as indicated. The buffer controls are an average of 16 and 11 animals for wild-type and *gcy-28*, respectively. Error bars indicate the SEM.



Supplementary Figure 4

Supplementary Figure 4. Genetic interactions between *gcy-28* and *egl-4* PKG loss-of-function and gain-of-function mutants.

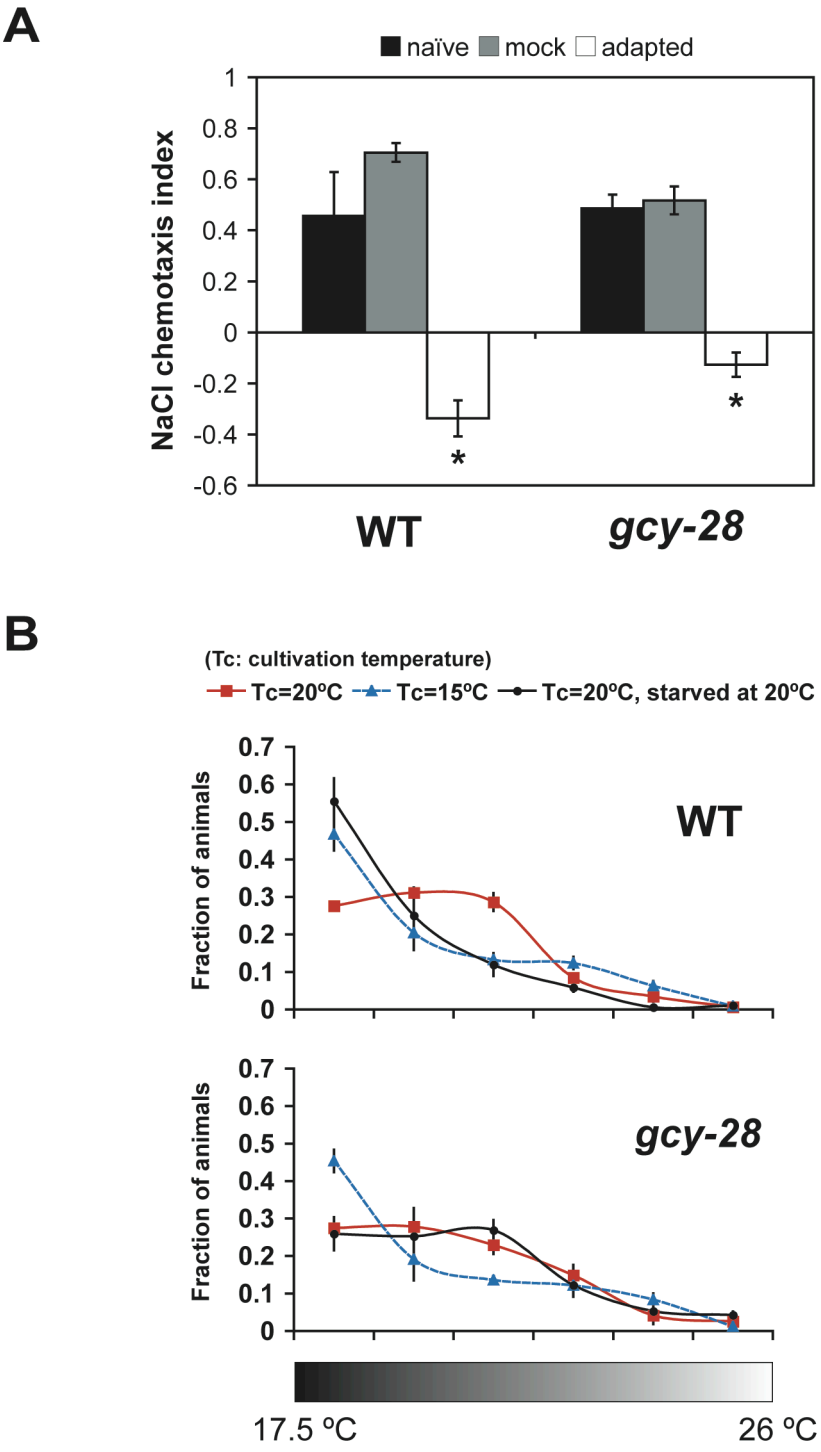
(A) Effect of an *egl-4* loss-of-function mutation on *gcy-28* chemotaxis. The double mutants have additive defects. (B) Effect of an *egl-4* gain-of-function mutation on *gcy-28* chemotaxis. The double mutants resemble *gcy-28* for butanone, and have a compound defect for benzaldehyde. Error bars represent SEM. * $p < 0.05$, Bonferroni t-test.



Supplementary Figure 5

Supplementary Figure 5. Ca^{2+} responses of AWC^{ON} neurons in *pkc-1* animals.

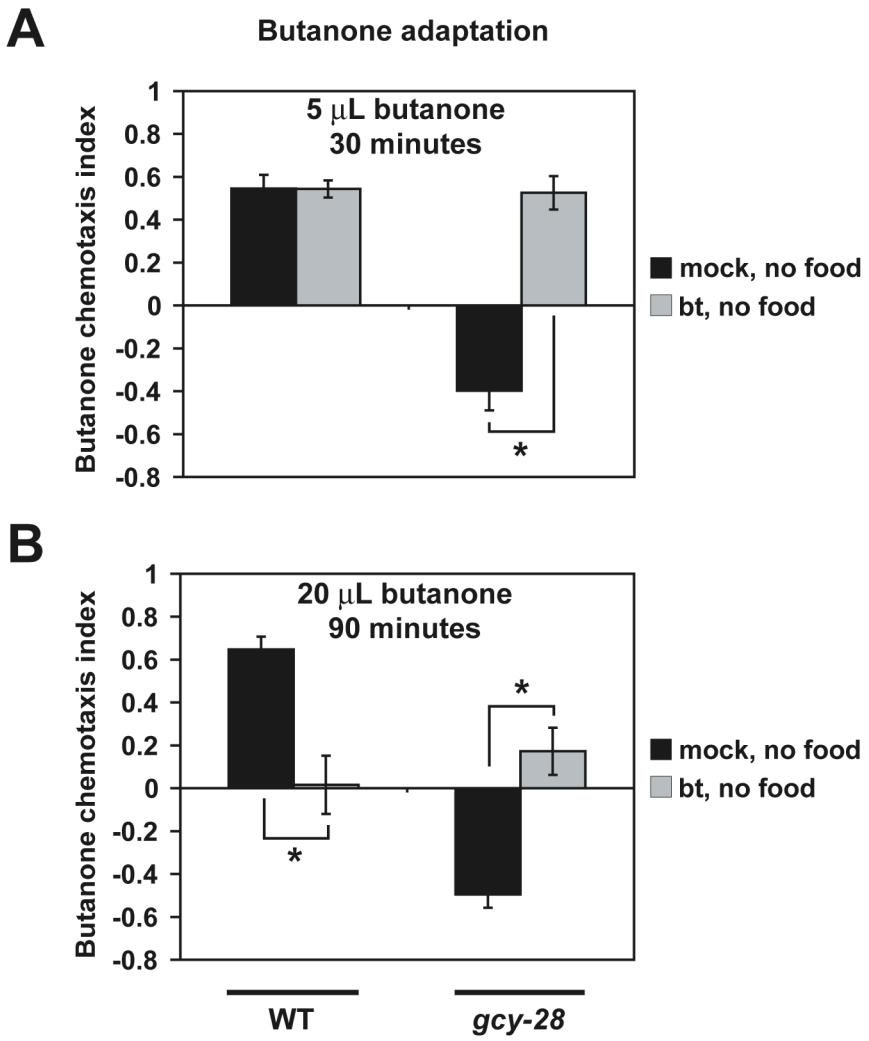
Dilution of butanone tested was 10^{-6}. The *pkc-1* trace is an average of 5 animals.



Supplementary Figure 6

Supplementary Figure 6. Salt and temperature plasticity in *gcy-28* mutants.

(A) Salt chemotaxis plasticity in wild-type and *gcy-28(tm2411)* animals. * $p < 0.05$ relative to both naïve and mock-treated animals, Bonferroni t-test. (B) Thermotaxis plasticity in wild-type and *gcy-28(tm2411)* animals. Animals were either raised at 20ºC (Tc = 20ºC), or were raised at 20ºC and shifted to 15ºC a day before the assay (Tc = 15ºC), or were raised at 20ºC and starved for one hour at 20ºC before the assay (Tc=20ºC, starved at 20ºC). *gcy-28* mutants showed thermotaxis to cultivation temperature (15ºC, 20ºC) but did not suppress thermotaxis upon starvation.



Supplementary Figure 7

Supplementary Figure 7. Butanone conditioning without food can rescue *gcy-28.*

The amount of butanone used for conditioning without food and the time of conditioning are indicated. Control animals were treated similarly except that butanone was not present during conditioning. Conditioning was carried out on NGM agar; similar results were obtained on assay agar (data not shown). (A) 30-minute butanone conditioning in the absence of food. (B) 90-minute butanone conditioning in the absence of food. Error bars represent SEM. * $p < 0.01$ relative to the respective control condition, Student's t-test.

Supplementary Methods

Strains

C. elegans strains were cultured using standard methods (Brenner, 1974). The following strains were used: wild-type Bristol (N2), CB4856 Hawaiian, CX713 *gcy-28(ky713) I,* FX02411 *gcy-28(tm2411) I*, CX8273 *gcy-28(ky887) I*, CX3695 *kyIs140 [str-2::gfp] I*, CX6343 *kyIs137 [str-2::gfp] V*, CX6482 *gcy-28(ky713) I; kyIs137 V*, KR1112 *unc-11(e47) dpy-5(e61) I; hDp9(I;f)*, CX2395 *dpy-5(e61) unc-101(m1) I*, IK105 *pkc-1(nj1) V*, CX10247 *gcy-28(tm2411) I; pkc-1(nj1) V*, CX4731 *nsy-1(ky542) II*, CX6510 *gcy-28(ky713) I; nsy-1(ky542) II*, CX6161 *nsy-5(ky634) I*, CX6519 *nsy-5(ky634) gcy-28(ky713) I*, CX6339 *ceh-36(ky640) X*, CX6483 *gcy-28(ky713) I; ceh-36(ky640) X*, CX3410 *odr-10(ky225) X*, CX4915 *odr-10(ky225) lin-15(n765) kyIs187 [str-2::odr-10] X*, CX6713 *gcy-28(ky713) I; odr-10(ky225) X*, CX6712 *gcy-28(ky713) I; odr-10(ky225) lin-15(n765) kyIs187 X*, KP828 *dgk-1(nu199) X*, CX9542 *gcy-28(ky713) I; dgk-1(nu199) X*, PR678 *tax-4(p678) III*, CX6819 *gcy-28(ky713) I; tax-4(p678) III*, MT1074 *egl-4(n479) IV*, CX8452 *gcy-28(ky713) I;egl-4(n479) IV*, DA521 *egl-4(ad450) IV*, CX8367 *gcy-28(ky713) I; egl-4(ad450) IV*, CX4991 *lim-4(ky403) X*, *CX6485 gcy-28(ky713) I; lim-4(ky403) X*, CX10 *osm-9(ky10) IV*, CX7072 *gcy-28(ky713) I; osm-9(ky10) IV*, CX10281 *kyEx2373 [str-2::GCaMP2.0, ofm-1::gfp]*, CX10223 *gcy-28(tm2411) I; kyEx2373*, CX10784 *pkc-1(nj1) V; kyEx2373*, CX7469 *kyEx903 [odr-2 2b::GCaMP1.0, ofm-1::gfp]*, CX8994 *gcy-28(tm2411) I; kyEx903*, CX8314 *gcy-28(ky713) I; kyEx1094 [t01a4.1c::t01a4.1c::gfp]*, CX7729 *gcy-28(ky713) I; kyEx1071 [t01a4.1c::t01a4.1c(ky713)::gfp]*, CX7624 *gcy-28(ky713) I; kyEx1016 [hsp-16-41::t01a4.1c SL2-gfp]*, CX7623 *gcy-28(ky713) I; kyEx1015 [H20::t01A4.1c::gfp]*,

CX9831 *gcy-28(ky713) I; kyEx2170 [odr-3::t01a4.1c::gfp]*, CX9718 *gcy-28(ky713) I; kyEx2134 [H20::t01a4.1d::gfp]*, CX9734 *gcy-28(ky713) I; kyEx2138 [odr-3:t01a4.1d::gfp]*, CX10586 *gcy-28(ky713) I; kyEx2642 [str-2::t01a4.1d::gfp]*, CX10707 *gcy-28(tm2411) I; dgk-1(nu199) X; kyEx2733 [odr-3::dgk-1.a SL2-gfp]*, CX9738 *gcy-28(tm2411) I; kyEx2142 [odr-3::pkc-1(C479A T480A) SL2-gfp]*. All transgenic strains were made essentially as described (Mello et al., 1991), with the co-injection marker *elt-2::GFP* except for the G-CaMP imaging strains, which used *unc-122::GFP*. Most test plasmids were injected at 20-50 ng/μL. *hsp16-41::gcy-28.c* plasmid was injected at ~5 ng/μL. At least three independent lines were tested for each rescuing experiment, except for the heat-shock rescue which was tested in two lines.

Isolation, mapping, and cloning of *gcy-28* alleles

N2 animals were mutagenized with EMS following standard protocols (Anderson, 1995). F2 animals were tested for butanone chemotaxis and those that failed to chemotax three times were kept for further analysis. After crossing *ky713* into *kyIs140 I [str-2::gfp]*, 12/12 F2 progeny without GFP were defective for butanone chemotaxis; this suggested *ky713* was on LGI. In three-factor mapping with *unc-11(e47) dpy-5(e61)* the butanone chemotaxis defect mapped between the two genes (9/16 Dpy non-Unc and 4/14 Unc non-Dpy were chemotaxis defective). The free duplication *hDp9* rescued the *ky713* chemotaxis defect in the strain *unc-11 ky713; hDp9*, suggesting that *ky713* lies to the left of *unc-38*. We generated a single nucleotide polymorphism (SNP) mapping strain (CX6649) by backcrossing the highly polymorphic strain CB4856 with *dpy-5(e61) unc-101(m1)*. CX6649 had CB4856 SNPs between markers *pkP1105* (-7.9) and *kyP25*

(+12.9) on LGI. We crossed CX6649 with the strain *unc-11(e47) ky713 dpy-5(e61)* and isolated Dpy non-Unc and Unc non-Dpy recombinants. *ky713* fell between the SNPs *pkP1111* (-1.22) and *kyP75* (-1.04), spanning a region of approximately 100 Kb. Upon sequencing the ORF T01A4.1 (*gcy-28*) we found a C to G mutation at position 43685 of the cosmid T01A4.

An additional allele, *gcy-28(ky887)* (from Isao Katsura, National Institute of Genetics, Mishima, Japan) has a small deletion in the exon unique to *gcy-28.a* that is predicted to cause a frameshift in this isoform. *gcy-28(ky887)* has no apparent chemotaxis defects, indicating that the *gcy-28.a* isoform is not critical for this function.

Molecular biology

gcy-28.c cDNA (gcy-X_1) was a generous gift from David Garbers (UT Southwestern Medical Center, TX). We used the primers: 5'–ATGATTCTAAGCGACGTAC–3' and 5'–GACGTCCGTGAGATCGAATTTCAC–3' to amplify the 5' end of *gcy-28.d* cDNA encoding the entire extracellular domain and part of the intracellular domain. This fragment replaced the 5' end of *gcy-28.c* up to a unique AvaI site in the intracellular domain to reconstruct the full-length *gcy-28.d* cDNA. The *gcy-28.d* 5' end could also be amplified using an SL1 primer and a sequence internal to T01A4.1. We were unable to amplify products for *gcy-28.b* using an SL1 primer or a 5' primer based on WormBase prediction (Release WS177). All rescuing *gcy-28* cDNA constructs were fused to GFP at the extreme C-terminus.

Primers for upstream regulatory regions were as follow:
gcy-28.a 5'–AGGGAAAAATGGAGAATCGAGCTG–3' and

5'–TCGGATACCATTCCCGCGGGGC–3';

gcy-28.c 5'–ATTGAATTGCTCTCTCCGCAGC–3' and

5'–AGCCTCATAGGTACATTCACGG–3';

gcy-28.d 5'–TACAATTGTAGTGAGCTTCG–3' and

5'–TTCGCACTCATCTCACCATTCC–3'.

AWC expression was driven by the *odr-3* promoter; pan-neuronal expression was driven by the H20 promoter; the heat-shock promoter was *hsp16-41*.

pkc-1 and *dgk-1* cDNAs were isolated from mixed stage RNA using the following primers: (*pkc-1*) 5'–CTGTTCACAGGCACCGTGCGCGTTC–3' and 5'–GTAGGTAAAATGCGGATTGATAAATG–3'; (*dgk-1*) 5'–ATGGCAGCTGAGGGGCACAATG–3' and 5'– TCAGAGAAAAGCGTCGCCTTCC–3'.

PKC-1(A160E) was constructed by introducing the appropriate mutations to the *pkc-1* cDNA.

Sequence analysis

For alignment of the cyclase domain, the GenBank accession numbers were: DmGC: NP_650505; HsGCA: AAF01340; sGCβ1: AAB94877. For alignment of the full-length proteins, sequences of *C. elegans* cyclases were obtained from WormBase (www.wormbase.org). The GCY-28.c isoform was used for sequence analysis. GCY-28.c and GCY-28.d are 80% identical, and alignments using either sequence produced similar results (data not shown). Sequences from cyclases of other species were selected from Fitzpatrick et al. (2006). GenBank accession numbers were:

Hs GCA: NP_000897; *Hs* GCB: NP_003986; *Hs* GCC: NP_004954; *Hs* GC2D: NP_000171; *Hs* GC2F: NP_001513; *Mm* GCA: NP_032753; *Mm* GCB: NP_776149; *Mm* GCC: NP_659504; *Mm* GC2E: NP_032218; *Mm* GCF: NP_001007577; *Mm* GCG: XP_129326; *Dm* (a): NP_611532: *Dm* (b): NP_650505; *Dm* (c): AAR31133; *Dm* (d): CAA51319; *Dm* (e) NP_648653; *Am* (a): XP01120461; *Am* (b): XP_623361; *Bm*: BAB32672; *Aa*: BAB85468; *Sp*: NP_999705.

Full-length sequences were aligned by ClustalW using default settings in Lasergene (DNASTAR, Madison, WI). A consensus tree was constructed from the aligned sequences using PHYLIP 3.65 software package (Joseph Felsenstein, University of Washington, Seattle, WA). Bootstrapping was performed on 100 replicates.

Salt plasticity and temperature plasticity assays

Salt learning assays were performed essentially as described (Tomioka et al., 2006). A 5 mm diameter agar plug containing 100 mM NaCl was placed near one edge of a 10 cm circular assay plate and the NaCl gradient was established overnight. Animals were washed and immersed for one hour at room temperature in buffer (1 mM $MgSO_4$, 1 mM $MgCl_2$, 5 mM phosphate buffer, pH 6.0) with or without 20 mM NaCl, then placed in the middle of the NaCl gradient.

For thermotaxis assays, a linear thermal gradient from 17.5 ºC to 26.0 ºC was established across an aluminum surface using thermoelectric control (Ryu and Samuel, 2002). Adult worms raised at the indicated temperature were washed and transferred to the middle of a 10 cm square plate with NGM agar. The plate was placed on the

aluminum surface, and after 45 minutes, animals were killed with chloroform to stop the assay and counted.

Anderson, P. (1995). Mutagenesis. Methods Cell Biol *48*, 31-58.

Brenner, S. (1974). The genetics of *Caenorhabditis elegans*. Genetics *77*, 71-94.

Mello, C.C., Kramer, J.M., Stinchcomb, D., and Ambros, V. (1991). Efficient gene transfer in *C. elegans*: extrachromosomal maintenance and integration of transforming sequences. Embo J *10*, 3959-3970.

Ryu, W.S., and Samuel, A.D. (2002). Thermotaxis in *Caenorhabditis elegans* analyzed by measuring responses to defined thermal stimuli. J Neurosci *22*, 5727-5733.

Tomioka, M., Adachi, T., Suzuki, H., Kunitomo, H., Schafer, W.R., and Iino, Y. (2006). The insulin/PI 3-kinase pathway regulates salt chemotaxis learning in *Caenorhabditis elegans*. Neuron *51*, 613-625.

CHAPTER 4

Genetic analysis of *gcy-28* function in AWC chemotaxis

Summary

Mutations in the *Caenorhabditis elegans* transmembrane guanylate cyclase *gcy-28* lead to a switch in behavioral preference for odors sensed by an AWC olfactory neuron. In naïve wild-type animals, butanone is an attractive odor sensed by AWC; however, *gcy-28* mutants avoid butanone. In this study, genetic experiments were used to study the underlying cause of the odor preference switch in AWC. *gcy-28* activity is mainly required in AWC for chemotaxis, but it is widely expressed. Rescue experiments demonstrate that cell non-autonomous activity of *gcy-28* can affect AWC chemotaxis in *gcy-28* mutants. *gcy-28* may act as a receptor for signals from other cells, because the extracellular domain of *gcy-28* is required for rescuing activity in AWC. Genetic analysis reveals more modulatory pathways for AWC chemotaxis: *gcy-28* interacts with a cAMP/PKA signaling pathway, as well as a large-conductance Ca^{2+}-activated K^{+} channel, to determine odor preference. These results identify modulatory inputs that may add flexibility to the AWC chemotaxis circuitry. Genetic interaction with mutants that abolish or enhance AWC-dependent turning behavior suggest that the efficiency of glutamatergic neurotransmission, the major AWC output, determines the extent of avoidance in *gcy-28* mutants.

Background

The AWC olfactory neurons of the nematode *C. elegans* sense food-related attractive odors (Bargmann et al., 1993). Even though attraction is the default behavior for AWC-sensed odors, there is remarkable plasticity in behavioral output from AWC (Bargmann, 2006). In particular, mutations in the receptor-type guanylate cyclase gene, *gcy-28*, switch responses to odors sensed by one AWC neuron from attraction to avoidance (Chapter 3a). Prolonged adaptation to odor also switches odor preference in one AWC neuron. Thus, AWC may encode alternate odor preferences depending on the animal's genetic or environmental context. How a single sensory neuron encodes both attraction and avoidance is unknown.

gcy-28 is homologous to the vertebrate natriuretic peptide receptors, which regulate developmental and physiological processes such as blood pressure and bone growth (Lopez et al., 1995; Oliver et al., 1997; Tamura et al., 2004; Tsuji and Kunieda, 2005). Natriuretic peptide receptors are ligand-regulated guanylate cyclases that bind small peptide ligands through their extracellular domains. The *C. elegans* genome does not contain any obvious homolog of these ligands, but *gcy-28* does have an extracellular domain with structural homology to the ligand-binding vertebrate receptors, suggesting that *gcy-28* activity may also be regulated by a ligand.

gcy-28 acts mostly in AWC to regulate odor preference (Chapter 3a). However, the expression pattern of *gcy-28* is broad and some isoforms of *gcy-28* rescue chemotaxis completely when expressed pan-neuronally, but rescue only partially when expressed in a smaller set of cells including AWC (Chapter 3a). These results suggest that activity of

gcy-28 in neurons other than AWC may affect AWC chemotaxis. *gcy-28* is also likely to have functions outside of chemotaxis (see Chapter 4).

In addition to *gcy-28*, *pkc-1*, which encodes a protein kinase C (PKC), is also required to specify odor preference in AWC (Okochi et al., 2005)(Chapter 3a). Both *gcy-28* and *pkc-1* act downstream of primary signal transduction and may alter synaptic transmission from AWC (Chapted 3a).

In this study, various genetic approaches were taken to probe the mechanism of odor avoidance in *gcy-28* mutants. *gcy-28* has cell non-autonomous effects on AWC chemotaxis, such that expression in some neurons suppresses chemotaxis and expression in others promotes it. Rescuing activity of *gcy-28* is abolished by deletion of its extracellular ligand-binding domain. Mutations that enhance synaptic transmission or activity of the AWC chemotaxis circuit suppress odor avoidance in *gcy-28* mutants. However, glutamatergic transmission is required for odor avoidance. These results suggest that the overall activity level of AWC may be integrated with modulatory inputs from other sensory neurons at the AWC synapse to specify odor preference in AWC chemotaxis.

Results

gcy-28.c can act cell non-autonomously to regulate AWC chemotaxis

The difference in the ability of *gcy-28.c* to rescue chemotaxis when expressed pan-neuronally and when expressed under the *odr-3* promoter (Fig. 5C and 5D, Chapter 3a) suggested that *gcy-28* may function at multiple sites in the nervous system to regulate AWC chemotaxis. To better understand the requirement for *gcy-28.c*, the cDNA was

expressed under different cell-specific promoters in *gcy-28* mutants and tested for rescuing activity.

Surprisingly, expression of *gcy-28.c* in AWC^{ON} using the *str-2* promoter rescued the butanone chemotaxis defect better than the *odr-3* promoter, which drives expression in AWC^{ON} and AWC^{OFF}, as well as AWB and sometimes ASH, AWA and ADF (Table 1 and 2). This difference suggests that expression of *gcy-28.c* in AWC^{OFF}, AWB or perhaps other cells interferes with AWC^{ON} chemotaxis. The *ceh-36* and *egl-2* promoters, which express in both AWCs but not in AWB or the other candidates, rescued the chemotaxis defects better than the *odr-3* promoter. Therefore, expression of *gcy-28* in AWB may antagonize AWC chemotaxis.

The *tax-4* promoter, which expresses in AWC and AWB, also rescued chemotaxis, but to a lesser extent than *str-2*, *ceh-36*, or *egl-2* promoters. Expressing *gcy-28.c* with the *tax-4* and either *des-2* or *odr-2 2b* promoters enhanced rescuing activity compared to just *tax-4* alone. The *odr-2 2b* promoter also enhanced rescuing activity when coexpressed with *odr-3*, *ceh-36*, and *egl-2* promoters. These results suggest that *gcy-28.*c activity in a certain set of cells promotes AWC chemotaxis and suppresses the negative effect of *gcy-28.*c expression in another set of cells. Furthermore, chemotaxis is promoted only when *gcy-28.c* is expressed in AWC, because neither the *des-2* nor the *odr-2 2b* promoter on their own have an effect on chemotaxis. *des-2* and *odr-2 2b* share expression in the IL2 cells (Table 2). However, IL2 expression by the *des-2* promoter needs to be comfirmed.

The *osm-3* promoter expresses in many ciliated neurons including IL2 (chemotaxis enhancing) and ASH (chemotaxis suppressing). Expression of *gcy-28.c* with

the *osm-3* promoter alone does not have an effect on AWC chemotaxis, but this promoter has a negative effect on *tax-4* promoter rescuing activity (Table 1). These results suggest that a balance between chemotaxis-enhancing and suppressing expression of *gcy-28.c* determines the overall rescue of chemotaxis.

gcy-28.d is required for AWC chemotaxis

Of three confirmed isoforms of *gcy-28*, *gcy-28.c* and *gcy-28.d* rescue *gcy-28* chemotaxis defects when expressed pan-neuronally (Chapter 3a) (Fig. 1A). However, only *gcy-28.d* rescues chemotaxis fully when expressed from the *odr-3* promoter. Furthermore, *gcy-28.d* is enriched in the axonal process of AWC whereas *gcy-28.c* is not. These results suggested that *gcy-28.d* is the most active form of *gcy-28* in AWC chemotaxis.

To further test this idea, we obtained *gcy-28(tm3028)* (Shohei Mitani, National Bioresource Project, Japan), which has a deletion that affects only the *gcy-28.d* isoform (Fig. 1A). *gcy-28(tm3028)* was defective for chemotaxis to AWC sensed odors, as predicted from the rescue experiments (Fig. 1B). Butanone avoidance in *gcy-28(tm3028)* was as strong as *gcy-28(tm2411)*, which is a deletion that affects all three isoforms of *gcy-28*. Chemotaxis of *gcy-28(tm3028)* mutants to benzaldehyde and 2,3-pentanedione was defective compared to wild-type animals, but was less defective compared to *gcy-28(tm2411)* mutants (Fig. 1B). These results suggest that *gcy-28.d* is required for proper butanone preference, but both *gcy-28.c* and *gcy-28.d* contribute to AWC chemotaxis in general. *gcy-28.a* is not required for AWC chemotaxis (Chapter 3a).

The extracellular domain of *gcy-28* is required for AWC chemotaxis

Some mammalian rGCs are activated by extracellular ligands, but others are ligand independent. As a test for potential ligand regulation of GCY-28 activity, a form of *gcy-28* with an extracellular domain deletion (*gcy-28(ΔECD)*) was expressed in *gcy-28* mutant (Fig. 2A). This mutant form retains the *gcy-28* signal sequence and transmembrane domain, and should be membrane localized. *gcy-28(ΔECD)* did not rescue *gcy-28* mutants for butanone chemotaxis when expressed under the *odr-3* promoter (Fig. 2B). The extracellular domain-deleted form of *gcy-28* was expressed properly and localized to the axonal processes of AWC like the full-length form (Fig. 2C). This result suggests that the extracellular domain is required for *gcy-28* activity, and that axonal localization is not sufficient for proper function of *gcy-28*. By contrast, a similar deleted form of *odr-1*, a ciliary rGC required for AWC sensory transduction, does retain *odr-1* activity (L'Etoile and Bargmann, 2000).

gcy-28 defects are genetically distinct from PKG signaling defects

gcy-28 encodes a transmembrane guanylyl cyclase (Chapter 3a) and one potential target of cGMP from GCY-28 was the cGMP-dependent kinase (PKG) encoded by *egl-4*. Comparison of *egl-4* and *gcy-28* chemotaxis phenotypes, as well as genetic interaction of *gcy-28* with *egl-4* loss-of-function and gain-of-function mutants suggested that EGL-4 is not a target of cGMP from GCY-28. To further support this conclusion, a *daf-3* mutant was crossed into *gcy-28*. *daf-3* is a co-SMAD transcription factor that strongly suppresses chemotaxis defects of *egl-4* mutants (Daniels et al., 2000). In *gcy-28; daf-3* double mutant aninmals there was weak suppression of butanone avoidance but no

suppression of 2,3-pentanedione chemotaxis (Fig. 3). This result is consistent with *gcy-28* and *egl-4* acting in distinct pathways to regulate AWC chemotaxis.

Genetic interactions of *gcy-28* with cAMP/PKA signaling pathway

To better understand the role of *gcy-28* in AWC chemotaxis, various signaling mutants were tested for genetic interactions with *gcy-28* mutants. The genetic interaction of *gcy-28* and a synaptic DAG/PKC signaling mutants suggested that strengthening synaptic signaling could suppress *gcy-28* chemotaxis defects (Chapter 3a). Another regulator of synaptic transmission, among other processes, is the cAMP/PKA signaling pathway (Schade et al., 2005). cAMP/PKA signaling acts in parallel to *unc-31*, a Ca^{2+}-dependent activator protein for secretion (CAPS) that is important for peptide secretion, to regulate neurotransmission (Charlie et al., 2006a; Zhou et al., 2007). *kin-2* encodes the regulatory subunit of PKA, and mutations in *kin-2* lead to constitutively active cAMP signaling phenotypes (Schade et al., 2005). Indeed, a *kin-2* mutation suppressed *gcy-28* chemotaxis defects nearly as well as a *dgk-1* mutant (Fig. 4A and Chapter 3a). The benzaldehyde and 2,3-pentanedione chemotaxis defects were completely suppressed and butanone chemotaxis was partially suppressed in *gcy-28; kin-2* double mutants. This result suggests that a defect in cGMP signaling can be suppressed by activating cAMP signaling.

One source of cAMP in *C. elegans* is ACY-1, a neuronal adenylyl cyclase required for viability, for cell-death induced by constitutively active $G_s\alpha$ signaling, and for chemotaxis to isoamyl alcohol (Berger et al., 1998; Moorman and Plasterk, 2002). An *acy-1* reduction-of-function mutant had a chemotaxis defect for butanone, but not for

benzaldehyde or 2,3-pentanedione (Fig. 4B). *gcy-28; acy-1* double mutants were mostly similar to *gcy-28* single mutants, except for a mild enhancement of the benzaldehyde chemotaxis defect (Fig. 4B). These results are consistent with cAMP and cGMP signaling regulating a overlapping cellular processes.

Genetic interaction of *gcy-28* with the BK channel mutant, *slo-1*

slo-1 encodes a large-conductance Ca^{2+}-activated K^{+} (BK) channel, and loss-of-function (lf) mutations in *slo-1* increases quantal content of neurotransmission at the neuromuscular junction (Wang et al., 2001). *slo-1(lf)* mutants have normal AWC chemotaxis, but when crossed into a *gcy-28* mutant, *slo-1* partially suppresses the *gcy-28* chemotaxis defects (Fig. 5). In *gcy-28; slo-1(lf)* double mutants butanone avoidance and benzaldehyde chemotaxis defects are suppressed, but the 2,3-pentanedione chemotaxis defect is not suppressed (Fig. 5).

The effect of a *slo-1* mutation on *gcy-28* chemotaxis resembles the effect of a cell-fate mutation that causes a 2 AWC^{OFF} phenotype (Chapter 3a). A *slo-1* gain-of-function mutation causes a 2 AWC^{ON} phenotype (Davies et al., 2003), so a reciprocal cell fate change could underlie suppression of *gcy-28* by *slo-1(lf)*. However, *gcy-28; slo-1(lf)* double mutants expressed *str-2* in one AWC per animal, suggesting that they have one AWC^{ON} neuron and one AWC^{OFF} neuron (data not shown). This result, along with the persistent pd chemotaxis in *slo-1(lf)* mutants, suggested that a cell fate change in AWC is not the basis of suppression of *gcy-28* by *slo-1*. Since there are now several additional markers for AWC^{ON} and AWC^{OFF}, this hypothesis could be re-examined in more detail.

Genetic interactions of *gcy-28* with AWC circuit signaling mutants

The neuronal pathways downstream of AWC that drive butanone avoidance in *gcy-28* mutants are unknown. To obtain an insight into these pathways, various mutations that are known to affect circuit properties of AWC signaling were crossed into *gcy-28* mutants and tested for chemotaxis. e*at-4* encodes a vesicular glutamate transporter, and *eat-4* mutants are defective for many sensory behaviors (Lee et al., 1999). In particular, *eat-4* reduces but does not eliminate AWC chemotaxis, and eliminates AWC-induced turning behavior, both due to its cell autonomous function in AWC (Chalasani et al., 2007). In a *gcy-28; eat-4* double mutant, all AWC function was lost. Butanone avoidance was abolished, suggesting that glutamate is required for butanone avoidance in *gcy-28* mutants (Fig. 6A), the benzaldehyde chemotaxis defect of *eat-4* mutants was enhanced by a *gcy-28* mutation, and similarly the two mutations had an additive effect on 2,3-pentanedione chemotaxis (Fig. 6A). These results suggest that *gcy-28* and *eat-4* act in parallel to regulate AWC chemotaxis.

The transmembrane guanylate cyclase *odr-1* is required for AWC chemotaxis and acts in the cilia to mediate olfactory signal transduction (L'Etoile and Bargmann, 2000). Animals over-expressing *odr-1* (ODR-1(OE)) have hyperactive AWC sensory signaling (Chalasani et al., 2007; L'Etoile and Bargmann, 2000). When *odr-1* was over-expressed in a *gcy-28* mutant, all AWC chemotaxis was lost. Over-expression of *odr-1* suppressed butanone avoidance in *gcy-28* and benzaldehyde chemotaxis was absent (Fig. 6B). Over-expression of *odr-1* causes a 2 AWC^{ON} phenotype and abolished chemotaxis to 2,3-pentanedione (Wes and Bargmann, 2001)(Fig. 6B).

One of the major synaptic partners of AWC is the AIY interneuron (White et al., 1986), which inhibits turning behavior and is inhibited by AWC (Chalasani et al., 2007; Gray et al., 2005). *ttx-3* is a LIM homeobox transcription factor required to specify AIY cell-fates (Altun-Gultekin et al., 2001; Hobert et al., 1997) and a *ttx-3* mutation increases AWC-induced turning (Gray et al., 2005). Butanone avoidance in *gcy-28; ttx-3* double mutants resembled *gcy-28* single mutants (Fig 6C). This result suggests that butanone avoidance does not require AIY, and that other synaptic partners of AWC are sufficient for the behavior. Benzaldehyde chemotaxis defect of *gcy-28* were partially suppressed by *ttx-3*.

Discussion

Investigating the role of *gcy-28* in AWC chemotaxis using genetic and structure-function approaches revealed complex effects of cells and signaling pathways on AWC odor preference. *gcy-28* acts mostly in AWC, but can influence AWC chemotaxis through other neurons that have positive and negative effects. GCY-28 activity requires the extracellular domain, suggesting the existence of a psiible ligand, and cGMP signaling through *gcy-28* acts in concert with a cAMP/PKA signaling pathway to regulate AWC chemotaxis. Glutamate signaling potentiates both attraction and avoidance of butanone. These results suggest that an olfactory sensory neuron integrates multiple intracellular and inter-neuronal signals to regulate flexible behaviors.

Cell non-autonomous regulation of AWC odor preference

AWC chemotaxis is modulated rapidly by odor conditioning, depending on the food context during the conditioning. In the absence of food, animals adapt to odors and even show avoidance of odors (Colbert and Bargmann, 1995)(Chapter 3a). Specifically, prolonged exposure to butanone in the absence of food causes a switch in AWC olfactory preference for butanone, similar to a naïve *gcy-28* mutant phenotype. It is possible that *gcy-28* activity is modulated by food availability, and that conditioning in the absence of food leads to down-regulation of *gcy-28* activity. In the presence of food, animals sensitize their response to odors (Torayama et al., 2007), and sensitization can rescue *gcy-28* chemotaxis defects (Chapter 3a). *gcy-28* rescue experiments suggest that altering *gcy-28* activity in a subset of neurons outside of AWC can modify AWC chemotaxis. These neurons may be involved in generating or responding to modulatory signals, such as the presence or absence food, that alter AWC circuit activity.

Integration of modulatory signals by a sensory neuron is seen in *C. elegans* gustatory plasticity, which is regulated in part by insulin signaling between an interneuron and a sensory neuron (Tomioka et al., 2006). The gustatory sensory neuron ASE mediates attraction to salt in naïve animals, but brief exposure to salt in the absence of food causes animals to avoid salt. Plasticity requires an insulin receptor and PI 3-kinase signaling in one ASE, ASER, and an insulin homolog in the interneuron AIA (Tomioka et al., 2006).

Similarly, a ligand for *gcy-28* produced by other cells may regulate *gcy-28* activity in AWC. The vertebrate homologs of *gcy-28*, the natriuretic peptide receptors, are regulated by natriuretic peptide binding to the extracellular domain (Potter et al., 2006). Natriuretic peptides act as endocrine signaling molecules and coordinate

responses to changes in physiological states (eg. blood pressure). Ligands for *gcy-28* may be produced in response to changes in the animal's internal state, such as starvation, which in turn regulate *gcy-28* activity to modify AWC odor preference.

The *gcy-28* rescue experiments suggest that AWB neurons and some *osm-3*-expressing neurons have a negative effect on AWC chemotaxis. AWB mediates avoidance of odors, but it is not known how AWB activity affects the AWC circuitry. AWB and AWC have common synaptic targets (White et al., 1986), which could be a site of integration. Many *osm-3*-expressing neurons have roles in food-dependent regulation of behavior (Chang et al., 2006; Hukema et al., 2006). Similarly, they may affect food-dependent modulation of AWC plasticity. The detailed mechanisms of these interactions are unknown, but several experiments point to the importance of peptide signaling to and from the sensory neurons. The food-related peptide INS-1 is required for starvation-induced plasticity in the salt-sensing ASE neurons (Tomioka et al., 2006), and an LDL-receptor motif-containing peptide, HEN-1, modulates interaction between the ASH and the olfactory neuron AWA (Ishihara et al., 2002).

Neurons that may have a positive influence on AWC chemotaxis are ASE and IL2. ASE neurons sense attractive salts (eg. NaCl), amino acids (eg. lysine) and other large organic molecules (eg. biotin) (Bargmann and Horvitz, 1991), and they have connectivity to interneurons that are similar to that of AWC and also have reciprocal connections with AWC (White et al., 1986). They have the ideal connectivity to directly or indirectly alter AWC signaling. The function of IL2 neurons is not well understood.

Mechanism of odor avoidance in *gcy-28* mutants

Genetic evidence suggests that butanone avoidance is associated with changes in AWC neurotransmission (Chapter 3a). GCY-28 is localized to axons and *gcy-28* mutants interact with a DAG/PKC signaling pathway that regulates synaptic transmission. Genetic interactions of *gcy-28* with the cAMP/PKA signaling pathway, which also regulates neurotransmission at the *C. elegans* neuromuscular junction (NMJ) (Charlie et al., 2006b; Schade et al., 2005), further underscores the convergence of signaling pathways at the synapse. cAMP/PKA signaling targets many components of the classical vesicle secretion machinery, such as SNAP25 (Nagy et al., 2004), but also regulates dense core vesicle secretion (Zhou et al., 2007). *acy-1* encodes an adenylate cyclase that probably acts upstream of PKA to enhance neurotransmission at the *C. elegans* NMJ (Charlie et al., 2006a). Induction of PKA by a *kin-2* mutation suppressed butanone avoidance. However, a loss of adenylate cyclase activity caused by the *acy-1* mutant did not have a butanone avoidance phenotype. In the absence of *acy-1*, the cGMP and PKC signaling pathways may be sufficient to maintain attraction in AWC. Alternatively, *acy-1* null mutations are lethal (Moorman and Plasterk, 2002), so the viable reduction-of-function mutant may have sufficient adenylate cyclase activity to prevent switching of odor preference. The cellular site of *kin-2* action has not yet been determined. In light of the cell non-autonomous regulation of AWC chemotaxis in *gcy-28* mutants, these genetic interpretations are preliminary.

The suppression of *gcy-28* by the Ca^{2+}-activated K^+ channel gene *slo-1* is also consistent with a synaptic defect being a major cause of the chemotaxis defects in *gcy-28* mutants. Again, however, the cellular site of *slo-1* action is not known. The mammalian *slo-1* channel is tightly associated with presynaptic Ca^{2+} channels, that regulate

neurotransmission, consistent with a synaptic function (Meir et al., 1999). In addition, *C. elegans slo-1* has developmental effects related to those of the presynaptic Ca^{2+} channel UNC-2 (Davies et al., 2003; Troemel et al., 1999). The subcellular localization of SLO-1 is also unkown. If it is present in AWC axons, a synaptic role is likely, but it could be acting in AWC cilia to modify the sensory response. Olfactory signal transduction in vertebrates as well as other invertebrates uses a stimulus-on response, that is, the sensory neurons depolarize in response to odor (Schild and Restrepo, 1998). However, odors may also inhibit olfactory neurons through Ca^{2+}-activated K^+ channels that open after activation of Ca^{2+}-permeable cAMP-gated channels (Castillo et al., 2005; Madrid et al., 2005). In *C. elegans* AWC olfactory neurons, odor removal induces large Ca^{2+} transients (Chalasani et al., 2007) (Chapter 3a), suggesting that the neuron is inhibited by odor. This is analogous to vertebrate visual transduction, in which light reduces cGMP levels in the photoreceptor and closes CNG channels (Stryer, 1986). If odor inhibits CNG channels in AWC, closing CNG channels could also close Ca^{2+}-activated K^+ channels. Careful characterization of signal transduction kinetics using electrophysiological methods will help to understand how AWC^{ON} can signal attraction and avoidance.

In wild-type *C. elegans*, glutamate released from AWC activates AIB – a turn-promoting interneuron, and inhibits AIY – a turn-suppressing interneuron (Gray et al., 2005), and promotes attraction to AWC odors. In *gcy-28* mutants glutamate transmission is required for butanone avoidance. This is consistent with the idea that misregulated glutamate signaling is the cause of odor preference switch. The fact that AIB calcium responses in *gcy-28* mutants to butanone are distinct from those of wild-type animals further supports the presence of alternative modes of signaling at the AWC-AIB synapse.

In one model, odor preference of AWC may be specified by the strength of glutamatergic signaling such that weak signals lead to avoidance and strong signals lead to attraction. Both AIB and AIY express glutamate-gated ionotropic (iGluR) and metabotropic (mGluR) receptors. The level of glutamate released from AWC may affect which receptor type is preferentially activated.

Signal processing and integration occurs even at the earliest stages of a sensory system. In the visual system, for example, the microenvironment of the cone synapse alters the shape of information transfer to downstream interneurons (DeVries et al., 2006). In the mouse olfactory system, activity of axonal CNG channels modulates synaptic transmission (Murphy and Isaacson, 2003). Understanding olfactory signaling in *C. elegans* will shed light on mechanisms of sensory processing and the behavioral effects of modulatory signaling pathways.

Materials and methods

Strains and reagents

C. elegans strains were cultured using standard methods (Brenner, 1974). The following strains were used: wild-type Bristol (N2), CX713 *gcy-28(ky713) I,* FX02411 *gcy-28(tm2411) I*, CX10222 *gcy-28(tm3028) I*, CB1376 *daf-3(e1376) X*, CX6987 *gcy-28(ky713) I; daf-3(e1376) X*, KG532 *kin-2(ce179) X*, CX8621 *gcy-28(ky713) I; kin-2(ce179) X*, BZ142 *slo-1(eg142) V*, CX8219 *gcy-28(ky713) I; slo-1 (eg142) V*, CX5 *eat-4(ky5) III*, CX7435 *gcy-28(ky713) I; eat-4(ky5) III*, CX6611 *kyIs330[ODR-1OE]*, CX7673 *gcy-28(ky713) I; kyIs330*, OH8 *ttx-3(mg158) X*, CX7433 *gcy-28(ky713) I, ttx-*

3(mg158) X, CX9569 *gcy-28(ky713) I; kyEx2040 [str-2::t01a4.1c::gfp]*, CX9831 *gcy-28(ky713) I; kyEx2170 [odr-3::t01a4.1c::gfp]*, CX7491 *gcy-28(ky713) I; kyEx906[tax-4::t01a4.1c]*, CX9221 *gcy-28(ky713) I; kyEx1853[egl-2::t01a4.1c]*, CX9467 *gcy-28(ky713) I; kyEx1997[ceh-36::t01a4.1c]*, CX9323 *gcy-28(ky713) I; kyEx1926 [des-2::t01a4.1c::gfp]*, CX9571 *gcy-28(ky713) I; kyEx2042[osm-3::t01a4.1c]*, CX7728 *gcy-28(ky713) I; kyEx1070[odr-2 2b::t01a4.1c]*, CX7790 *gcy-28(ky713) I; kyEx1095[odr-3::t01a4.1c, odr-2 2b::t01a4.1c]*, CX7629 *gcy-28(ky713) I; kyEx1022[tax-4::t01a4.1c, odr-2 2b::t01a4.1c]*, CX9282 *gcy-28(ky713) I; kyEx1901[tax-4::t01a4.1c, osm-3::t01a4.1c]*, CX9321 *gcy-28(ky713) I; kyEx1924[tax-4::t01a4.1c, des-2::t01a4.1c]*, CX7868 *gcy-28(ky713) I; kyEx1155[egl-2::t01a4.1c, odr-2 2b::t01a4.1c]*, CX9470 *gcy-28(ky713) I; kyEx2000[ceh-36::t01a4.1c, odr-2 2b::t01a4.1c]*, CX7629 *gcy-28(ky713) I; kyEx1022[osm-3::t01a4.1c, odr-2 2b::t01a4.1c]*, CX10424 *gcy-28(ky713) I; kyEx2507[odr-3::t01a4.1d(ΔECD)::gfp]*. All transgenics were made essentially as described (Mello et al., 1991), with the co-injection marker *elt-2::GFP* (pJM23) unless noted otherwise. Most test plasmids were injected at 20-50 ng/µL.

Odor reagents were obtained from Sigma-Aldrich (St. Louis, MO).

Molecular biology

Extracellular domain deletion of *gcy-28.d* was made using the following primers: 5'–GATAAGAGCAAGTGTCCGCAGGGaTATCCACTTCATGTCTAT CTTC–3' and 5'–GAAGATAGACATGAAGTGGATAtCCCTGCGGACACTTGCTCTTATC–3', to create a unique EcoRV site in a fragment of *gcy-28.d* cDNA flanked by the start codon and a unique AvaI site. This construct was cut with EcoRV and BsrBI to remove most of

the extracellular domain, and one nucleotide was inserted at the ligation site to fix a frameshift. The frameshifted 5' end replaced the wild-type 5' end of the complete *gcy-28.d* cDNA fused to GFP at the 3' end.

Behavioral assays

Population chemotaxis assays were performed on assay agar (1.6 % agar, 1 mM $MgSO_4$, 1 mM $MgCl_2$, 5 mM phosphate buffer, pH 6.0) in 10 cm square plates. Unless otherwise indicated, odor dilutions in ethanol were 2-butanone 1:1,000; 2,3-pentanedione 1:10,000; benzaldehyde.

References

Altun-Gultekin, Z., Andachi, Y., Tsalik, E. L., Pilgrim, D., Kohara, Y., and Hobert, O. (2001). A regulatory cascade of three homeobox genes, *ceh-10*, *ttx-3* and *ceh-23*, controls cell fate specification of a defined interneuron class in *C. elegans*. Development *128*, 1951-1969.

Bargmann, C. I., Chemosensation in *C. elegans* (October 25, 2006), *WormBook*, ed. The *C. elegans* Research Community, WormBook, 10.1895/wormbook.1.123.1, http://www.wormbook.org

Bargmann, C. I., Hartwieg, E., and Horvitz, H. R. (1993). Odorant-selective genes and neurons mediate olfaction in *C. elegans*. Cell *74*, 515-527.

Bargmann, C. I., and Horvitz, H. R. (1991). Chemosensory neurons with overlapping functions direct chemotaxis to multiple chemicals in *C. elegans*. Neuron *7*, 729-742.

Berger, A. J., Hart, A. C., and Kaplan, J. M. (1998). G alphas-induced neurodegeneration in *Caenorhabditis elegans*. J Neurosci *18*, 2871-2880.

Brenner, S. (1974). The genetics of *Caenorhabditis elegans*. Genetics *77*, 71-94.

Castillo, K., Bacigalupo, J., and Wolff, D. (2005). Ca2+-dependent K+ channels from rat olfactory cilia characterized in planar lipid bilayers. FEBS Lett *579*, 1675-1682.

Chalasani, S. H., Chronis, N., Tsunozaki, M., Gray, J. M., Ramot, D., Goodman, M. B., and Bargmann, C. I. (2007). Dissecting a circuit for olfactory behaviour in *Caenorhabditis elegans*. Nature *450*, 63-70.

Chang, A. J., Chronis, N., Karow, D. S., Marletta, M. A., and Bargmann, C. I. (2006). A distributed chemosensory circuit for oxygen preference in *C. elegans*. PLoS Biol *4*, e274.

Charlie, N. K., Schade, M. A., Thomure, A. M., and Miller, K. G. (2006a). Presynaptic UNC-31 (CAPS) is required to activate the G alpha(s) pathway of the *Caenorhabditis elegans* synaptic signaling network. Genetics *172*, 943-961.

Charlie, N. K., Thomure, A. M., Schade, M. A., and Miller, K. G. (2006b). The Dunce cAMP phosphodiesterase PDE-4 negatively regulates G alpha(s)-dependent and G alpha(s)-independent cAMP pools in the *Caenorhabditis elegans* synaptic signaling network. Genetics *173*, 111-130.

Colbert, H. A., and Bargmann, C. I. (1995). Odorant-specific adaptation pathways generate olfactory plasticity in *C. elegans*. Neuron *14*, 803-812.

Daniels, S. A., Ailion, M., Thomas, J. H., and Sengupta, P. (2000). *egl-4* acts through a transforming growth factor-beta/SMAD pathway in *Caenorhabditis elegans* to regulate multiple neuronal circuits in response to sensory cues. Genetics *156*, 123-141.

Davies, A. G., Pierce-Shimomura, J. T., Kim, H., VanHoven, M. K., Thiele, T. R., Bonci, A., Bargmann, C. I., and McIntire, S. L. (2003). A central role of the BK potassium channel in behavioral responses to ethanol in *C. elegans*. Cell *115*, 655-666.

DeVries, S. H., Li, W., and Saszik, S. (2006). Parallel processing in two transmitter microenvironments at the cone photoreceptor synapse. Neuron *50*, 735-748.

Gray, J. M., Hill, J. J., and Bargmann, C. I. (2005). A circuit for navigation in *Caenorhabditis elegans*. Proc Natl Acad Sci U S A *102*, 3184-3191.

Hobert, O., Mori, I., Yamashita, Y., Honda, H., Ohshima, Y., Liu, Y., and Ruvkun, G. (1997). Regulation of interneuron function in the *C. elegans* thermoregulatory pathway by the *ttx-3* LIM homeobox gene. Neuron *19*, 345-357.

Hukema, R. K., Rademakers, S., Dekkers, M. P., Burghoorn, J., and Jansen, G. (2006). Antagonistic sensory cues generate gustatory plasticity in *Caenorhabditis elegans*. Embo J *25*, 312-322.

Ishihara, T., Iino, Y., Mohri, A., Mori, I., Gengyo-Ando, K., Mitani, S., and Katsura, I. (2002). HEN-1, a secretory protein with an LDL receptor motif, regulates sensory integration and learning in *Caenorhabditis elegans*. Cell *109*, 639-649.

L'Etoile, N. D., and Bargmann, C. I. (2000). Olfaction and odor discrimination are mediated by the *C. elegans* guanylyl cyclase ODR-1. Neuron *25*, 575-586.

Lee, R. Y., Sawin, E. R., Chalfie, M., Horvitz, H. R., and Avery, L. (1999). EAT-4, a homolog of a mammalian sodium-dependent inorganic phosphate cotransporter, is necessary for glutamatergic neurotransmission in *Caenorhabditis elegans*. J Neurosci *19*, 159-167.

Lopez, M. J., Wong, S. K., Kishimoto, I., Dubois, S., Mach, V., Friesen, J., Garbers, D. L., and Beuve, A. (1995). Salt-resistant hypertension in mice lacking the guanylyl cyclase-A receptor for atrial natriuretic peptide. Nature *378*, 65-68.

Madrid, R., Delgado, R., and Bacigalupo, J. (2005). Cyclic AMP cascade mediates the inhibitory odor response of isolated toad olfactory receptor neurons. J Neurophysiol *94*, 1781-1788.

Meir, A., Ginsburg, S., Butkevich, A., Kachalsky, S. G., Kaiserman, I., Ahdut, R., Demirgoren, S., and Rahamimoff, R. (1999). Ion channels in presynaptic nerve terminals and control of transmitter release. Physiol Rev *79*, 1019-1088.

Mello, C. C., Kramer, J. M., Stinchcomb, D., and Ambros, V. (1991). Efficient gene transfer in *C. elegans*: extrachromosomal maintenance and integration of transforming sequences. Embo J *10*, 3959-3970.

Moorman, C., and Plasterk, R. H. (2002). Functional characterization of the adenylyl cyclase gene *sgs-1* by analysis of a mutational spectrum in *Caenorhabditis elegans*. Genetics *161*, 133-142.

Murphy, G. J., and Isaacson, J. S. (2003). Presynaptic cyclic nucleotide-gated ion channels modulate neurotransmission in the mammalian olfactory bulb. Neuron *37*, 639-647.

Nagy, G., Reim, K., Matti, U., Brose, N., Binz, T., Rettig, J., Neher, E., and Sorensen, J. B. (2004). Regulation of releasable vesicle pool sizes by protein kinase A-dependent phosphorylation of SNAP-25. Neuron *41*, 417-429.

Okochi, Y., Kimura, K. D., Ohta, A., and Mori, I. (2005). Diverse regulation of sensory signaling by *C. elegans* nPKC-epsilon/eta TTX-4. Embo J *24*, 2127-2137.

Oliver, P. M., Fox, J. E., Kim, R., Rockman, H. A., Kim, H. S., Reddick, R. L., Pandey, K. N., Milgram, S. L., Smithies, O., and Maeda, N. (1997). Hypertension, cardiac hypertrophy, and sudden death in mice lacking natriuretic peptide receptor A. Proc Natl Acad Sci U S A *94*, 14730-14735.

Potter, L. R., Abbey-Hosch, S., and Dickey, D. M. (2006). Natriuretic peptides, their receptors, and cyclic guanosine monophosphate-dependent signaling functions. Endocr Rev *27*, 47-72.

Schade, M. A., Reynolds, N. K., Dollins, C. M., and Miller, K. G. (2005). Mutations that rescue the paralysis of *Caenorhabditis elegans ric-8* (synembryn) mutants activate the G alpha(s) pathway and define a third major branch of the synaptic signaling network. Genetics *169*, 631-649.

Schild, D., and Restrepo, D. (1998). Transduction mechanisms in vertebrate olfactory receptor cells. Physiol Rev *78*, 429-466.

Stryer, L. (1986). Cyclic GMP cascade of vision. Annu Rev Neurosci *9*, 87-119.

Tamura, N., Doolittle, L. K., Hammer, R. E., Shelton, J. M., Richardson, J. A., and Garbers, D. L. (2004). Critical roles of the guanylyl cyclase B receptor in endochondral ossification and development of female reproductive organs. Proc Natl Acad Sci U S A *101*, 17300-17305.

Tomioka, M., Adachi, T., Suzuki, H., Kunitomo, H., Schafer, W. R., and Iino, Y. (2006). The insulin/PI 3-kinase pathway regulates salt chemotaxis learning in *Caenorhabditis elegans*. Neuron *51*, 613-625.

Torayama, I., Ishihara, T., and Katsura, I. (2007). *Caenorhabditis elegans* integrates the signals of butanone and food to enhance chemotaxis to butanone. J Neurosci *27*, 741-750.

Troemel, E. R., Sagasti, A., and Bargmann, C. I. (1999). Lateral signaling mediated by axon contact and calcium entry regulates asymmetric odorant receptor expression in *C. elegans*. Cell *99*, 387-398.

Tsuji, T., and Kunieda, T. (2005). A loss-of-function mutation in natriuretic peptide receptor 2 (Npr2) gene is responsible for disproportionate dwarfism in *cn/cn* mouse. J Biol Chem *280*, 14288-14292.

Wang, Z. W., Saifee, O., Nonet, M. L., and Salkoff, L. (2001). SLO-1 potassium channels control quantal content of neurotransmitter release at the *C. elegans* neuromuscular junction. Neuron *32*, 867-881.

Wes, P. D., and Bargmann, C. I. (2001). *C. elegans* odour discrimination requires asymmetric diversity in olfactory neurons. Nature *410*, 698-701.

White, J. G., Southgate, E., Thomson, J. N., and Brenner, S. (1986). The structure of the nervous system of the nematode *Caenorhabditis elegans*. Phil Trans R Soc Lond B *314*, 1-340.

Zhou, K. M., Dong, Y. M., Ge, Q., Zhu, D., Zhou, W., Lin, X. G., Liang, T., Wu, Z. X., and Xu, T. (2007). PKA activation bypasses the requirement for UNC-31 in the docking of dense core vesicles from *C. elegans* neurons. Neuron *56*, 657-669.

Promoter #2	Promoter #1							
	tax-4	*str-2*	*odr-3*	*ceh-36*	*egl-2*	*osm-3*	*des-2*	*odr-2 2b*
none	**0.43***	**0.78****	0.14	**0.62***	**0.69***	-0.01	-0.08	0.16
osm-3	-0.05							
des-2	**0.86****							
odr-2 2b	**0.73****		**0.55***	**0.84****	**0.81****	-0.15		

Table 4-1. Fractional rescue of butanone chemotaxis in *gcy-28* mutants
gcy-28(ky713) mutants carrying *gcy-28.c* cDNA driven under one or two promoters were tested for butanone chemotaxis. Numbers are calculated as (chemotaxis index (CI) of test strain - CI *gcy-28(ky713)*)/(CI wild-type - CI *gcy-28(ky713)*). Fraction of 1.0 represents complete rescue (wild-type level), 0 represents no rescue (*gcy-28* level) and negative fractions represent enhancement of the defect. CI averages from at least 4 assays done on at least two days were used. Results for benzaldehyde chemotaxis were qualitatively similar. * $p < 0.05$ relative to both wild-type and *gcy-28* mutant, ** $p < 0.05$ relative to *gcy-28* mutant, Bonferroni *t*-test.

Expressed neurons	Promoter							
	str-2	*odr-3*	*ceh-36*	*tax-4*	*egl-2*	*osm-3*	*des-2*	*odr-2 2b*
AWC	√†	√	√	√	√			
AWB		√		√				
ASE			√	√	√	√		
ASG				√		√		√
ASH		(√)				√		
ASI/ ASJ/ ASK				√		√		
ADL/ ADF		(√)				√		
AFD				√	√			
IL2					√	√	(√)	√
AQR/ PQR/ BAG/ URX				√	√			
AIB								√
others		(√)					√	√

Table 4-2. Expression pattern of promoters
Expression patterns were either observed directly in the transgenic lines or based on informations on WormBase (www.wormbase.org).
† Expression in AWC^{ON} only

Promoters		Butanone				Benzaldehyde			
		rescue	WT	*gcy-28*	fraction	rescue	WT	*gcy-28*	fraction
str-2		0.24	0.47	-0.58	0.78	0.57	0.85	0.35	0.44
odr-3		-0.29	0.64	-0.44	0.14	0.21	0.88	0.25	-0.06
ceh-36		0.16	0.58	-0.51	0.62	0.50	0.88	0.26	0.39
tax-4		-0.13	0.49	-0.60	0.43	0.28	0.79	-0.08	0.41
egl-2		0.22	0.57	-0.58	0.69	0.66	0.81	0.13	0.79
osm-3		-0.59	0.47	-0.58	-0.01	0.11	0.85	0.35	-0.48
des-2		-0.63	0.46	-0.54	-0.08	0.16	0.85	0.24	-0.12
odr-2 2b		-0.38	0.60	-0.57	0.16	0.14	0.87	0.09	0.07
mgl-1		-0.72	0.66	-0.57	-0.12	0.14	0.85	0.07	0.09
glr-1		-0.31	0.57	-0.46	0.14	0.44	0.88	0.50	-0.15
glr-3		-0.71	0.44	-0.53	-0.18	-0.04	0.79	0.33	-0.81
odr-11d		-0.77	0.67	-0.57	-0.16	-0.25	0.91	-0.04	-0.22
odr-3	*odr-2 2b*	0.07	0.57	-0.54	0.55	0.38	0.79	-0.08	0.53
ceh-36	*odr-2 2b*	0.40	0.58	-0.51	0.84	0.67	0.88	0.26	0.66
tax-4	*odr-2 2b*	0.27	0.58	-0.58	0.73	0.71	0.84	0.16	0.81
egl-2	*odr-2 2b*	0.32	0.54	-0.61	0.81	0.65	0.85	0.31	0.63
osm-3	*odr-2 2b*	-0.66	0.57	-0.50	-0.15	-0.27	0.76	-0.16	-0.12
ceh-14	*odr-2 2b*	-0.20	0.61	-0.46	0.24	0.38	0.87	0.24	0.22
flp-8	*odr-2 2b*	-0.18	0.61	-0.46	0.26	0.27	0.87	0.24	0.05
gcy-31	*odr-2 2b*	-0.26	0.61	-0.46	0.19	0.30	0.87	0.24	0.09
tax-4	*glr-1*	-0.15	0.57	-0.46	0.30	0.41	0.88	0.50	-0.23
glr-3	*odr-2 2b*	-0.41	0.62	-0.61	0.16	0.08	0.80	-0.03	0.13
tax-4	*des-2*	0.32	0.46	-0.54	0.86	0.69	0.85	0.24	0.73
tax-4	*osm-3*	-0.60	0.53	-0.55	-0.05	0.37	0.81	0.29	0.16
egl-2	*glr-3*	0.15	0.52	-0.49	0.63	0.66	0.81	0.34	0.67

(Table 4-3)

Promoters			rescue	WT	*gcy-28*	fraction	rescue	WT	*gcy-28*	fraction
tax-4	*odr-2 2b*	*mgl-1*	0.32	0.49	-0.60	0.85	0.63	0.79	-0.08	0.81
odr-3	*odr-2 2b*	*mgl-1*	0.12	0.49	-0.60	0.66	0.41	0.79	-0.08	0.56
tax-4	*ttx-3*	*odr-11d*	-0.21	0.51	-0.56	0.33	0.31	0.78	0.09	0.32
odr-3	*osm-3*	*odr-2 2b*	0.20	0.80	-0.18	0.39	0.50	0.89	0.36	0.26
egl-2	*odr-2 2b*	*glr-3*	0.54	0.52	-0.49	1.02	0.76	0.81	0.34	0.89
odr-3	*ceh-14*	*odr-2 2b*	0.30	0.69	-0.28	0.60	0.43	0.77	0.23	0.37
odr-3	*flp-8*	*odr-2 2b*	0.28	0.76	-0.37	0.58	0.54	0.87	0.22	0.49
odr-3	*gcy-31*	*odr-2 2b*	0.34	0.69	-0.28	0.64	0.52	0.77	0.23	0.53

Table 4-3. Chemotaxis index of *gcy-28* mutants rescued with different promoters
gcy-28(ky713) mutants carrying *gcy-28.c* cDNA driven under one, two or three promoters were tested for butanone (1:1000) and benzaldehyde (1:200) chemotaxis ("rescue" column). Same day controls are listed for comparison ("WT" and "*gcy-28*" columns). Chemotaxis indices (CIs) are averages of at least four assays performed on at least two different days. The "fraction" column represents the fractional rescue, which is calculated as (CI of test strain - CI *gcy-28(ky713)*)/(CI wild-type - CI *gcy-28(ky713)*). Fraction of 1.0 represents complete rescue (wild-type level), 0 represents no rescue (*gcy-28* level) and negative fractions represent enhancement of the defect.

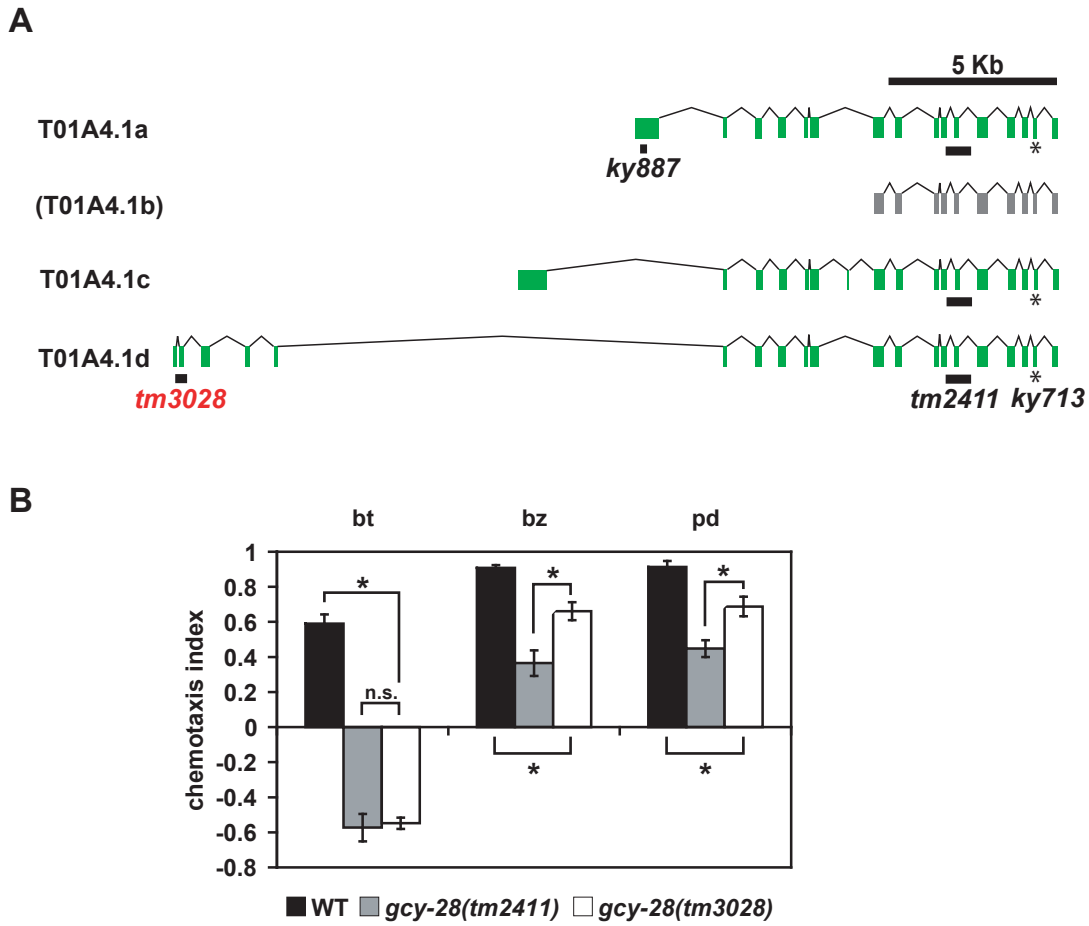


Figure 4-1. Effect of a *gcy-28.d*-specific deletion on chemotaxis
(A) Genomic region encoding *gcy-28*. Deletions are indicated by a solid bar and a point mutation is indicated by an asterisk. The *tm3028* deletion removes part of exon 1 and all of exon 2 from t01a4.1d. (B) Chemotaxis of *gcy-28* deletion alleles *tm2411* and *tm3028*. * $p < 0.05$, n.s. not significant, Bonferroni *t*-test. Error bars indicate SEM.

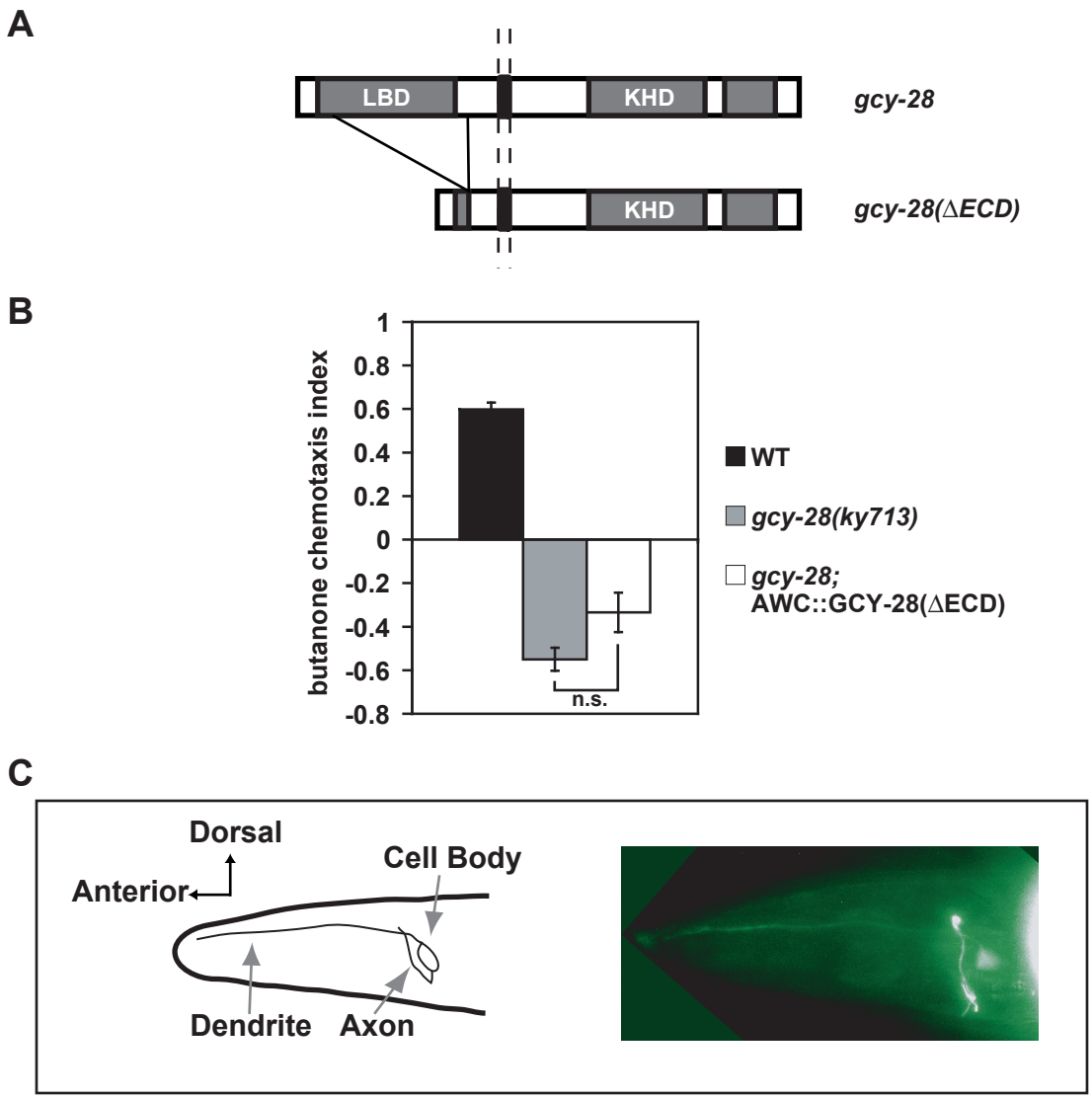


Figure 4-2. Effect of extracellular domain deletion on *gcy-28* rescuing activity
(A) Predicted location of deletion in the extracellular domain of GCY-28. (B) Chemotaxis of *gcy-28(ky713)* mutants expressing an extracellular-domain deleted *gcy-28* in AWC using the *odr-3* promoter. n.s. not significant, Bonferroni *t*-test. (C) Subcellular localization of GFP-tagged GCY-28(ΔECD) expressed in AWC.

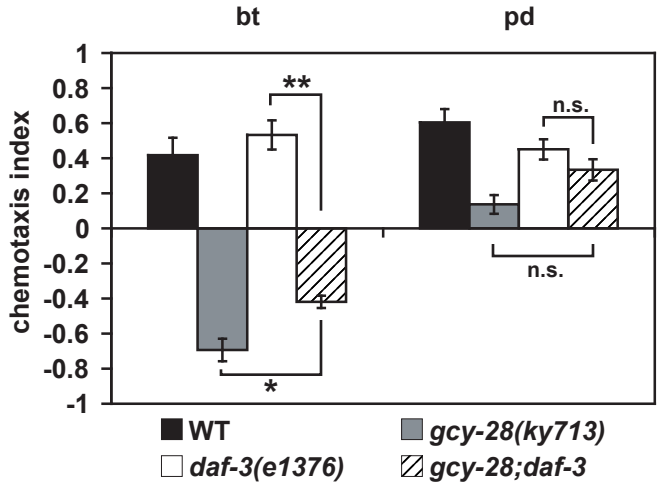


Figure 4-3. Genetic interaction between *gcy-28* and *daf-3*, a suppressor of PKG mutants

Effect of co-SMAD transcription factor, *daf-3*, on *gcy-28* chemotaxis. * $p < 0.05$, ** $p < 0.01$, Bonferroni *t*-test. Error bars indicate SEM.

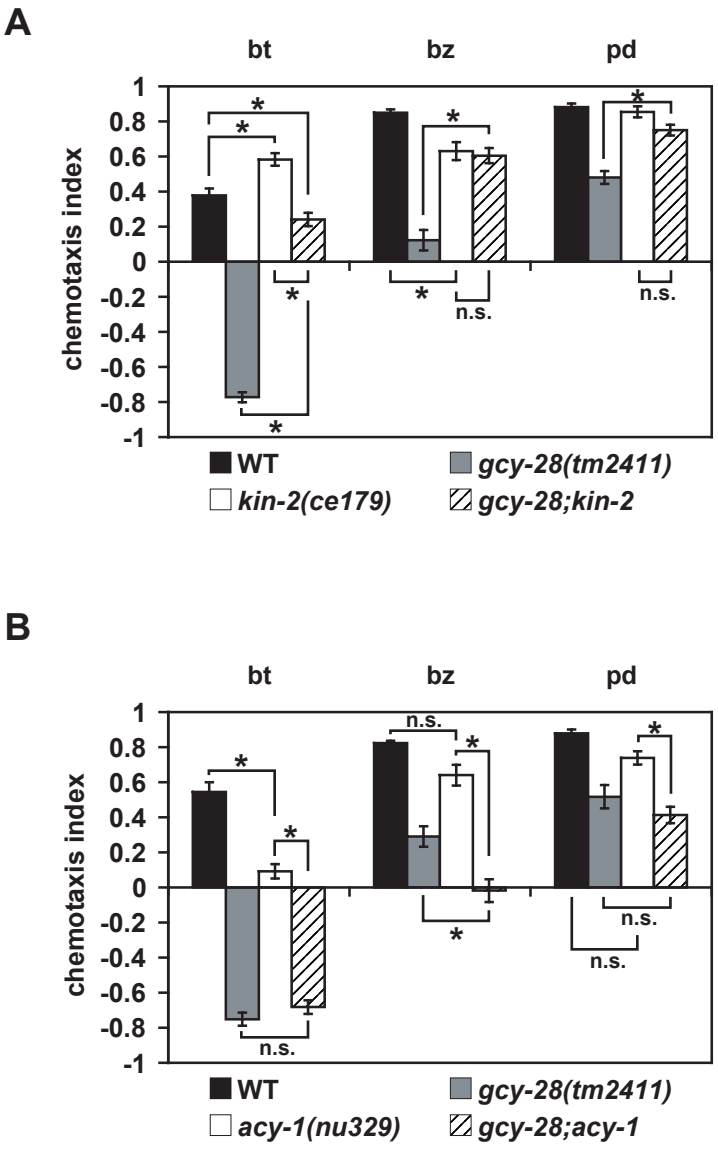


Figure 4-4. Genetic interaction between *gcy-28* and cAMP signaling
(A) Effect of a mutation in the regulatory subunit of PKA, *kin-2*, on *gcy-28* chemotaxis. (B) Chemotaxis of an adenylate cyclase, *acy-1*, and its interaction with *gcy-28*. * $p <$ 0.05, n.s. not significant, Bonferroni *t*-test. Error bars indicate SEM.

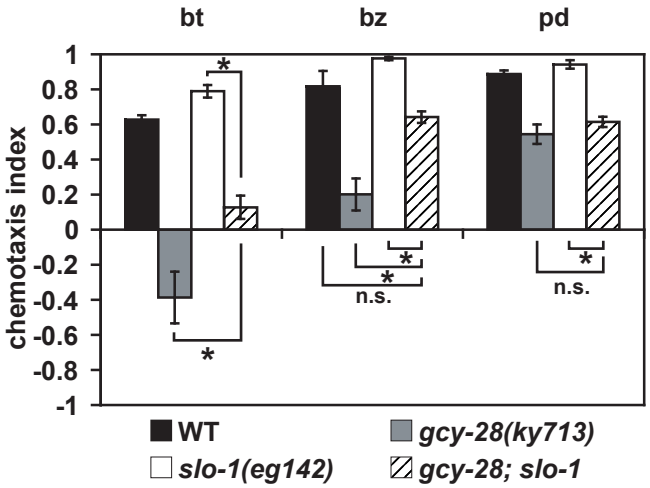


Figure 4-5. Genetic interaction between *gcy-28* and the BK channel mutant, *slo-1*
Effect of a mutation in *slo-1*, a large conductance Ca^{2+}-regulated K^{+} channel, on *gcy-28* chemotaxis. * $p < 0.05$, n.s. not significant, Bonferroni *t*-test. Error bars indicate SEM.

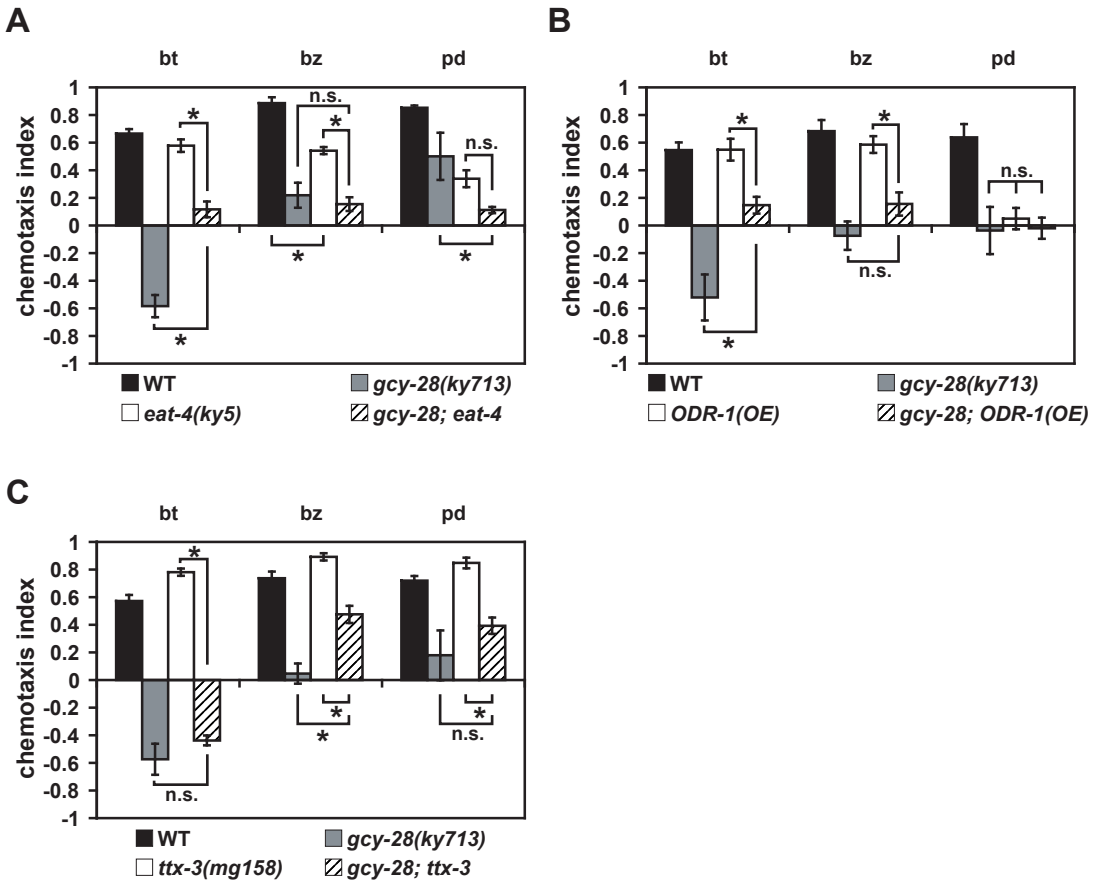


Figure 4-6. Genetic interaction between *gcy-28* and circuit mutants
(A) Effect of a vesicular glutamate transporter mutation, *eat-4*, on *gcy-28* chemotaxis. (B) Effect of overexpressing olfactory sensory guanylate cyclase, ODR-1, on *gcy-28* chemotaxis. (C) Effect of an AIY interneuron cell-fate mutation, *ttx-3*, on *gcy-28* chemotaxis. * $p < 0.05$, n.s. not significant, Bonferroni *t*-test. Error bars indicate SEM.

CHAPTER 5

cGMP signaling regulates hypo-osmotic stress responses in *C. elegans*

Summary

Maintaining an appropriate water balance is critical for all organisms. Here, the nematode *Caenorhabditis elegans* was used as a model system to dissect the molecular and cellular mechanisms of responses to hypo-osmotic stress. Wild-type animals, when shifted from high to low osmotic environments, reduce their locomotion speed while continuing to move. Animals with mutations in the receptor-type guanylate cyclase *gcy-28* have a transient acute paralysis during hypo-osmotic stress. cGMP signaling acting in neurons prevents hypo-osmotic paralysis in *gcy-28* mutants and a cGMP-dependent protein kinase acts downstream of the cyclase. *gcy-28* is a homolog of the mammalian atrial natriuetic peptide receptor, which functions to regulate blood pressure and water homeostasis. Therefore neuronal cGMP signaling in *C. elegans* plays an important and possibly conserved function in water homeostasis. Genetic analysis suggests that the putative mechanosensory neurons, PVD and FLP, regulate the hypo-osmotic stress response, perhaps functioning as osmosensors.

Background

In nematodes, locomotion is closely linked to proper regulation of water balance. Nematodes have a high internal hydrostatic pressure (called a hydrostatic skeleton) against which their longitudinally oriented muscles contract in a coordinated fashion to generate sinusoidal movement (Harris and Crofton, 1957; Wallace, 1968). The hydrostatic skeleton is maintained by keeping internal osmotic pressure higher than that of the surrounding media through osmoregulatory mechanisms and by regulating muscle tone. Different species of nematodes have adapted to survive in diverse environments, such as the ocean, the soil and inside other organisms, and many are able to osmoregulate in response to fluctuations in their osmotic environment (Wright, 2004). For example, in the marine parasitic nematode *Pseudoterranova decipiens*, the osmotic pressure in the pseudocoelum increases linearly with a slope about 0.25 relative to an increase in the environmental osmotic pressure (Fuse et al., 1993). Metabolic respiration blockers abolish this regulation, consistent with a role for active mechanisms of osmoregulation. However, the molecular and cellular mechanisms of osmoregulation in nematodes are partially understood.

C. elegans responds to osmotic stress by regulating internal levels of glycerol (Lamitina et al., 2004). In the short term, hyperosmotic stress causes shrinking and paralysis due to the loss of water. Within certain range of osmotic step sizes, animals eventually accumulate glycerol and recover motility. Glycerol regulation is part of the long-term response to osmotic stress – glycerol content increases with a $t_{1/2}$ ~8 hrs in hyperosmotic conditions, and dercreases with a $t_{1/2}$ ~4 hrs when shifted back to hypo-osmotic media (Lamitina et al., 2004). Hyper-osmotic stress-resistant (Osr) mutants have

elevated basal levels of glycerol, which prevents acute water loss when animals are placed in high osmotic environments (Solomon et al., 2004; Wheeler and Thomas, 2006).

Water homeostasis in vertebrates is under the control of a network of neuroendocrine signaling pathways (Antunes-Rodrigues et al., 2004). The atrial natriuretic peptide (ANP) system is a major component of this network (reviewed in (Potter et al., 2006)). ANP is released in the heart atrium when blood pressure rises and acts through its receptor guanylate cyclase A (GCA) in the kidneys, and the vasculature to reduce blood volume. Lack of GCA leads to chronic as well as acute hypertension (Holtwick et al., 2002; Lopez et al., 1995). GCA is expressed in the central nervous system, but its function in the brain is not well characterized (Gutkowska et al., 1997).

In the *C. elegans* genome there are 27 transmembrane guanylate cylases (Ortiz et al., 2006) of which one, *gcy-28*, belongs to the family of natriuretic peptide receptors (Chapter 3a). Axonal *gcy-28* and cGMP signaling is required in the AWC olfactory neuron to specify odor preference between attraction and avoidance (Chapter 3a). However, *gcy-28* has at least three structurally distinct isoforms and is widely expressed in the nervous system as well as many other tissue types, so it may have roles in other processes (Ortiz et al., 2006)(Chapter 3a). By analogy with ANP receptors, one potential role for *gcy-28* is in regulation of water balance.

This study describes the short-term response of *C. elegans* to hypo-osmotic stress and shows that *gcy-28* and cGMP signaling prevents hypo-osmotic stress-induced paralysis. cGMP signaling is required in the nervous system and acts through a protein kinase G-dependent signaling pathway. These results reveal a conservation in the physiological function of cGMP signaling across disparate phyla. Genetic analysis

implicates a set of putative mechanosensory neurons as regulators of the hypo-osmotic stress response in *C. elegans*.

Results

gcy-28 is defective for hypo-osmotic stress-induced increase in body size

The acute response of *C. elegans* to hypo-osmotic stress was observed by transferring animals from high osmolality media, which is isosmotic to their growth media, to low osmolality media (Fig. 1A). The animals were video recorded and analyzed for changes in body size and locomotion speed (See Materials and methods). Wild-type *C. elegans* increased their body length immediately upon being transferred from media containing 300 mM NaCl to media containing 50 mM NaCl, probably due to the influx of water (Fig. 1B). This result is consistent with a previous report that showed an increase in body volume during hypo-osmotic stress (Lamitina et al., 2004). Also consistent with previous reports, hypo-osmotic stress did not cause lethality (Lamitina et al., 2004)(data not shown).

Because atrial natriuretic peptide receptors act to reduce blood volume in mammals, *gcy-28* mutants were tested to see if the *C. elegans* homolog was also required for responses to increases in volume. When *gcy-28* mutants were exposed to hypo-osmotic stress, they increased their body size to a larger extent than wild-type animals (Fig. 1B). This result suggests that *gcy-28* normally acts to limit the net influx of water into the animal.

Hypo-osmotic stress affects locomotion speed

To understand the effects of hypo-osmotic stress on behavior, the animal's locomotion speed was measured. Wild-type *C. elegans* moved at ~0.15 mm/sec on media isosmotic to their growth media (Fig. 2A and B). When shifted to hypo-osmotic media, animals moved more slowly, averaging ~0.06 mm/sec (Fig. 2A and B). The frequency histogram of locomotion speeds showed that in the first 200 seconds of hypo-osmotic stress, animals moved at a wide range of speeds (Fig. 2B). The flat distribution may represent a variable response to hypo-osmotic shock as well as an immediate response to transferring animals (Zhao et al., 2003). The speed distribution gradually changed over the next few minutes such that a single peak representing the average locomotion speed emerged (Fig. 2B). Over the course of 40 minutes of hypo-osmotic stress, animals first reduced their speed gradually and then recovered back to a steady speed of ~0.1 mm/sec (Fig. 1A inset). Occasionally animals stopped moving and appeared transiently paralyzed; these animals often appeared straight with one or two kinks along the body. An animal was defined as being paralyzed if it moved more slowly than 0.01 mm/sec, and the fraction of paralyzed animals over the course of the assay was determined (Fig. 2B and C). No wild-type animals were paralyzed in isosmotic conditions, but in hypo-osmotic conditions, there was a constant low level of paralysis as different animals became transiently paralyzed at different times (Fig. 2C, 3A and data not shown). A larger osmotic down shift resulted in a higher fraction of paralyzed animals (Fig. 3B).

gcy-28 mutants on isosmotic media were slightly faster than wild-type animals (Fig. 2D and E). Upon shifting to hypo-osmotic media, *gcy-28* animals showed a rapid but transient reduction in speed accompanied by paralysis of a large fraction of animals (Fig. 2D, E, F and Fig. 3A). This observation suggested that *gcy-28* animals are defective

in their acute behavioral response to hypo-osmotic stress. A larger osmotic down step caused a more severe paralysis in *gcy-28* mutants (compare Fig. 3A and B). These results suggest that *gcy-28* is required to maintain locomotion during hypo-osmotic stress.

The paralysis caused by shifting NaCl may be due to a specific change in NaCl concentration or due to the change in osmotic pressure. To distinguish between the two possibilities a similar osmotic step was generated using sucrose as the solute. Wild-type animals showed little paralysis when transferred from a high sucrose plate to a low sucrose plate (Fig. 3C), but *gcy-28* animals showed a rapid and transient paralysis (Fig. 3C). These results suggest that *gcy-28* mutants are generally defective in behavioral adaptation to changes in external osmotic strength.

Neuronal cGMP signaling is required for the hypo-osmotic stress response

The hypo-osmotic paralysis defect of *gcy-28* mutants was rescued by expressing a *gcy-28.c* cDNA under its own upstream regulatory region (Fig. 3D). Introducing a mutation in the cyclase domain of *gcy-28* abolished rescuing activity (Fig. 3D). These results suggest that guanylate cyclase activity is necessary for preventing paralysis during hypo-osmotic stress.

The behavioral defects in *gcy-28* mutants could be due to defects at sites of water exchange, such as the gut or hypodermis, due to defects in the locomotory system such as the muscles, or due to defects in neurons that regulate water exchange and/or locomotion. To distinguish between these possibilities, *gcy-28* was expressed in various tissues in *gcy-28* mutants. The *gcy-28* hypo-osmotic paralysis defect was rescued by expressing *gcy-28* using a pan-neuronal promoter (Fig. 3E and Table 1) whereas expression in the

gut, hypodermis or the body wall muscles did not rescue the defect (Table 1). In fact, expression of *gcy-28.c* in hypodermis and gut enhanced the *gcy-28* mutant defect.

A *gcy-28* clone that lacked the extracellular domain partially rescued the hypo-osmotic paralysis defect when expressed from a pan-neuronal promoter (Fig. 3F). Deletion of the extracellular domain suppressed the transient increase in paralysis during hypo-osmotic stress, but it also raised the base line level of paralysis (Fig. 3F). A general reduction in locomotory speed was observed in *gcy-28* mutants carrying the extracellular deletion construct (average speed ± SEM on isosmotic media = 0.15 ± 0.01 mm/sec (*gcy-28)* and 0.088 ± 0.013 mm/sec (*gcy-28* ΔECD rescue), n = 3 assays each), perhaps dues to unregulated cyclase activity. Note that the *gcy-28* mutant had a higher rate of locomotion compared to wildtype (Fig. 2A and D). These results suggest that neuronal cGMP levels may determine overall locomotory speed as well as the extent of paralysis induced by hypo-osmotic stress.

A major effector of cGMP signaling is the cGMP-dependent protein kinase (PKG). *egl-4* is a *C. elegans* homolog of PKG that is required for sensory behaviors and for regulation of development (Daniels et al., 2000; Fujiwara et al., 2002; L'Etoile et al., 2002). *egl-4* mutants were also defective for responses to hypo-osmotic stress (Fig. 4); they showed a marked increase in body size compared to wild-type animals (Fig. 4A) and were rapidly and transiently paralyzed when placed under hypo-osmotic stress (Fig. 4B and C). The locomotory phenotype resembled the *gcy-28* phenotype both in its rapid onset and its time course, suggesting that *egl-4* may act in the same pathway as *gcy-28* to regulate hypo-osmotic stress responses. When *gcy-28; egl-4* double mutants were tested for hypo-osmotic paralysis, they were as defective as the *gcy-28* single mutant in

magnitude of the response, but were more similar to *egl-4* mutants in their rapidity in the onset of paralysis (Fig. 4C). The similar phenotype of the single and double mutants suggests that *gcy-28* and *egl-4* act mostly in the same pathway, although they may have minor roles in hypo-osmotic stress response that are independent of each other. A mutation in another target of cGMP, the cyclic nucleotide-gated channel *tax-4*, did not affect hypo-osmotic paralysis (Table 1).

If *egl-4* acts downstream of *gcy-28*, expression of the extracellular domain-deleted *gcy-28*, which may have unregulated cyclase activity, should not have an effect in *egl-4* mutants. Indeed, *gcy-28(ΔECD)* did not suppress the *egl-4* hypo-osmotic paralysis defect (Fig. 4E). Therefore *gcy-28* acts upstream of or in parallel to *egl-4* to prevent hypo-osmotic stress-induced paralysis.

Why do *gcy-28* and *egl-4* mutants become paralyzed during hypo-osmotic stress? In one scenario, hypo-osmotic stress may prevent muscle contraction by inhibiting motorneuron functions such as neurotransmission. *gcy-28* mutants, as well as *egl-4* mutants, were resistant to the acetylcholinesterase inhibitor aldicarb (Fig. 5)(Daniels et al., 2000), suggesting that acetylcholine release at the neuromuscular junction (NMJ) was reduced. *gcy-28* and *egl-4* may strengthen synaptic transmission at the NMJ in order to maintain locomotion during hypo-osmotic stress. Another possible cause for paralysis, not mutually exclusive, is that in the mutants the hydrostatic skeleton becomes too stiff due to the increased pressure. In that case, the normal function of *gcy-28* and *egl-4* may be to reduce that internal pressure by acting in osmoregulatory neurons.

Harsh touch-sensitive neurons regulate the hypo-osmotic stress response

The specific defects of *gcy-28* and *egl-4* animals suggest that responses to hypo-osmotic stress are regulated by neuronal signaling. To study the mechanism of osmosensing during hypo-osmotic stress, candidate mechanosensory and osmosensory mutants were tested. Osmotic gradients in biological systems generate mechanical forces in the form of membrane stretch (Kung, 2005). Therefore mechanosensory systems are good candidates for osmosensors. *C. elegans* senses touch along its body using a set of mechanosensory neurons (Chalfie et al., 1985) and many mutants defective in the touch response have been isolated (Syntichaki and Tavernarakis, 2004). *mec-3* encodes a LIM homeodomain transcription factor that specifies cell fates for the light-touch mechanoreceptors (ALM, AVM, PLM) and additional putative mechanoreceptors (FLP, PVD) (Kaplan and Horvitz, 1993; Way and Chalfie, 1989). *mec-3* mutants were defective for the hypo-osmotic stress response and showed a rapid and transient increase in paralysis when exposed to a NaCl downstep (Fig. 6A) or a sucrose down step (Fig. 6B). Thus behavioral adaptation to hypo-osmotic stress may require mechanosensory neurons.

To determine which of the *mec*-3-expressing cells were important, several other mutants for touch sensation were tested. *mec-4* encodes a degenerin/epithelium Na^+ channel (DEG/ENaC) that forms the pore-forming subunit of the mechanosensitive DEG/ENaC protein complex. *mec-4* is required for mechanosensory behavior as well as for mechanosensitive currents in the light-touch sensitive neurons (Driscoll and Chalfie, 1991; O'Hagan et al., 2005; Suzuki et al., 2003). A gain-of-function mutation in *mec-4*, *mec-4(e1611dm)*, leads to degeneration of the touch neurons ALM, AVM and PLM but spares FLP and PVD (Driscoll and Chalfie, 1991). The *mec-4(e1611dm)* mutant did not show hypo-osmotic paralysis (Fig. 6B). Thus the light touch neurons may not be

required for the hypo-osmotic stress response, and the *mec-3* hypo-osmotic stress paralysis defect may be caused by defective PVD and FLP neurons. A loss-of-function mutant of *mec-4*, *mec-4(u253*lf*)*, also did not have a hypo-osmotic paralysis defect (Fig. 6C), confirming that light touch sensation is not required for this response.

Another subunit of the mechanosensitive DEG/ENaC protein complex is *mec-6*, which is expressed in a wider set of cells, including the light touch cells and PVD (Chelur et al., 2002). *mec-6* mutants became paralyzed upon a downshift in osmolality (Fig. 6D). This result suggests that a DEG/ENaC protein complex may be important for mediating the hypo-osmotic stress response.

Expression of *gcy-28.c* cDNA in the PVD and FLP neurons did not rescue the *gcy-28* mutant defects (Fig. 5F). This result suggests that cGMP signaling is required in neurons other than PVD and FLP.

The *osr-1* mutant is resistant to effects of hyperosmotic stress in *C. elegans* (Solomon et al., 2004). This mutant was not defective for behavioral adaptation to hypo-osmotic stress (Table 2), suggesting that genetically distinct mechanisms regulate responses to increase and decrease in osmotic pressure.

Discussion

In this study, a novel assay was used to measure acute behavioral adaptation to hypo-osmotic stress in *C. elegans*. A rapid downshift in external osmolality causes slowing of wild-type animals, which may represent an active or a passive response to changes in osmotic pressure. Genetic manipulations in mechanosensitive cells suggest that the PVD and FLP neurons are candidate cells for an osmosensor that detect the initial changes.

Our results show that neuronal cGMP signaling is an important regulator of behavioral adaptation to changes in water balance. In *C. elegans*, *gcy-28* is required in neurons for proper responses to osmotic stress. In rats, ANP applied to neurons in the the hypothalamus can reduce secretion of vasopressin – a hormone with effects on blood volume opposite to ANP (Samson et al., 1987). ANP also reduces glutamatergic neurotransmission from osmosensory neurons that synapse onto vasopressin-secreting population of cells in the hypothalamus, an effect that is mimicked by cGMP analogs (Richard and Bourque, 1996). Thus a neuronal function for natriuretic peptide and cGMP signaling in regulating physiological adaptation to osmotic changes may be conserved across distant phyla.

The PKG *egl-4* may act downstream of *gcy-28* to regulate osmotic responses, although it remains to be seen whether *egl-4* is required in neurons. In vertebrates there are two forms of PKG, PKGI and PKGII, and both have functions in water homeostasis (Hofmann et al., 2006). PKGI is required for vasorelaxation induced by cGMP (Pfeifer et al., 1998), while PKGII inhibits renin secretion in the kidneys (Wagner et al., 1998). PKGI knockout mice have hypertension when young, but not when older (Pfeifer et al., 1998), while the PKGII knockout mice are normotensive (Hofmann et al., 2006). It is not known whether vertebrate PKGs have functions in the nervous system to control water balance. Effectors of cGMP signaling include other pathways, such as phosphodiesterases and cyclic nucleotide-gated channels. Different tissues in vertebrates use different cGMP signaling pathways to regulate water homeostasis (Potter et al., 2006), and species-specific divergence in signaling pathways may also exist.

Nevertheless, some functions of PKG in water homeostasis may be conserved across disparate species.

Regulation of *gcy-28* activity by hypo-osmotic stress

It is not known how *gcy-28* activity is regulated by osmotic changes, or which neurons require *gcy-28*. The activity of a vertebrate homolog of *gcy-28*, guanylate cyclase B (GCB), is inhibited by hyperosmotic stress through a Ca^{2+}- and receptor dephosphorylation-dependent processes (Potthast et al., 2004). In these cells, GCB does not sense osmotic stimuli directly, but is regulated downstream of the osmosensitive step in the same cell. Similarly in *C. elegans*, osmotic stimuli could be sensed by a cell that secretes a ligand to regulate *gcy-28* activity.

The hypo-osmotic paralysis observed in *gcy-28* and *egl-4* mutants may be a result of defects in acute signaling, or of chronic defects in internal water balance. In the former model, hypo-osmotic stimuli could activate *gcy-28* and *egl-4* signaling to counter the stress; in the latter model, signaling could be required to maintain a basal state that is more resistant to osmotic stress. A chronic defect would parallel the phenotype in GCA knockout mice, in which basal blood pressure is elevated (Lopez et al., 1995). Direct measurement of water content as well as cGMP levels and PKG activity levels will be required to distinguish between the possibilities. An indirect measure of body turgidity could also be obtained through the use of microfluidic devices that measure stiffness of individual animals (Park et al., 2007).

The paralysis observed in the mutants studied here was transient, and animals tended to recover within ten minutes. In addition, the mutants tested in this study are all

likely neuronal defects. Thus, neuronal regulation of the hypo-osmotic response may be important for adaptation to acute changes in osmotic pressure. A slower, non-neuronal process tof glycerol and fluid regulation can re-adjust water balance to restore locomotion in wild-type as well as various mutant animals. The excretory cell, hypodermis and the gut are two potential sites of regulation through which extrusion of excess fluid may restore locomotion (Fuse et al., 1993; Nelson and Riddle, 1984; Wright, 2004).

Osmosensing in *C. elegans*

C. elegans senses osmotic stimuli through the polymodal nociceptive neuron ASH (Bargmann et al., 1990; Hilliard et al., 2005). When crawling animals encounter a region of high osmolarity, they undergo a stereotyped avoidance behavior that is initiated by sensory transduction in ASH. Osmotic avoidance requires the TRP channels *osm-9* and *ocr-2*, which localize to the ciliated ending of the neuron at the tip of the head (Kahn-Kirby and Bargmann, 2006). Many TRP channels have been implicated in osmosensing in other systems. In particular, mammalian TRPV4 is gated by hypo-osmotic changes in cell culture (Liedtke et al., 2000), and when expressed in *C. elegans osm-9* mutants it can restore ASH osmotic responses (Liedtke et al., 2003).

This study implicates the PVD and FLP neurons in mediating responses to systemic hypo-osmotic stress. These neurons have extensively branching dendrites that cover a large area around the animal, with PVD covering most of the body and FLP covering the head region (Wormatlas, www.wormatlas.org)(Tsalik et al., 2003). The unique shape of the two neurons makes them good candidate neurons to monitor systemic changes in osmotic or hydrostatic pressure. Components of the light touch transduction

machinery are candidates for molecular sensors for hydrostatic pressure. PVD and FLP express some of the *mec* genes required for light touch sensation (*mec-6*, *mec-7*, and *mec-10* but not *mec-4*). *osm-9* is also expressed in PVD, and TRP channels may function as sensors there as well as in ASH. Preliminary results showed that *osm-9* and *ocr-2* animals are defective for the hypo-osmotic stress response (Table 2). In addtition, the *C. elegans* genome contains 30 DEG/ENaC family members that could interact with *mec-6* (Syntichaki and Tavernarakis, 2004), so these are also candidate sensors.

The hypo-osmotic stress response shows requirement for molecular components of both mechanosensation (*mec-6*) and osmosensation (*osm-9*). It would be interesting to understand if and how these related but distinct mechanisms for mechanical force detection interact to sense systemic changes in osmotic pressure.

Materials and methods

Strains and reagents

C. elegans strains were cultured using standard methods (Brenner, 1974). The following strains were used: wild-type Bristol (N2), CX713 *gcy-28(ky713) I,* FX02411 *gcy-28(tm2411) I*, CX9192 *egl-4(n479) IV*, CX8452 *gcy-28(ky713) I;egl-4(n479) IV*, CX8767 *mec-3(e1338) IV*, CB1611 *mec-4(e1611) X*, TU253 *mec-4(u253) X*, CB1472 *mec-6(e1342) I*, AM1 *osr-1(rm1) I*, CX4533 *ocr-1(ok132) IV*, RB1374 *ocr-3(ok1559) X*, CX3036 *osm-9(ky161) IV*, MT3665 *osm-9(n1601) IV*, VC818 *trp-4(gk341) I*, RB1052 *trpa-1(ok999) IV*, TU185 *deg-3(u701) V*, FK103 *tax-4(ks28) III*, PR678 *tax-4(p678) III*, CX4544 *ocr-2(ak47) V*, CX8314 *gcy-28(ky713) I; kyEx1094 [t01a4.1c::t01a4.1c::gfp]*,

CX7729 *gcy-28(ky713) I; kyEx1071 [t01a4.1c::t01a4.1c(ky713)::gfp]*, CX7623 *gcy-28(ky713) I; kyEx1015 [H20::t01A4.1c::gfp]*, CX7625 *gcy-28(ky713) I; kyEx1018 [myo-3::t01A4.1c::gfp]*, CX8425 *gcy-28(ky713) I; kyEx1406 [col-19::t01A4.1c::gfp]*, CX8995 *gcy-28(ky713) I; kyEx1738 [elt-2::t01A4.1c::gfp]*, CX8793 *gcy-28(ky713) I; kyEx1617 [H20::t01A4.1c(ΔECD)::gfp]*, CX8856 *gcy-28(ky713) I; kyEx1655 [des-2Δ::t01a4.1c::gfp]*, CX8837 *egl-4(n479) IV; kyEx1644 [H20::t01A4.1c(ΔECD)::gfp]*. All transgenics were made essentially as described (Mello et al., 1991), with either *elt-2::GFP* (pJM23), *elt-2::CFP*, or *unc-122::GFP* as co-injection marker. Odor reagents were obtained from Sigma-Aldrich (St. Louis, MO).

Molecular biology

Rescuing *gcy-28.c* constructs have been described previously (Chapter 3a). Extracellular domain deletion of *gcy-28.c* was made using the following primers: 5'–GGTTACGATAAGAGCAAGTGCCCGGGTTATCCACTTCATGTC–3' and 5'–GACATGAAGTGGATAACCCGGGCACTTGCTCTTATCGTAACC–3', to create a unique SmaI site in a fragment of *gcy-28.c* cDNA flanked by the start codon and a unique AvaI site. This construct was cut with SmaI and HincII and religated to remove most of the extracellular domain. The deleted 5' end replaced the wild-type 5' end of the complete *gcy-28.c* cDNA fused to GFP at the 3' end.

Behavioral assays

For hypo-osmotic stress assays, NGM plates with different amounts of solutes were made prior to the assay. Unless otherwise indicated, NaCl was used for the growth and assay

plates. Growth plates contained either 300 mM NaCl or 500 mM sucrose, and assay plates contained equivalent amounts of solute to the growth plate for the iso-osmotic condition, or contained either 50 mM NaCl, 10 mM NaCl or 100 mM sucrose for the hypo-osmotic conditions. Growth plates were seeded with OP50 and allowed to dry two days at room temperature. All plates were then sealed with parafilm and stored at 4 ºC for up to one month before use.

The standard hypo-osmotic stress assay was carried out as follows. Adult animals were picked onto growth plates and their progeny were raised at 20 ºC for five days. Up to 12 young adults that had less than a row of embryos in the gonad were picked onto unseeded, iso-osmotic plates and were starved for 20~30 minutes. Starved animals were transferred to the assay plate and their behavior recorded for ten minutes at two frames per second. Videos were analyzed using a MATLAB script (Ramot et al., 2008) to determine the locomotion speed and body length. The locomotion speed excluded periods in a given track of an animal that were classified as pirouettes (reversals and turns) (Pierce-Shimomura et al., 1999). Body length was defined as the length of a thresholded image of an animal that was thinned to a single line. It has been shown that water content of nematodes correlates linearly with their body length (Piggott et al., 2002). Body length was determined at the end of the starvation period as well as during the assay to allow direct comparison between the same set of animals. Data represents at least two assays performed on at least separate days, unless otherwise noted.

Aldicarb assays were performed essentially as described (Lackner et al., 1999).

References

Antunes-Rodrigues, J., de Castro, M., Elias, L. L., Valenca, M. M., and McCann, S. M. (2004). Neuroendocrine control of body fluid metabolism. Physiol Rev *84*, 169-208.

Bargmann, C. I., Thomas, J. H., and Horvitz, H. R. (1990). Chemosensory cell function in the behavior and development of *Caenorhabditis elegans*. Cold Spring Harb Symp Quant Biol *55*, 529-538.

Brenner, S. (1974). The genetics of *Caenorhabditis elegans*. Genetics *77*, 71-94.

Chalfie, M., Sulston, J. E., White, J. G., Southgate, E., Thomson, J. N., and Brenner, S. (1985). The neural circuit for touch sensitivity in *Caenorhabditis elegans*. J Neurosci *5*, 956-964.

Chelur, D. S., Ernstrom, G. G., Goodman, M. B., Yao, C. A., Chen, L., R, O. H., and Chalfie, M. (2002). The mechanosensory protein MEC-6 is a subunit of the *C. elegans* touch-cell degenerin channel. Nature *420*, 669-673.

Daniels, S. A., Ailion, M., Thomas, J. H., and Sengupta, P. (2000). *egl-4* acts through a transforming growth factor-beta/SMAD pathway in *Caenorhabditis elegans* to regulate multiple neuronal circuits in response to sensory cues. Genetics *156*, 123-141.

Driscoll, M., and Chalfie, M. (1991). The *mec-4* gene is a member of a family of *Caenorhabditis elegans* genes that can mutate to induce neuronal degeneration. Nature *349*, 588-593.

Fujiwara, M., Sengupta, P., and McIntire, S. L. (2002). Regulation of body size and behavioral state of *C. elegans* by sensory perception and the EGL-4 cGMP-dependent protein kinase. Neuron *36*, 1091-1102.

Fuse, M., Davey, K. G., and Sommerville, R. I. (1993). Osmoregulation in the parasitic nematode *Pseudoterranova decipiens*. J Exp Biol *175*, 127-142.

Gutkowska, J., Antunes-Rodrigues, J., and McCann, S. M. (1997). Atrial natriuretic peptide in brain and pituitary gland. Physiol Rev *77*, 465-515.

Harris, J. E., and Crofton, H. D. (1957). Structure and Function in the Nematodes: Internal Pressure and Cuticular Structure in *Ascaris*. J Exp Biol *34*, 116-130.

Hilliard, M. A., Apicella, A. J., Kerr, R., Suzuki, H., Bazzicalupo, P., and Schafer, W. R. (2005). In vivo imaging of *C. elegans* ASH neurons: cellular response and adaptation to chemical repellents. Embo J *24*, 63-72.

Hofmann, F., Feil, R., Kleppisch, T., and Schlossmann, J. (2006). Function of cGMP-dependent protein kinases as revealed by gene deletion. Physiol Rev *86*, 1-23.

Holtwick, R., Gotthardt, M., Skryabin, B., Steinmetz, M., Potthast, R., Zetsche, B., Hammer, R. E., Herz, J., and Kuhn, M. (2002). Smooth muscle-selective deletion of guanylyl cyclase-A prevents the acute but not chronic effects of ANP on blood pressure. Proc Natl Acad Sci U S A *99*, 7142-7147.

Kahn-Kirby, A. H., and Bargmann, C. I. (2006). TRP channels in *C. elegans*. Annu Rev Physiol *68*, 719-736.

Kaplan, J. M., and Horvitz, H. R. (1993). A dual mechanosensory and chemosensory neuron in *Caenorhabditis elegans*. Proc Natl Acad Sci U S A *90*, 2227-2231.

Kung, C. (2005). A possible unifying principle for mechanosensation. Nature *436*, 647-654.

L'Etoile, N. D., Coburn, C. M., Eastham, J., Kistler, A., Gallegos, G., and Bargmann, C. I. (2002). The cyclic GMP-dependent protein kinase EGL-4 regulates olfactory adaptation in *C. elegans*. Neuron *36*, 1079-1089.

Lackner, M. R., Nurrish, S. J., and Kaplan, J. M. (1999). Facilitation of synaptic transmission by EGL-30 Gqalpha and EGL-8 PLCbeta: DAG binding to UNC-13 is required to stimulate acetylcholine release. Neuron *24*, 335-346.

Lamitina, S. T., Morrison, R., Moeckel, G. W., and Strange, K. (2004). Adaptation of the nematode *Caenorhabditis elegans* to extreme osmotic stress. Am J Physiol Cell Physiol *286*, C785-791.

Liedtke, W., Choe, Y., Marti-Renom, M. A., Bell, A. M., Denis, C. S., Sali, A., Hudspeth, A. J., Friedman, J. M., and Heller, S. (2000). Vanilloid receptor-related osmotically activated channel (VR-OAC), a candidate vertebrate osmoreceptor. Cell *103*, 525-535.

Liedtke, W., Tobin, D. M., Bargmann, C. I., and Friedman, J. M. (2003). Mammalian TRPV4 (VR-OAC) directs behavioral responses to osmotic and mechanical stimuli in *Caenorhabditis elegans*. Proc Natl Acad Sci U S A *100 Suppl 2*, 14531-14536.

Lopez, M. J., Wong, S. K., Kishimoto, I., Dubois, S., Mach, V., Friesen, J., Garbers, D. L., and Beuve, A. (1995). Salt-resistant hypertension in mice lacking the guanylyl cyclase-A receptor for atrial natriuretic peptide. Nature *378*, 65-68.

Mello, C. C., Kramer, J. M., Stinchcomb, D., and Ambros, V. (1991). Efficient gene transfer in *C. elegans*: extrachromosomal maintenance and integration of transforming sequences. Embo J *10*, 3959-3970.

Nelson, F. K., and Riddle, D. L. (1984). Functional study of the *Caenorhabditis elegans* secretory-excretory system using laser microsurgery. J Exp Zool *231*, 45-56.

O'Hagan, R., Chalfie, M., and Goodman, M. B. (2005). The MEC-4 DEG/ENaC channel of *Caenorhabditis elegans* touch receptor neurons transduces mechanical signals. Nat Neurosci *8*, 43-50.

Ortiz, C. O., Etchberger, J. F., Posy, S. L., Frokjaer-Jensen, C., Lockery, S., Honig, B., and Hobert, O. (2006). Searching for neuronal left/right asymmetry: genomewide analysis of nematode receptor-type guanylyl cyclases. Genetics *173*, 131-149.

Park, S. J., Goodman, M. B., and Pruitt, B. L. (2007). Analysis of nematode mechanics by piezoresistive displacement clamp. Proc Natl Acad Sci U S A *104*, 17376-17381.

Pfeifer, A., Klatt, P., Massberg, S., Ny, L., Sausbier, M., Hirneiss, C., Wang, G. X., Korth, M., Aszodi, A., Andersson, K. E.*, et al.* (1998). Defective smooth muscle regulation in cGMP kinase I-deficient mice. Embo J *17*, 3045-3051.

Pierce-Shimomura, J. T., Morse, T. M., and Lockery, S. R. (1999). The fundamental role of pirouettes in *Caenorhabditis elegans* chemotaxis. J Neurosci *19*, 9557-9569.

Piggott, S. J., Liu, Q. Z., Glazer, I., and Wright, D. J. (2002). Does osmoregulatory behaviour in entomopathogenic nematodes predispose desiccation tolerance? Nematology *4*, 483-487.

Potter, L. R., Abbey-Hosch, S., and Dickey, D. M. (2006). Natriuretic peptides, their receptors, and cyclic guanosine monophosphate-dependent signaling functions. Endocr Rev *27*, 47-72.

Potthast, R., Abbey-Hosch, S. E., Antos, L. K., Marchant, J. S., Kuhn, M., and Potter, L. R. (2004). Calcium-dependent dephosphorylation mediates the hyperosmotic and lysophosphatidic acid-dependent inhibition of natriuretic peptide receptor-B/guanylyl cyclase-B. J Biol Chem *279*, 48513-48519.

Ramot, D., Johnson, B. E., Berry, T. L., Jr., Carnell, L., and Goodman, M. B. (2008). The Parallel Worm Tracker: a platform for measuring average speed and drug-induced paralysis in nematodes. PLoS ONE *3*, e2208.

Richard, D., and Bourque, C. W. (1996). Atrial natriuretic peptide modulates synaptic transmission from osmoreceptor afferents to the supraoptic nucleus. J Neurosci *16*, 7526-7532.

Samson, W. K., Aguila, M. C., Martinovic, J., Antunes-Rodrigues, J., and Norris, M. (1987). Hypothalamic action of atrial natriuretic factor to inhibit vasopressin secretion. Peptides *8*, 449-454.

Solomon, A., Bandhakavi, S., Jabbar, S., Shah, R., Beitel, G. J., and Morimoto, R. I. (2004). *Caenorhabditis elegans* OSR-1 regulates behavioral and physiological responses to hyperosmotic environments. Genetics *167*, 161-170.

Suzuki, H., Kerr, R., Bianchi, L., Frokjaer-Jensen, C., Slone, D., Xue, J., Gerstbrein, B., Driscoll, M., and Schafer, W. R. (2003). In vivo imaging of *C. elegans* mechanosensory neurons demonstrates a specific role for the MEC-4 channel in the process of gentle touch sensation. Neuron *39*, 1005-1017.

Syntichaki, P., and Tavernarakis, N. (2004). Genetic models of mechanotransduction: the nematode *Caenorhabditis elegans*. Physiol Rev *84*, 1097-1153.

Tsalik, E. L., Niacaris, T., Wenick, A. S., Pau, K., Avery, L., and Hobert, O. (2003). LIM homeobox gene-dependent expression of biogenic amine receptors in restricted regions of the *C. elegans* nervous system. Dev Biol *263*, 81-102.

Wagner, C., Pfeifer, A., Ruth, P., Hofmann, F., and Kurtz, A. (1998). Role of cGMP-kinase II in the control of renin secretion and renin expression. J Clin Invest *102*, 1576-1582.

Wallace, H. R. (1968). The Dynamics of Nematode Movement. Annual Review of Phytopathology *6*, 91-114.

Way, J. C., and Chalfie, M. (1989). The *mec-3* gene of *Caenorhabditis elegans* requires its own product for maintained expression and is expressed in three neuronal cell types. Genes Dev *3*, 1823-1833.

Wheeler, J. M., and Thomas, J. H. (2006). Identification of a novel gene family involved in osmotic stress response in *Caenorhabditis elegans*. Genetics *174*, 1327-1336.

Wright, D. J. (2004). Osmoregulatory and excretory behavior. In: Gaugler R. and Bilgrami, A. L. (eds) *Nematode Behavior.* CAB International, Wallingford, UK, pp. 177-196.

Zhao, B., Khare, P., Feldman, L., and Dent, J. A. (2003). Reversal frequency in *Caenorhabditis elegans* represents an integrated response to the state of the animal and its environment. J Neurosci *23*, 5319-5328.

Genotype:	*gcy-28(ky713)*	
Promoter	With cDNA	Without cDNA
H20 (pan-neuronal)	0.056	0.34
col-19 (hypodermis)	0.8	0.37
myo-3 (muscle)	0.68	0.37
elt-2 (gut)	0.48	0.36

Table 5-1. Tissue-specific rescue of *gcy-28* mutants
Fraction of animals paralyzed 200 seconds after transferring to low osmolality plate. Promoters used to express *gcy-28.c* cDNA are indicated. Each rescue strain was tested in parallel with a control *gcy-28(ky713)* strain. Each data point represents one or two assays, with about 12 animals each. Data was smoothed to represent an average over 10 seconds.

genotype	Test strain	WT	*gcy-28 (ky713)*
ocr-1(ok132)	0.16	0.05	0.51
ocr-2(ak47)	0.88*	0.024	0.43
ocr-3(ok1559)	0.49*	0.12	0.72
osm-9(ky161)	0.78*	0.15	0.73
osm-9(n1601)	0.92*	0.15	0.73
trp-4(gk341)	0.6*	0.12	0.72
trpa-1(ok999)	0.15	0.12	0.72
deg-3(u701)	0.35*	0.036	0.48
tax-4(ks28)	0.11	0.029	0.52
tax-4(p678)	0.02	0.029	0.52
osr-1 (rm1)	0.13	0.048	0.31

Table 5-2. Candidate mutants tested for hypo-osmotic stress response
Fraction of animals paralyzed 200 seconds after transferring to low osmolality plate. Genotypes tested are indicated. Each strain was tested in parallel with wild-type and *gcy-28(ky713)* controls. *ocr-1, ocr-2*, *ocr-3*, *osm-9*, *trp-4* and *trpa-1* are TRP channel homologs, *deg-3* belongs to the DEG/ENaC family of channels related to *mec-4* and *mec-10*, *tax-4* is a CNG channel subunit, and *osr-1* is a novel gene that regulates hyperosmotic stress responses in *C. elegans*. Each data point represents one or two assays, with about 12 animals each. Data was smoothed to represent an average over 10 seconds. Asterisks mark results showing a potential defect in the response.

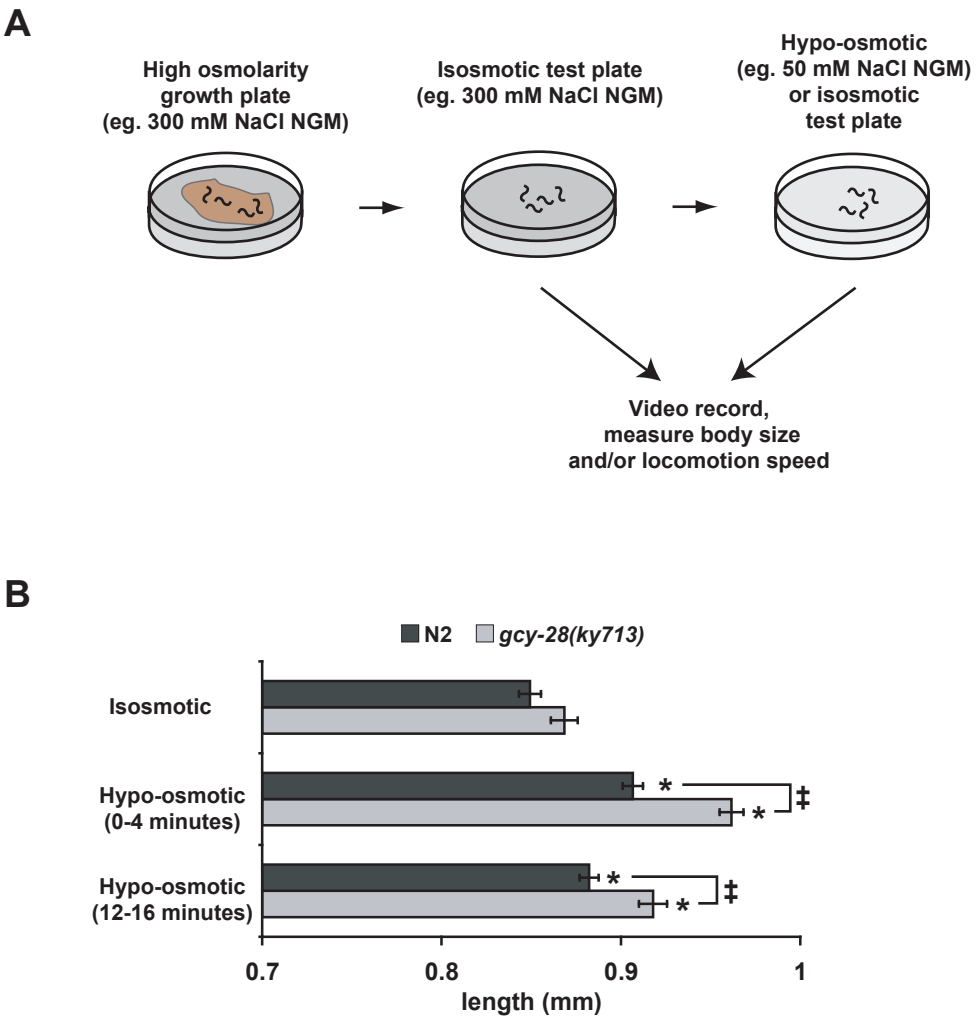


Figure 5-1. Measuring the effect of hypo-osmotic stress on *C. elegans*
(A) Protocol for hypo-osmotic stress assay. (B) Effect of hypo-osmotic stress on body length in wild-type and *gcy-28(ky713)* mutant animals. n = 15 assays each. * $p < 0.05$ relative to isosmotic control, ‡ $p < 0.05$, Bonferroni *t*-test. Error bars indicate SEM.

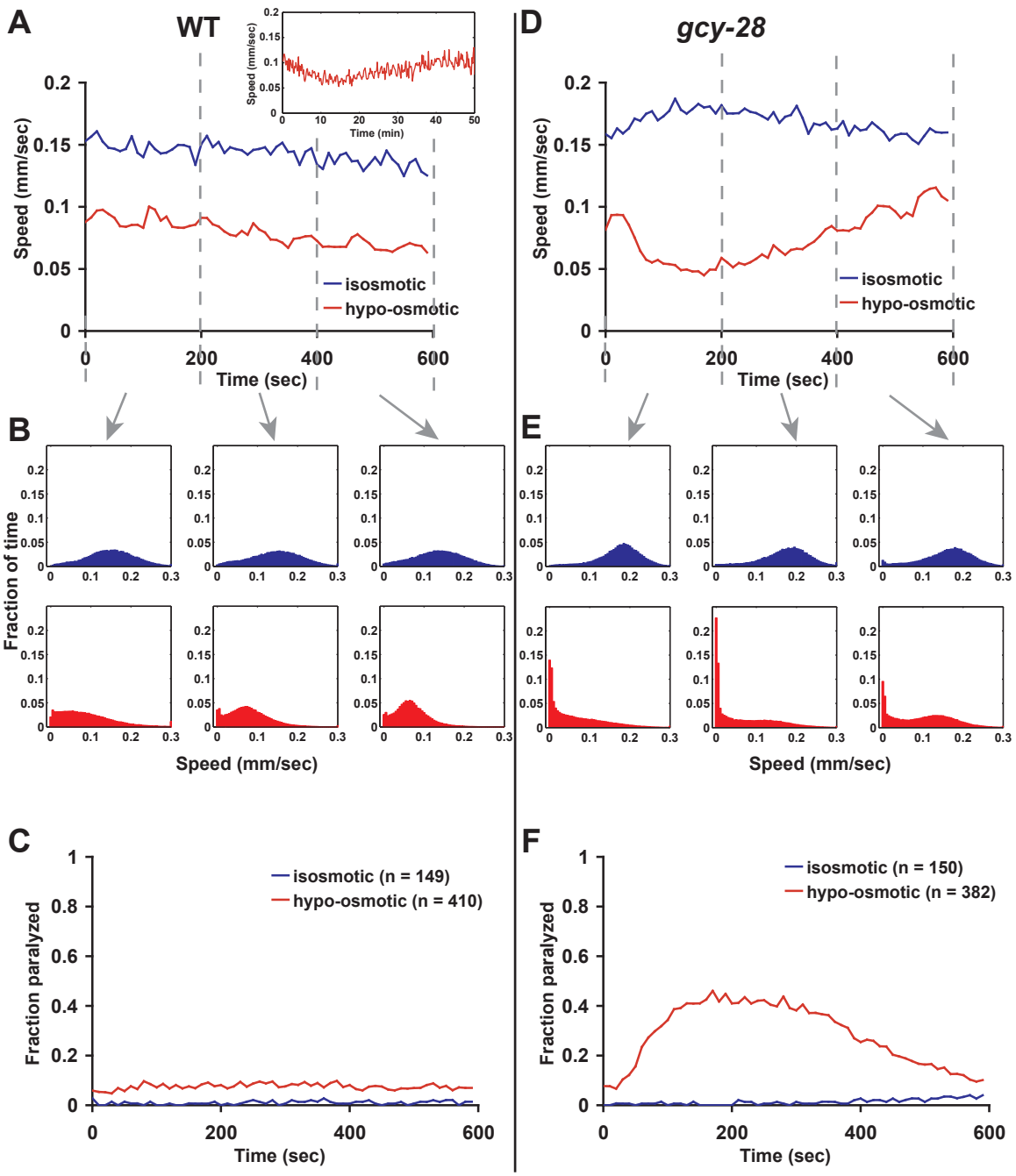


Figure 5-2. Effect of hypo-osmotic stress on locomotion in wild-type and *gcy-28* mutant animals

Analysis of locomotion rate in wild-type (A-C) and gcy-28 mutant (D-F) animals. (A and D) Representative trace (average of ~12 animals each) for the time course of locomotion rate immediately after shifting to isosmotic (blue) or hypo-osmotic (red) media. (A inset) Speed of wild-type animals in hypo-osmotic media up to 50 minutes. (B and E) Frequency histogram of speed distributions. Each histogram represents speed distributions in successive 200-second windows after shifting to the assay media. (C and F) Time course of paralysis. Animals moving slower than 0.01 mm/sec were classified as paralyzed. n is the total number of animals tracked.

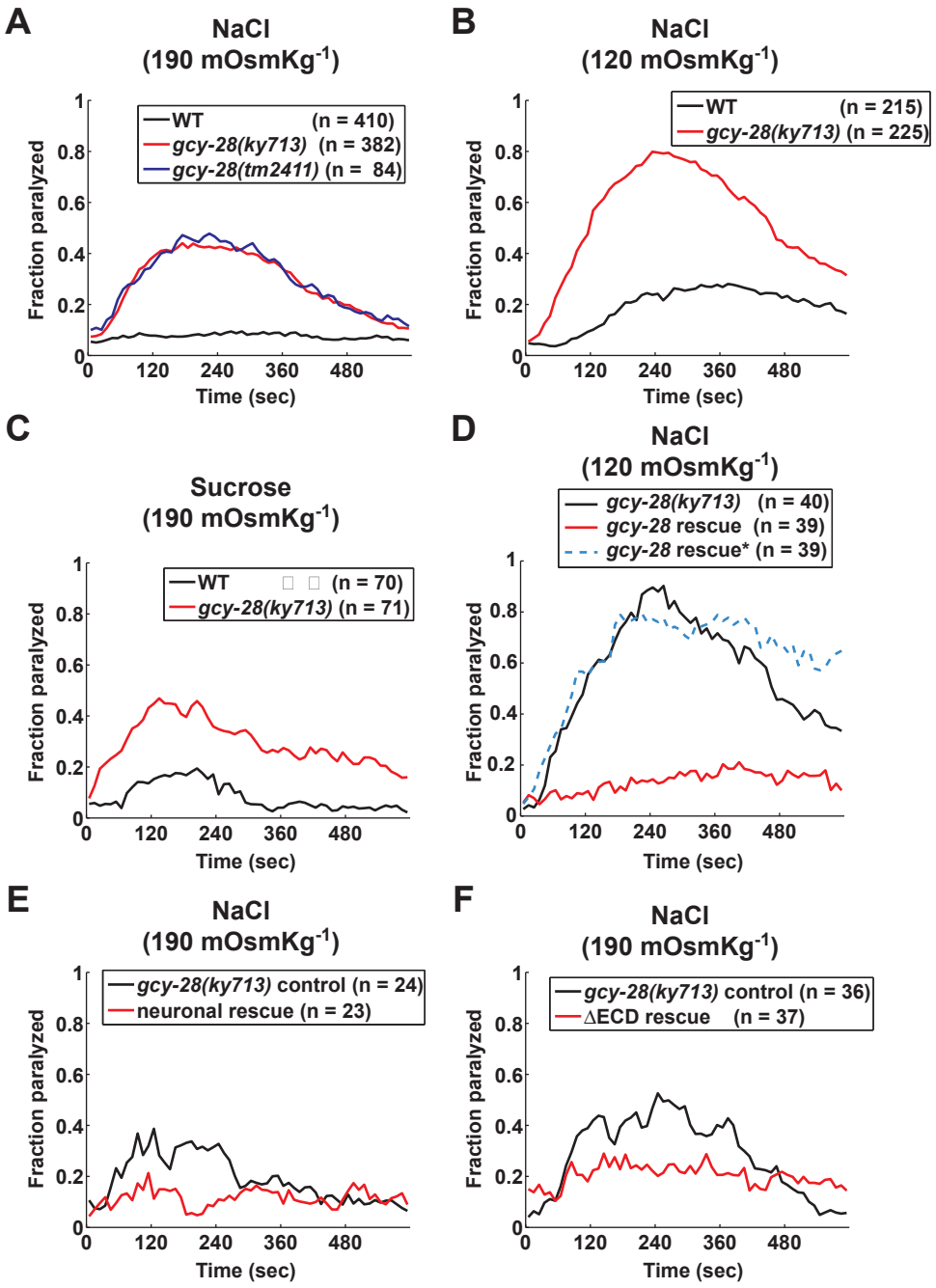


Figure 5-3. Hypo-osmotic stress-induced paralysis in *gcy-28* mutants
The solute used to adjust osmolality is indicated, and the osmolality of the test media is indicated in parentheses underneath. The growth media was at 590 mOsmKg^{-1}. (A) Response to hypo-osmotic stress in wild-type and two loss-of-function alleles of *gcy-28* mutant animals. (B) Paralysis induced by a larger reduction in osmolality compared to (A). (C) Hypo-osmotic stress induced by sucrose. (D) Effect of expressing *gcy-28.c* cDNA under the *gcy-28* promoter in *gcy-28(ky713)* mutants. A cDNA with the *ky713* mutation was also tested and is indicated by and asterisk. (E) Expression of *gcy-28.c* cDNA under a pan-neuronal *H20* promoter. (F) Expression of an extracellular domain-deleted *gcy-28.c* cDNA under a pan-neuronal *H20* promoter.

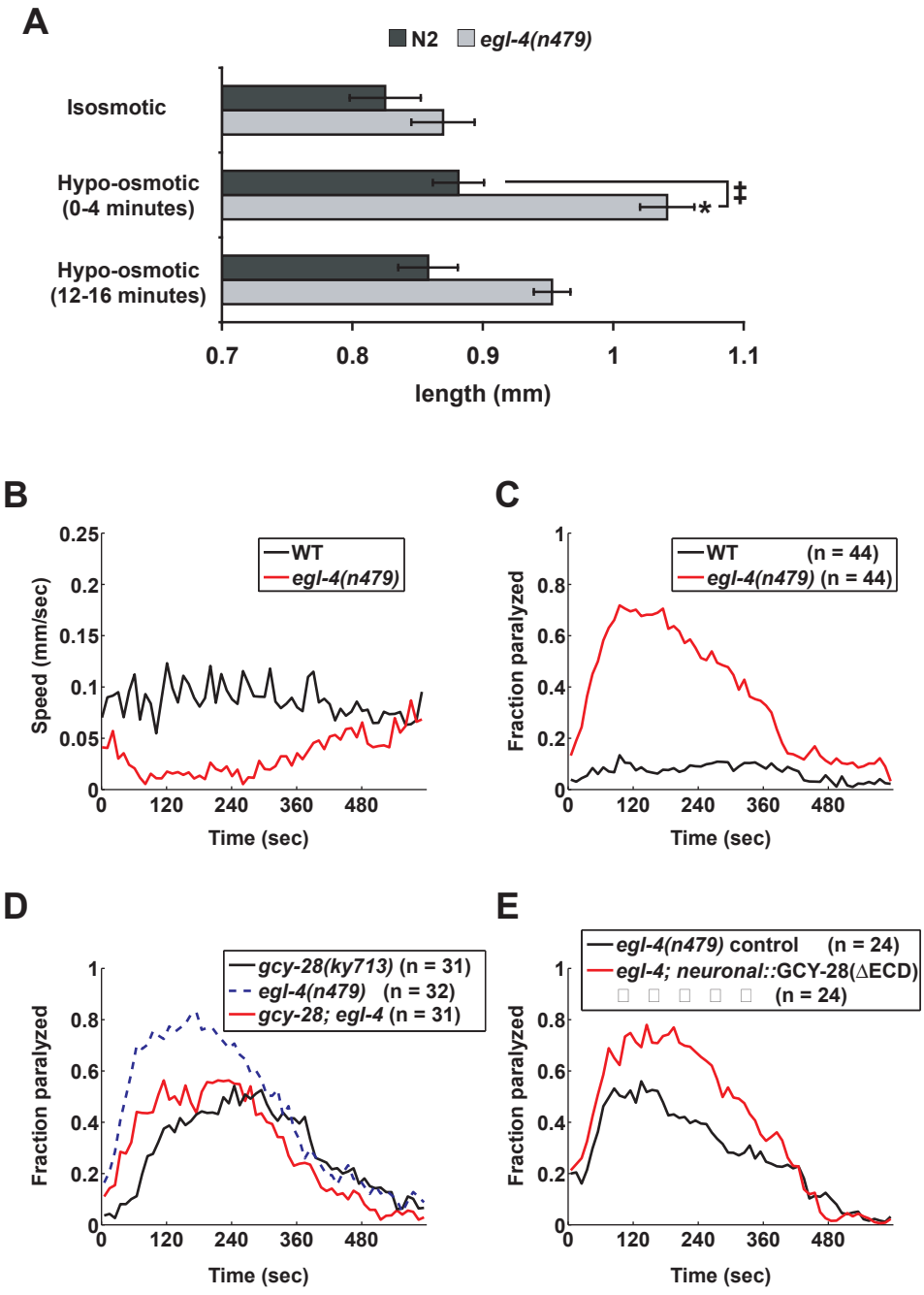


Figure 5-4. Hypo-osmotic stress response of PKG *egl-4* mutants

(A) Effect of hypo-osmotic stress on body length in wild-type and *egl-4(n479)* mutant animals. n = 3 assays each. * $p < 0.05$ relative to isosmotic control, ‡ $p < 0.05$, Bonferroni *t*-test. Error bars indicate SEM. (B) Representative trace (average of ~12 animals each) for the time course of locomotion rate immediately after shifting to isosmotic (blue) or hypo-osmotic (hypo-osmotic) media. (C) Paralysis time course. (D) *gcy-28, egl-4* single and double mutants. (E) Expression of an extracellular domain-deleted *gcy-28* cDNA under a pan-neuronal *H20* promoter in *egl-4* mutants.

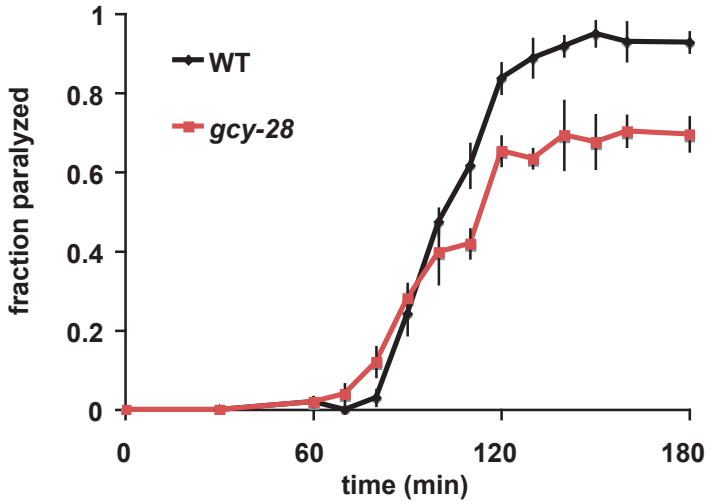


Figure 5-5. Aldicarb resistance in *gcy-28* mutants
Time course of paralysis induced by 1 mM aldicarb in the growth media. n = 5 assays with ~20 animals each. Error bars indicate SEM.

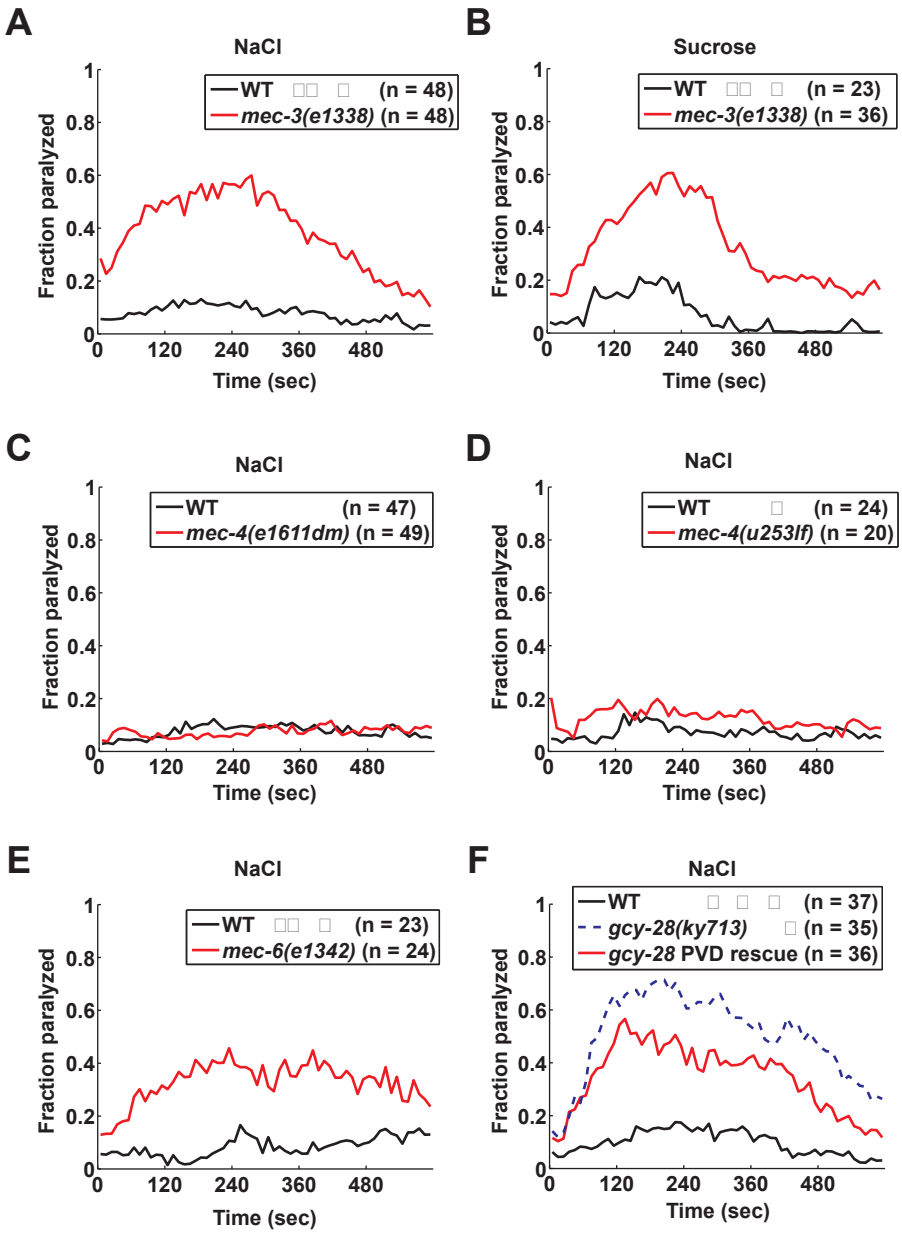


Figure 5-6. Hypo-osmotic stress-induced paralysis in mechanosensory mutants
The solute used to adjust osmolality is indicated. (A) Hypo-osmotic stress induced by NaCl in *mec-3* LIM-homeodomain transcription factor mutants that lack most mechanosensory cells. (B) Hypo-osmotic stress induced by sucrose in *mec-3* mutants. (C) Paralysis time course in the DEG/ENaC subunit *mec-4* gain-of-function mutant that lack a subset of mechanosensory cells. (D) Paralysis time course in *mec-4* loss-of-function mutants that lack mechanosensitive responses in a subset of mechanosensory cells. (E) Paralysis time course in the DEG/ENaC subunit *mec-6* mutant that is expressed in many mechanosensory cells. (F) Paralysis time course of *gcy-28(ky713)* animals expressing *gcy-28.c* cDNA in PVD and FLP using a truncated *des-2* promoter.

CHAPTER 6

Perspectives and Future Directions

A. Olfactory discrimination (Chapter 2)

I used a discrimination assay to study the mechanisms by which the *C. elegans* sensory system codes odor quality. In one case where a loss of neuronal diversity leads to strong discrimination defects (Wes and Bargmann, 2001), the animal uses a combinatorial code to represent odor quality. My results indicate that discrimination between some odor pairs may result from cell-intrinsic mechanisms, not combinatorial codes. However, a screen for discrimination between such an odor pair did not yield any mutants.

There are several ways to continue this work. If there is a rare mutation that gives rise to a discrimination defect, a larger screen may be needed to isolate animals carrying such a mutation. As in any screen, there are reasons that even a larger screen could fail. There may be redundancy among multiple genes, or pleiotropic effects of genes may mask behavioral defects. One interesting possible reason that discrimination mutants are hard to find is that cell-intrinsic mechanisms that allow odor discrimination are also required for olfactory transduction itself. In both behavior and neuronal activity, response to a step stimulus is phasic, that is, the largest responses are observed soon after the stimulus changes and then the response relaxes towards baseline as the stimulus remains constant. A return to baseline activity during constant stimulus presentation, or adaptation, is thought to play a part in maintaining the large dynamic range observed in many sensory systems (Burns and Baylor, 2001). Rapid adaptation may be necessary for proper chemotaxis in odor gradients and could also allow for discrimination between odors sensed by the same neuron. For example, a regulatory player in many GPCR signaling pathways is the GPCR kinase GRK-2 (Pitcher et al., 1998). GRK-2 down regulates signaling through ligand-activated GPCRs by phosphorylating the cytoplasmic

tail of the GPCR, which is then bound by arrestins that terminate signaling. Thus GRK-2 is important for proper signaling and allows for selective down regulation of activated pathways in sensory signaling. The mutant for the *C. elegans* GRK-2 homolog, *grk*-2, is defective for chemotaxis, indicating that receptor down regulation may be essential for gradient sensing (Fukuto et al., 2004). Unfortunately, this defect precludes anaylsis of discrimination in *grk-2* mutants. A more quantitative analysis of behavior based on animal-tracking assays that measure instantaneous odor responses, may help to analyze odor detection and discrimination. A microfluidic device that presents odors to freely moving animals can be used to track rapid behavioral responses to odors, such as turns and speed changes. This time-resolved mothod can be used to distinguish chemotaxis mutants that do not sense odors at all from those that have altered kinetics of behavioral responses.

Comprehensive analysis of odor responses using these behavioral methods combined with Ca^{2+} imaging of sensory neurons and interneurons could be performed for several odors that are sensed by one neuron but discriminated by the animal. Factors such as the time course and dose dependence of responses may be obtained. From these data, it will be possible to formulate hypotheses about how odor quality is coded at the level of the neurons and translated into behavior. For example, different odors may evoke different temporal patterns of AWC activity, similar to what is seen in the bitter tasting neurons of larval *Manduca sexta* (Glendinning et al., 2002). Discrimination between odors may be tested by either presentation of two odors at the same time, or through a cross-adaptation protocol, where animals are conditioned with one odor and tested for responses to another. Various chemotaxis defective as well as other candidate

mutants may be tested in a similar way to genetically define different components of the response. For example, the AWC adaptation-defective *osm-9* and *ocr-2* mutants may have quantitative defects in behavior when presented with two odors sensed by AWC.

B. Switching odor preference in AWC (Chapters 3 and 4)

Olfactory and gustatory behavior is highly plastic and is modified readily by context-dependent sensory experience. During adaptation or sensitization, plasticity in the sensory neuron involves quantitative reduction or enhancement of attraction. In gustatory learning, salt preference switches from attraction to avoidance, and this switch may be a result of changes in the relative strengths of distinct groups of neurons that mediate either attraction or avoidance (Hukema et al., 2006; Tomioka et al., 2006). In olfaction, AWC^{ON} normally drives attraction, but mutations in *gcy-28* and *pkc-1* cause AWC^{ON} to drive avoidance. As described in this thesis, regulation of AWC^{ON} output between attraction and avoidance by cGMP and PKC signaling could create plasticity in a small anatomically stable neural circuit.

The molecular mechanisms underlying the preference switch are not clear, and experiments addressing these questions offer an interesting avenue for future research. Signaling upstream of *gcy-28* is not understood and it would be important to identify the ligand for *gcy-28*. The expression pattern for the ligand for *gcy-28* could suggest which environmental cues may regulate *gcy-28* and behavioral plasticity. It could also shed light on how *gcy-28* regulates plasticity in other sensory modalities, such as thermotaxis and salt chemotaxis. The behavioral switch in preference suggests that there is a change in AWC^{ON} circuit coding. There are examples of switching of coding in other systems,

so this may be a more general phenomenon in sensory systems. Finally, *gcy-28* causes a dramatic switch in behaviors mediated by the AWC^{ON} neuron, but not the AWC^{OFF} neuron, further underscoring the difference in physiology between the two neurons. A better mechanistic understanding of the functional cause and consequences of AWC asymmetry will shed light on how sensory information is processed and integrated by a defined nervous system.

Mechanisms of odor preference switching

Odor avoidance in *gcy-28* mutants can be rescued acutely in adults, by heat-shock expression of *gcy-28*, pharmacological activation of DAG signaling, or by association of odor with food. Therefore, *gcy-28* is not a necessary component AWC signaling, but instead regulates the balance between two parallel outputs, one driving attraction and the other driving repulsion. The balance between these signaling pathways determines the overall outcome of chemotaxis. *gcy-28*, *pkc-1*, and odor/food pairing favor attractive signaling, and *dgk-1* and adaptation favor repulsive signaling. Thus, regulation is imposed on an underlying circuit capable of driving opposite behaviors.

A similar principle is observed in a more complicated innate behavior; the choice between mating and aggression in mice. The TRP channel TrpC2 is expressed in the sensory neurons of the vomeronasal organ (VNO), and mediates sensory transduction in response to conspecific pheromonal cues (Leypold et al., 2002; Liman et al., 1999; Stowers et al., 2002). A genetic lesion of TrpC2 causes male mice to mate with both males and females, where they would normally show aggressive behavior to males, and causes female mice to display male courtship behavior to both males and females

(Kimchi et al., 2007; Stowers et al., 2002). The behavioral switch in females is not caused by developmental defects because removing the VNO in adult females phenocopies the TrpC2 mutant phenotype. Therefore, regulatory input from TrpC2-expressing sensory neurons suppresses an underlying neural circuit for male mating behavior in female mice.

There are two main approaches needed to address the mechanisms underlying the odor preference switch in AWC. First, a better understanding of physiological responses to odor in the AWC circuit is necessary to identify where signaling pathways diverges between attraction and repulsion. Given that *in vivo* Ca^{2+} imaging shows no obvious difference between wild-type and *gcy-28* animals in AWC^{ON}, it is unlikely that primary signal transduction is affected in the mutant. However, there may be subtle differences in membrane potential that may not be detected by Ca^{2+} indicators. Comparisons of G-CaMP Ca^{2+} signals and electrophysiological measurements show that the indicator does not always detect single action potentials (Mao et al., 2008); it seems likely that it does not fully report the graded changes in membrane potential expected in worm neurons (Davis and Stretton, 1989). Electrophysiology is a sensitive method to directly measure membrane potential and has been used in multiple *C. elegans* sensory neurons to characterize resident ion channels and currents (O'Hagan et al., 2005; Ramot et al., 2008). An analysis of the endogenous active channels in AWC^{ON} in wild-type and *gcy-28* animals, and a comparison of those channels in AWC^{ON} and AWC^{OFF} cells could provide information about the substrate for plasticity. It would be desirable to monitor AWC^{ON} voltage directly, but chemosensory signaling is disrupted by current recording techniques. A method combining a voltage sensitive dye and its interaction with membrane bound

GFP through fluorescent energy transfer may allow direct measurement of membrane potential in live animals (Chanda et al., 2005).

Another possible route would be a more detailed analysis of AWC^{ON} synaptic transmission. Glutamate is required for AWC odor attraction in wild-type animals, and avoidance in *gcy-28* animals. Therefore, differential regulation of glutamate release may underlie the difference in behavioral outcome. In *Aplysia*, cholinergic interneurons in the buccal ganglia connect to each other through a biphasic chemical synapse (Gardner and Kandel, 1972); in which acetylcholine released on the interneurons activates both hyperpolarizing and depolarizing currents. A similar biphasic synapse could support AWC plasticity and there is reason to think that the mechanism is plausible. Glutamate from AWC normally suppresses activity of the AIY interneuron, but in the absence of its inhibitory glutamate receptor, AIY shows Ca^{2+} transients when AWC is activated (Chalasani et al., 2007). This observation suggests that AIY may have dual responses to glutamate from AWC. A genetic analysis of glutamate receptors expressed in interneurons downstream of AWC may identify receptors with opposite polarities within the some target neuron. A biphasic synapse model would suggest that one receptor (eg. inhibitory) would be important for attraction, and another receptor (eg. excitatory) for repulsion. In this model, I expect different patterns of glutamate release from wild-type and *gcy-28* mutants animals. To test this hypothesis, it would be important to quantify odor-evoked synaptic vesicle release from the AWC axon. Optical techniques can be used to do these experiments in live animals using pH-sensitive GFP tagged to synaptic vesicle proteins, such as synaptobrevin and the vesicular glutamate transporter (Dittman and Kaplan, 2006; Voglmaier et al., 2006).

The AIB Ca^{2+} transients in response to butanone were different between wild-type and *gcy-28* mutant animals, but the full nature of the change is unclear. Additional experiments should be conducted to develop these results further, including testing for a broader range of odors and concentrations, comparison of AIB responses downstream of AWC^{ON} and AWC^{OFF}, and cell-autonomy of the effect. Measuring AIB responses in the *pkc-1* mutant, whose behavior is similar to that of *gcy-28*, will help determine what aspect of the AIB response is most closely correlated with avoidance behavior. The AIB response in wild-type animals is relatively weak. Butanone is sensed by only AWC^{ON}, which forms synapses onto both AIBL and AIBR neurons. One interesting possibility is that AIB responses are lateralized. To understand whether AWC^{ON} communicates differently with the two AIBs, imaging could be conducted after marking the AWC^{ON} or AWC^{OFF} neuron in the AIB G-CaMP animals.

A better-controlled stimulus and more quantitative analysis of behavior could help to distinguish between mechanisms of attraction and repulsion. In chemotaxis assays, an odor gradient is created and animals moving in the gradient should experience a gradual change in odor concentration as a function of time. By contrast, *in vivo* Ca^{2+} imaging experiments are carried out using a rapid step change in concentration of odor. Therefore, the shape of the stimulus in the two assays is different. Delivering a stimulus that mimicks the chemotaxis assay gradient is difficult because the shape of the gradient is not defined and is not stable in time. To make the two assays more comparable it may be easiest to test the behavior of animals using odor stimuli that can be reproduced in Ca^{2+} imaging experiments. Through experiments currently being developed by D. Albrecht, an odor step stimulus can be used to analyze behavioral responses in custom-

made microfluidic devices. Characterizing the behavioral response to defined stimuli should lead to a better understanding of wild-type and mutant chemotaxis (Clark et al., 2007; Suzuki et al., 2008; Zariwala et al., 2003).

Physiological consequences of AWC asymmetry

gcy-28 odor avoidance is only observed in the AWC^{ON} neuron and not the AWC^{OFF} neuron. This observation suggests that the AWC^{OFF} neuron may not have a repulsive mode of signaling. Therefore, differences between gene expression patterns in AWC^{ON} and AWC^{OFF} neurons might be used to identify candidate mechanisms of odor avoidance in *gcy-28* mutants. Expression profiling of specific neurons marked with GFP has identified genes specifically expressed in these neuron types (Colosimo et al., 2004; Zhang et al., 2002). However, expression profiling requires embryonic cell cultures, which are obtained by dissociation of early-stage embryos (Christensen et al., 2002), whereas AWC^{ON}/AWC^{OFF} asymmetry is determined during late embryogenesis and requires cell-cell interactions (Chuang and Bargmann, 2005; Chuang et al., 2007; Troemel et al., 1999). Initial experiments suggest that AWC^{ON} neuron fates are not properly specified in culture. An alternative approach such as polyA tagging of mRNA pools within mature AWC neurons may allow comparison of AWC^{ON} and AWC^{OFF} (Von Stetina et al., 2007). This approach ha successfully been used to identify transcripts unique to ASER and ASEL (Kunitomo et al., 2005). To determine which of the candidate genes is required to generate the difference between AWC^{ON} and AWC^{OFF}, each candidate gene could be expressed in AWC neurons of *gcy-28* mutants to see if any one or combination of genes alters *gcy-28* behavior. For example, a gene expressed only

in AWC^{ON} may, when expressed in AWC^{OFF} in a *gcy-28* mutant background, turn AWC^{OFF} into an avoidance neuron.

Regulation of *gcy-28* activity

Because the specific GCY-28.d extracellular domain is required for full rescuing activity, GCY-28 may be regulated by a ligand. Identifying a ligand may help understand which cells and what environmental cues are involved in *gcy-28* regulation. A genetic screen for butanone avoidance mutants, analogous to the screen that yielded *gcy-28*, is an obvious approach to identify mutations in the ligand.

Odor conditioning up to one hour causes olfactory adaptation in AWC specific to the odor, except for certain odor pairs like benzaldehyde and isoamyl alcohol, which cross-adapt with each other (Colbert and Bargmann, 1995). Longer conditioning with butanone causes a change in AWC^{ON} that generalizes to other AWC^{ON} odors. Therefore, regulation of entire neurons may play a role in parallel to odor-specific regulation of sensory transduction pathways to generate olfactory plasticity in *C. elegans.* Sensitization of AWC to butanone was reported as being odor specific (Torayama et al., 2007). However, our results suggest that sensitization generalizes to other odors sensed by AWC^{ON}. Differences in experimental protocol, may have led to the different results, but these results are also consistent with regulation at the level of the entire neuron. Other sensory modalities may also have regulation at the whole-neuron level. Gustatory learning in ASER is a process that generalizes to all chemicals sensed by ASER (Saeki et al., 2001).

Switching coding and behavior

What is the role of the behavioral switch in AWC^{ON} in normal *C. elegans* behavior ? There are a few examples of behavioral switching with known cellular mechanisms in other systems that could be informative. Young *Drosophila* larvae accept fructose-containing media, but avoid it before metamorphosis. This switch in behavior is correlated with the different physiological needs of feeding larvae and non-feeding pupae. In *Drosophila*, appetitive behavior and avoidance behavior are mediated by different sets of neurons, and a developmentally regulated switch turns on fructose sensitivity in the aversive neurons (Xu et al., 2008). In *C. elegans*, males are attracted to pheromone that hermaphrodites find repulsive. This sex switch involves a change in both sex-specific and sex non-specific sensory neurons (Srinivasan et al., 2008; White et al., 2007).

At the level of neural circuits, there is an example of polarity switching in the retinal ganglion cells from On to Off in the vertebrate visual system (Geffen et al., 2007). Recordings from ganglion cells in the salamander retina show that a subset of neurons that respond to light decreases in its receptive field (Off response) become sensitive to light increases (On response) transiently when there is a large contrast change in the periphery. Thus, the ganglion cell encodes opposite outputs depending on the stimulus context. This shift occurs on the order of 100 ms in a much more complex circuit, and mechanisms underlying the switch are likely to be different from *C. elegans* olfactory behavior. However, given the several parallels between worm olfaction and vertebrate vision (Chalasani et al., 2007), it is interesting to draw another parallel between the vertebrate visual system and *C. elegans* olfaction: the stimulus context (temporal context

for olfaction, spatial context for vision) may switch the output from the sensory system (attraction to avoidance for AWC, Off to On response for retinal ganglion cells).

C. Adaptive behaviors during osmotic stress (Chapter 5)

C. elegans responds to a rapid drop in external osmolality by increasing its body size and altering its locomotion pattern. The increase in body size may reflect the influx of water from the environment due to osmotic pressure. cGMP signaling, through *gcy-28* and the PKG encoded by *egl-4*, regulates the extent of the body size increase. Hypo-osmotic stress also causes acute paralysis that is strongly enhanced in the absence of cGMP signaling by *gcy-28* and *egl-4*. Acute paralysis upon hypo-osmotic stress is also observed in a subset of mutants defective for touch sensation, implicating the putative harsh-touch neuron PVD or the nose-touch neuron FLP in regulating hypo-osmotic stress responses.

It is likely that *gcy*-28 and *egl-4* act downstream of the osmosensory step in the hypo-osmotic stress response. My results suggest that *gcy-28* does not act in PVD/FLP, because rescue of the hypo-osmotic responses was not observed by expression of *gcy-28* under the PVD/FLP-selective *des-2* promoter. To further define the genetic pathway of hypo-osmotic stress responses, the relationship between PVD/FLP and *gcy-28*/*egl-4* should be established. If cGMP signaling is required in neurons that receive a signal from osmosensing PVD/FLP neurons, a consistutively active *gcy-28* extracellular domain deletion or an *egl-4* gain-of-function mutant (Raizen et al., 2006) might suppress *mec-3* (PVD/FLP cell fate) or *mec-6* (ENaC channel-defective) mutants. It would also be interesting to determine the neurons in which cGMP signaling is required by rescue of

gcy-28 or *egl-4* defects. Motor neurons are possible candidates, for example. This information may help understand the paralysis observed in the mutants.

PVD and FLP are ideal candidates for sensory neurons that detect changes in systemic osmotic pressure because of their morphology and their gene expression patterns. To confirm their role in this process, cell-specific rescue experiments should be conducted in the defective mutants *mec-3*, *mec-6*, and *osm-9*. If *mec-3* and *mec-6* do rescue in PVD and FLP in the mutants, it will be interesting to use Ca^{2+} imaging to look for osmotic pressure-induced Ca^{2+} signaling in PVD/FLP.

Among all the sensory modalities, mechanosensation has the largest number of unanswered questions in terms of the molecular basis of sensation. In mammals, touch-sensitive fibers innervating the skin can be classified into several different classes depending on the type of stimulus to which they respond (Johnson, 2001). These fibers belong to dorsal root ganglion cells that express different sets of mechanosensitive and osmosensitive channels (Lumpkin and Caterina, 2007). A current model is that diverse classes of molecular mechanosensors, expressed in diverse mechanosensitive neurons, may represent the need to code different types of mechanical stimuli into distinct neuronal representations. Similarly, in *C. elegans*, gentle touch along the body and nose touch are sensed by different neurons, and the genetic requirements for the two behaviors are different (Syntichaki and Tavernarakis, 2004). Future work on the role of PVD/FLP in osmosensation may demonstrate how the nematode uses different sets of neurons to distinguish between different types of mechanical stimuli.

References

Burns, M. E., and Baylor, D. A. (2001). Activation, deactivation, and adaptation in vertebrate photoreceptor cells. Annu Rev Neurosci *24*, 779-805.

Chalasani, S. H., Chronis, N., Tsunozaki, M., Gray, J. M., Ramot, D., Goodman, M. B., and Bargmann, C. I. (2007). Dissecting a circuit for olfactory behaviour in *Caenorhabditis elegans*. Nature *450*, 63-70.

Chanda, B., Blunck, R., Faria, L. C., Schweizer, F. E., Mody, I., and Bezanilla, F. (2005). A hybrid approach to measuring electrical activity in genetically specified neurons. Nat Neurosci *8*, 1619-1626.

Christensen, M., Estevez, A., Yin, X., Fox, R., Morrison, R., McDonnell, M., Gleason, C., Miller, D. M., 3rd, and Strange, K. (2002). A primary culture system for functional analysis of *C. elegans* neurons and muscle cells. Neuron *33*, 503-514.

Chuang, C. F., and Bargmann, C. I. (2005). A Toll-interleukin 1 repeat protein at the synapse specifies asymmetric odorant receptor expression via ASK1 MAPKKK signaling. Genes Dev *19*, 270-281.

Chuang, C. F., Vanhoven, M. K., Fetter, R. D., Verselis, V. K., and Bargmann, C. I. (2007). An innexin-dependent cell network establishes left-right neuronal asymmetry in *C. elegans*. Cell *129*, 787-799.

Clark, D. A., Gabel, C. V., Lee, T. M., and Samuel, A. D. (2007). Short-term adaptation and temporal processing in the cryophilic response of *Caenorhabditis elegans*. J Neurophysiol *97*, 1903-1910.

Colbert, H. A., and Bargmann, C. I. (1995). Odorant-specific adaptation pathways generate olfactory plasticity in *C. elegans*. Neuron *14*, 803-812.

Colosimo, M. E., Brown, A., Mukhopadhyay, S., Gabel, C., Lanjuin, A. E., Samuel, A. D., and Sengupta, P. (2004). Identification of thermosensory and olfactory neuron-specific genes via expression profiling of single neuron types. Curr Biol *14*, 2245-2251.

Davis, R. E., and Stretton, A. O. (1989). Signaling properties of *Ascaris* motorneurons: graded active responses, graded synaptic transmission, and tonic transmitter release. J Neurosci *9*, 415-425.

Dittman, J. S., and Kaplan, J. M. (2006). Factors regulating the abundance and localization of synaptobrevin in the plasma membrane. Proc Natl Acad Sci U S A *103*, 11399-11404.

Fukuto, H. S., Ferkey, D. M., Apicella, A. J., Lans, H., Sharmeen, T., Chen, W., Lefkowitz, R. J., Jansen, G., Schafer, W. R., and Hart, A. C. (2004). G protein-coupled receptor kinase function is essential for chemosensation in *C. elegans*. Neuron *42*, 581-593.

Gardner, D., and Kandel, E. R. (1972). Diphasic Postsynaptic Potential: A Chemical Synapse Capable of Mediating Conjoint Excitation and Inhibition. Science *176*, 675-678.

Geffen, M. N., de Vries, S. E., and Meister, M. (2007). Retinal ganglion cells can rapidly change polarity from Off to On. PLoS Biol *5*, e65.

Glendinning, J. I., Davis, A., and Ramaswamy, S. (2002). Contribution of different taste cells and signaling pathways to the discrimination of "bitter" taste stimuli by an insect. J Neurosci *22*, 7281-7287.

Hukema, R. K., Rademakers, S., Dekkers, M. P., Burghoorn, J., and Jansen, G. (2006). Antagonistic sensory cues generate gustatory plasticity in *Caenorhabditis elegans*. Embo J *25*, 312-322.

Johnson, K. O. (2001). The roles and functions of cutaneous mechanoreceptors. Current Opinion in Neurobiology *11*, 455-461.

Kimchi, T., Xu, J., and Dulac, C. (2007). A functional circuit underlying male sexual behaviour in the female mouse brain. Nature *448*, 1009-1014.

Kunitomo, H., Uesugi, H., Kohara, Y., and Iino, Y. (2005). Identification of ciliated sensory neuron-expressed genes in *Caenorhabditis elegans* using targeted pull-down of poly(A) tails. Genome Biol *6*, R17.

Leypold, B. G., Yu, C. R., Leinders-Zufall, T., Kim, M. M., Zufall, F., and Axel, R. (2002). Altered sexual and social behaviors in trp2 mutant mice. Proc Natl Acad Sci U S A *99*, 6376-6381.

Liman, E. R., Corey, D. P., and Dulac, C. (1999). TRP2: a candidate transduction channel for mammalian pheromone sensory signaling. Proc Natl Acad Sci U S A *96*, 5791-5796.

Lumpkin, E. A., and Caterina, M. J. (2007). Mechanisms of sensory transduction in the skin. Nature *445*, 858-865.

Mao, T., O'Connor, D. H., Scheuss, V., Nakai, J., and Svoboda, K. (2008). Characterization and subcellular targeting of GCaMP-type genetically-encoded calcium indicators. PLoS ONE *3*, e1796.

O'Hagan, R., Chalfie, M., and Goodman, M. B. (2005). The MEC-4 DEG/ENaC channel of *Caenorhabditis elegans* touch receptor neurons transduces mechanical signals. Nat Neurosci *8*, 43-50.

Pitcher, J. A., Freedman, N. J., and Lefkowitz, R. J. (1998). G protein-coupled receptor kinases. Annu Rev Biochem *67*, 653-692.

Raizen, D. M., Cullison, K. M., Pack, A. I., and Sundaram, M. V. (2006). A novel gain-of-function mutant of the cyclic GMP-dependent protein kinase *egl-4* affects multiple physiological processes in *Caenorhabditis elegans*. Genetics *173*, 177-187.

Ramot, D., Macinnis, B. L., and Goodman, M. B. (2008). Bidirectional temperature-sensing by a single thermosensory neuron in *C. elegans*. Nat Neurosci.

Saeki, S., Yamamoto, M., and Iino, Y. (2001). Plasticity of chemotaxis revealed by paired presentation of a chemoattractant and starvation in the nematode *Caenorhabditis elegans*. J Exp Biol *204*, 1757-1764.

Srinivasan, J., Kaplan, F., Ajredini, R., Zachariah, C., Alborn, H. T., Teal, P. E., Malik, R. U., Edison, A. S., Sternberg, P. W., and Schroeder, F. C. (2008). A blend of small molecules regulates both mating and development in *Caenorhabditis elegans*. Nature.

Stowers, L., Holy, T. E., Meister, M., Dulac, C., and Koentges, G. (2002). Loss of sex discrimination and male-male aggression in mice deficient for TRP2. Science *295*, 1493-1500.

Suzuki, H., Thiele, T. R., Faumont, S., Ezcurra, M., Lockery, S. R., and Schafer, W. R. (2008). Functional asymmetry in *Caenorhabditis elegans* taste neurons and its computational role in chemotaxis. Nature *454*, 114-117.

Syntichaki, P., and Tavernarakis, N. (2004). Genetic models of mechanotransduction: the nematode *Caenorhabditis elegans*. Physiol Rev *84*, 1097-1153.

Tomioka, M., Adachi, T., Suzuki, H., Kunitomo, H., Schafer, W. R., and Iino, Y. (2006). The insulin/PI 3-kinase pathway regulates salt chemotaxis learning in *Caenorhabditis elegans*. Neuron *51*, 613-625.

Torayama, I., Ishihara, T., and Katsura, I. (2007). *Caenorhabditis elegans* integrates the signals of butanone and food to enhance chemotaxis to butanone. J Neurosci *27*, 741-750.

Troemel, E. R., Sagasti, A., and Bargmann, C. I. (1999). Lateral signaling mediated by axon contact and calcium entry regulates asymmetric odorant receptor expression in *C. elegans*. Cell *99*, 387-398.

Voglmaier, S. M., Kam, K., Yang, H., Fortin, D. L., Hua, Z., Nicoll, R. A., and Edwards, R. H. (2006). Distinct endocytic pathways control the rate and extent of synaptic vesicle protein recycling. Neuron *51*, 71-84.

Von Stetina, S. E., Watson, J. D., Fox, R. M., Olszewski, K. L., Spencer, W. C., Roy, P. J., and Miller, D. M., 3rd (2007). Cell-specific microarray profiling experiments reveal a comprehensive picture of gene expression in the *C. elegans* nervous system. Genome Biol *8*, R135.

Wes, P. D., and Bargmann, C. I. (2001). *C. elegans* odour discrimination requires asymmetric diversity in olfactory neurons. Nature *410*, 698-701.

White, J. Q., Nicholas, T. J., Gritton, J., Truong, L., Davidson, E. R., and Jorgensen, E. M. (2007). The sensory circuitry for sexual attraction in *C. elegans* males. Curr Biol *17*, 1847-1857.

Xu, J., Sornborger, A. T., Lee, J. K., and Shen, P. (2008). *Drosophila* TRPA channel modulates sugar-stimulated neural excitation, avoidance and social response. Nat Neurosci *11*, 676-682.

Zariwala, H. A., Miller, A. C., Faumont, S., and Lockery, S. R. (2003). Step response analysis of thermotaxis in *Caenorhabditis elegans*. J Neurosci *23*, 4369-4377.

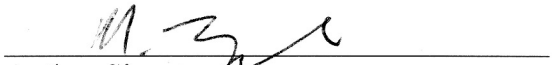
Zhang, Y., Ma, C., Delohery, T., Nasipak, B., Foat, B. C., Bounoutas, A., Bussemaker, H. J., Kim, S. K., and Chalfie, M. (2002). Identification of genes expressed in *C. elegans* touch receptor neurons. Nature *418*, 331-335.

Publishing Agreement

It is the policy of the University to encourage the distribution of all theses and dissertations. Copies of all UCSF theses and dissertations will be routed to the library via the Graduate Division. The library will make all theses and dissertations accessible to the public and will preserve these to the best of their abilities, in perpetuity.

Please sign the following statement:

I hereby grant permission to the Graduate Division of the University of California, San Francisco to release copies of my thesis or dissertation to the Campus Library to provide access and preservation, in whole or in part, in perpetuity.



Author Signature

Aug. 21, 2008

Date